REMOVAL OF HEXAVALENT CHROMIUM AND CADMIUM FROM WATER USING CARBON BASED ADSORBENTS

BY

FAHAD ABDULAZIZ AL-KHALDI

A Dissertation Presented to the

DEANSHIP OF GRADUATE STUDIES

KING FAHD UNIVERSITY OF PETROLEUM & MINERALS

DHAHRAN, SAUDI ARABIA

In Partial Fulfillment of the

Requirements for the Degree of

DOCTOR OF PHILOSOPHY

In

CHEMICAL ENGINEERING

June, 2011

KING FAHD UNIVERSITY OF PETROLEUM & MINERALS
DHAHRAN, SAUDI ARABIA

DEANSHIP OF GRADUATE STUDIES

This dissertation, written by **Fahad Abdulaziz Al-Khaldi** under the direction of his dissertation advisor and approved by his dissertation committee, has been presented to and accepted by the Dean of Graduate Studies, in partial fulfillment of the requirements for the degree of **DOCTOR OF PHIOLOSOPHY IN CHEMICAL ENGINEERING.**

Dissertation Committee

Prof. Basel F. Abu-Sharkh
Thesis Advisor

Dr. S. M. Javaid Zaidi
Co-advisor

Dr. Usamah Al-Mubaiyedh
Department Chairman

Dr. Muataz A. Atieh
Member

Dr. Salam Zummo
Dean of Graduate Studies

Dr. Mazen M. Khaled
Member

21/6/11
Date

Dr. Alaadin A. Bukhari
Member

DEDICATION

This work is dedicated to my beloved ***parents***, my ***wife***, my ***children***, my ***brothers***, and my ***sisters***.

أهـــــــــداء

لمن جـــهد في تـربـيـتي ..... أمـي و أبـي الكـرام.

لمن شغل بشغلي و أهـتم بهمـي ..... زوجتي الحبـيـبـة.

لمن لزم نصـحي و شُـــد به أزري ..... أخوتـــي الأعـزاء.

لمن صبر على شدتي و تعاطف معي ..... أبنائي و بناتي الأعـزاء.

ACKNOWLEGDGEMENTS

I really want to give my deepest gratitude to all my thesis Committee members for all the support they provided me with during my research work. Special thanks to committee chairman, ***Dr. Basil Abu-Sharkh***, and ***Dr. Muataz Ali Atieh*** for their special support and day to day guidance during the entire development phase of this study. I also want to thank all other committee members, ***Dr. S. M. Javid Zaidi, Dr. Mazen Khaled and Dr. Aladdin Bukhari*** for their constructive guidance, valuable advices and cooperation.

I am very grateful to ***King Fahd University of Petroleum & Minerals*** (KFUPM) and would like to thank all the KFUPM members and graduate students for the friendship they showed during the time of this study. Finally, all my gratitude to my family: my ***mother***, my ***wife***, my ***children,*** all my ***brothers*** and my ***sisters*** for their love, patience, encouragement and prayers.

TABLE OF CONTENTS

LIST OF TABLES

LIST OF FIGURES

ABSTRACT

Full Name **FAHAD ABDULAZIZ AQUL AL-KHALDI**

Title of Study ***REMOVAL OF HEXAVALENT CHROMIUM AND CADMIUM FROM WATER USING CARBON BASED ADSORBENTS***

Major Field **CHEMICAL ENGINEERING**

Date of Degree **JUNE 2011**

This study presents potential application of different forms of carbon including: carbon nanotubes, carbon nanofibers, activated carbon, and fly ash into the removal of some of the high toxic heavy metals that may present in water resources. The study was based on intensive experimental work to measure the removal percentage of hexavalent chromium and cadmium from water under different situations. Therefore, this study was carried out to evaluate the environmental application of carbon in its different forms, through the experimental removal of chromium hexavalent and cadmium divalent ions from water. Five parameters were studied during this experimental work: the pH of solution, the agitation speed, the contact time, the carbon dosage rate, and concentration of the heavy metal in water. Matrix design was developed in this experimental study in order to find the optimal conditions of the Cr (VI) and Cd (II) removal from water. In addition to these four forms of carbon, each form was modified for carboxylic group addition. All the eight forms of carbon used were characterize using filed emission scanning electron microscopy (FESEM) and transmission electron microscopy (TEM) in order to measure the diameter and length of the adsorbent. The results showed that the highest

removal for Cd (II) was observed for the unmodified fly ash with over 95 % removal at pH=7 and agitation speed higher than 150 rpm when allowed in contact for more than 2 hours. In contrast, the highest removal for Cr(VI) was observed for modified AC with almost 100 % removal at pH=3 and agitation speed higher than 200 rpm when allowed for more than 2 hours and for adsorbent dosage higher than 75mg in 100 ml of water. These high removal efficiencies for Cd (II) by fly ash were likely attributed to the strong tendency towards chemical bonding between the Cd (II) ions and metals content of fly ashes. For Cr (VI) removal, the removal efficiencies by AC and modified AC increases significantly with increases in agitation speed from 150 rpm to 200 rpm. This was most likely due to the fact that, the increase of agitation speed, improves the diffusion of chromium ions towards the surface of the AC. The adsorption isotherm plot was well fitted with experimental data. Lastly, it is expected that this project will help finding inexpensive water treatment technology in near future.

THESIS ABSTRACT (ARABIC)

ملخص الرسالة

الإســــــــــــم: فهد بن عبدالعزيز بن عقل الخالدي

عنوان الرسالة: ازالة الكادميوم والكرميوم (6) من الماء باستخدام مواد كربونية ماصة

التخصـــــــص: هندســـة كيميـــــائية

تعرض هذه الدراسة أمكانية أستخدام أنواع مختلفة من الكربون، و تشمل أنابيب النانو الكربونية و الياف النانو الكربونبة و الفحم الصناعي (الكربون النشط) و الرماد الصناعي، في تنقية المياه من المعادن الثقيلة الخطرة على صحة الأنسان . و قد أعتمدت هذه الدراسة على تجارب مكثفة من أجل دراسة مقدار تنقية المياه من هذه المعادن الذائبة تحت تأثير ظروف مختلفة. من خلال هذه التجارب تمت دراسة تأثير خمس متغيرات على مقدار التنقية وهي: حمضية الماء و سرعة الخلط و مدة التنقيع و كمية المادة الكربونية المضافة و تركيز المعادن الذائبة في الماء . و تم تصميم و ترتيب هذه التجارب لتحديد الظروف الأمثل للحصول على أفضل تنقية لأيونات كل من معدن الكادميوم و معدن الكروميوم (6) الذائبة في الماء. وقد تمت دراسة أثر إضافة مجموعة الكربوكسليك على أسطح المواد الكربونية الماصة في مقدار تنقية المياه من هذه المعادن الخطرة . و قد أوضحت النتائج أن أعلى نسبة إزالة لمعدن الكادميوم بلغت 95% و ذلك بأستخدام 50 ملجرام من الرماد الصناعي لكل 100 مللتر من المحلول عند حامضية معتدلة (pH7) و سرعة خلط 150 دورة بالدقيقة. في المقابل فأن أعلى نسبة إزالة لمعدن الكروميوم بلغت 100% و ذلك بأستخدام 75 ملجرام من الفحم الصناعي لكل 100 مللتر من المحلول عند حامضية منخفضة (pH3) و سرعة خلط 200 دورة بالدقيقة. و يمكن إيعاز كفائة ا لرماد الصناعي في تنقية معدن الكادميوم ال ذائب في المياه الى محتوى المعادن الموجود في الرماد الصناعي ال ذي يساهم في مقدار كمية الأمتصاص . و قد لوحظ الزيادة المطردة في كمية إمتصاص أيونات معدن الكروميوم (6) بالفحم الصناعي عند رفع سرعة الخلط من 150 الى 200 دورة في الدقيقة. و هذه الزيادة يمكن تفسيرها بتحسن انتشار أيونات معدن الكروميوم (6) داخل فراغات الفحم الصناعي عند زيادة سرعة الخلط. بأستخدام نتائج التجارب، تم وضع المعادلات الرياضية الممثلة لعمليات الامتصاص الخاصة بكل مادة من المواد المستخدمة. و من المتوقع أن تساهم هذه الدراسة في إيجاد بدائل أقتصادية لمعالجة المياه من المعادن الثقيلة الذائبة في المستقبل القريب. و تقدم الدراسة إمكانية تطبيق بعض التوصيات في المجال تنقية مياه الشرب و المياه المعالجة مما سيساهم في تطوير الأقتصاد الوطني عن طريق زيادة كفائة محطات المعالجة الحالية.

CHAPTER I

INTRODUCTION

1.1 General Introduction

Heavy metals could be very harmful to human health if found in potable water system. Different heavy metals have different effects; but in general they have severe effects to human body including reduced growth, cancer, organ damage, nervous system damage, and may eventually cause death. Prolonged exposure to some metals, such as cadmium and chromium (VI), may also cause kidneys failure and cancer to human body [1].

Currently there are many water treatment technologies that purify water from all kinds of contaminants, including heavy metals. Such water treatments include thermal desalination, membranes, ion-exchange, sedimentation, physical separation and filtration, and many others. Heavy metals are generally removed during the advanced water treatment technologies, such as thermal and membranes; however, when the pollutants concentrations are low or the treatment is required just for removing single pollutant, these treatment technologies become extremely expensive and the requirement to find more cost effective water treatment technologies becomes essential. Two promising alternatives for the selective removal of heavy metals are nano-technology and carbon based waste material such as fly ash.

Nanotechnology is relatively a new field and it is the field that deals with engineering and manipulating matter at the nanoscale (1-100 nm). There is a potential for producing new small scale materials, called nanomaterials that can be used to develop new water treatment methods or enhance the current water treatment technologies. The treatment can range from ground water treatment to produce potable water to more completed treatment of treating wastewater contaminated with toxic metal ions, organic and inorganic solutes, and microorganisms' pollutants. The last decade witnessed a significant advancement in every side of the nanotechnology including the nanoparticles, nanolayers, and nanostructured biological materials. The extensive work on nanotechnology is estimated to continue for the next 20-30 years and it will cover all fields of science and technology [2].

Among the different nanotechnologies available today, special interest was devoted to nanostructures carbon materials. Carbon nanostructure materials received considerable commercial importance since their discovery in 1991 [3]. According to Dresselhaus, Carbon nanotubes (CNTs) and carbon nanofibers (CNFs) are among the most eminent materials in the first rank of the nanotechnology revolution with rapidly growing interest over the last decade [4]. Carbon nanotubes (CNTs) and carbon nanofibers (CNFs) are members of the carbon family with superior properties that make them potentially useful in many applications in nanotechnology including the water. Their properties, including their exceptional mechanical and electrical properties, highly chemical stability, and large specific area, have attracted considerable researchers' interest [5]. The research in this exciting field has been in continuous evolution for application in almost all science and engineering fields [6]. New development in nanotechnology could play a major rule in resolving issues

relating to today problems and current technologies' limitations including the problem of water shortage and water quality.

The other promising alternative for the low cost water treatment technology is the use of fly ashes. One of the fly ashes recent applications is water treatment to remove inorganic and organic pollutants. Fly ash is one of the residues generated in the combustion process of coal and liquid fuels, and represents the fine particles that rise with the flue gases. The fly ash contains many materials based on the fuel used and combustion conditions. Fly ash content of unburned carbon can vary significantly from as high as 90% by weight [7] to just traces of hydrocarbons. High content of unburned carbon can be expected when heavy liquid fuel is used; however, for coal the major components of the fly ash are number of oxides such as silicon, aluminum, iron and calcium with traces of other heavy metals.

Fly ash is being used as an additive to Portland cements to increase the cement resistance to corrosion. Another commonly use for coal fly ash is as filler for building projects in the construction industry. The lightweight property of fly ash makes it important part of concrete used in construction projects such as bridges. When demand for cement decreases, the uses of fly ash in application such as land fill and as a soil stabilizer and improving agent, become an option by civil engineering to help satisfying the growing social interest for recycling and reuse of natural resources [8].

Recent researches concluded that fly ash has a superior adsorption property for heavy metals that can be used in remediation of polluted water [9]. The fly ashes produced in Saudi Arabia and other GCC’s members are mostly heavy fuel oil based sly ashes;

therefore, unlike the coal fly ash, the unburned carbon content in these ashes is expected to be high. This could make them good adsorbent agents for use in water treatment and other chemical engineering application fields.

1.2 Significance of Study

Carbon based adsorbents can provide an environmental solution to water and wastewater treatment. Activated carbon and nano-carbons have been evaluated for heavy metals removal; however, this study evaluated the effectiveness of four different carbon based adsorbents for the removal of heavy metals, at low initial concentrations, from water. These four adsorbents are activated carbon, CNTs, CNFs, and fly ashes. Treatment of water or waste water with low initial concentrations of heavy metals is the challenge to face when considering cost effective treatment technologies.

In addition, there are limited researches in uses of fly ashes as adsorbent agent for heavy metals removal from water; however, the fly ashes used in these limited studies are of significant difference from the fly ashes available in this region. Therefore, this study should break a new ground in water and wastewater treatment by using the fly ashes generated locally and helps achieving the growing social interest for recycling and reuse of natural resources in this region.

Moreover, metals normally forms complex compounds in water that are soluble at different water conditions. Therefore, this study evaluated the heavy metals removal for two different heavy metals with two different ionic charges: cadmium (Cd^{2+}) and chromium (VI) primarily present in water as chromate (CrO_4^{2-}) and dichromate

($Cr2O_7^{2-}$) ions [10]. These two different forms of metals ions provide a wider spectrum that helps better understanding the adsorption of heavy metals by these four carbon based adsorbents.

1.3 Objective of the Study

The objective of this work of research is to find an economical alternative for the remediation of contaminated water and wastewater, with initial low concentration of heavy metals contaminants. This objective can be summarized per the following:

1. Introduce liquid fuel fly ash as a new adsorbent for heavy metals removal.
2. To remove cadmium and chromium (VI) by using:
    a. CNTs.
    b. CNFs
    c. Activated Carbon
    d. Locally produced Fly Ashes
3. Modify the above four carbon based adsorbents with the addition of carboxylic group (COOH) to improve the removal efficiency.
4. To optimize the process parameters such as pH, dosage of adsorbents, agitation speed and contact time in order to maximize the removal of cadmium and chromium (VI).

5. To study the adsorption isotherms those describe the distribution of the adsorbate species between liquid and adsorbents using different models such as Langmuir and Freundlich adsorption isotherms.
6. To study the sorption kinetics that describes the adsorbate uptake rate. This rate evidently controls the residence time of adsorbate at solid liquid interface.

CHAPTER II

LITERATURE REVIEW

2.1 Carbon Nanotubes

2.1.1 What is Carbon Nanotubes

Carbon has the property to exist in many molecular forms, known as allotropes of carbon. These allotropes can be considered as different structural modifications of carbon element [11]. Carbon nanotubes (CNTs) are allotropes of carbon described as a rolled-up tubular shell of graphene sheets. These graphene sheets are made of benzene-type hexagonal rings of carbon atoms as can be seen in Figure 2.1.1. Figure-2.1.1 shows a graphene sheet made of C atoms (a) placed at the corners of hexagons forming the lattice with arrows AA and ZZ denoting the rolling direction of the sheet to make (b) a (5,5) armchair nanotube and (c) a (10,0) zigzag nanotube [12].

CNTs were discovered in 1991 by Sumio Ijima of NEC Laboratory in Tsukuba, Japan, using arc-discharge method and they were characterized by High-Resolution Transmission Electron Microscope (HRTEM) [5]. Chemical bonding in nanotubes is best described by Applied quantum chemistry, specifically, orbital hybridization. "The chemical bonding of nanotubes is composed entirely of sp2 bonds, similar to those of graphite. These bonds, which are stronger than the sp3 bonds found in alkanes, provide nanotubes with their unique strength. Moreover, nanotubes naturally align themselves into "ropes" held together by Van Der Waals forces" [13]. The reported

nanostructure cylindrical shape was found to have length-to-diameter ratio of up to 132,000,000:1, significantly larger than any other material [12].

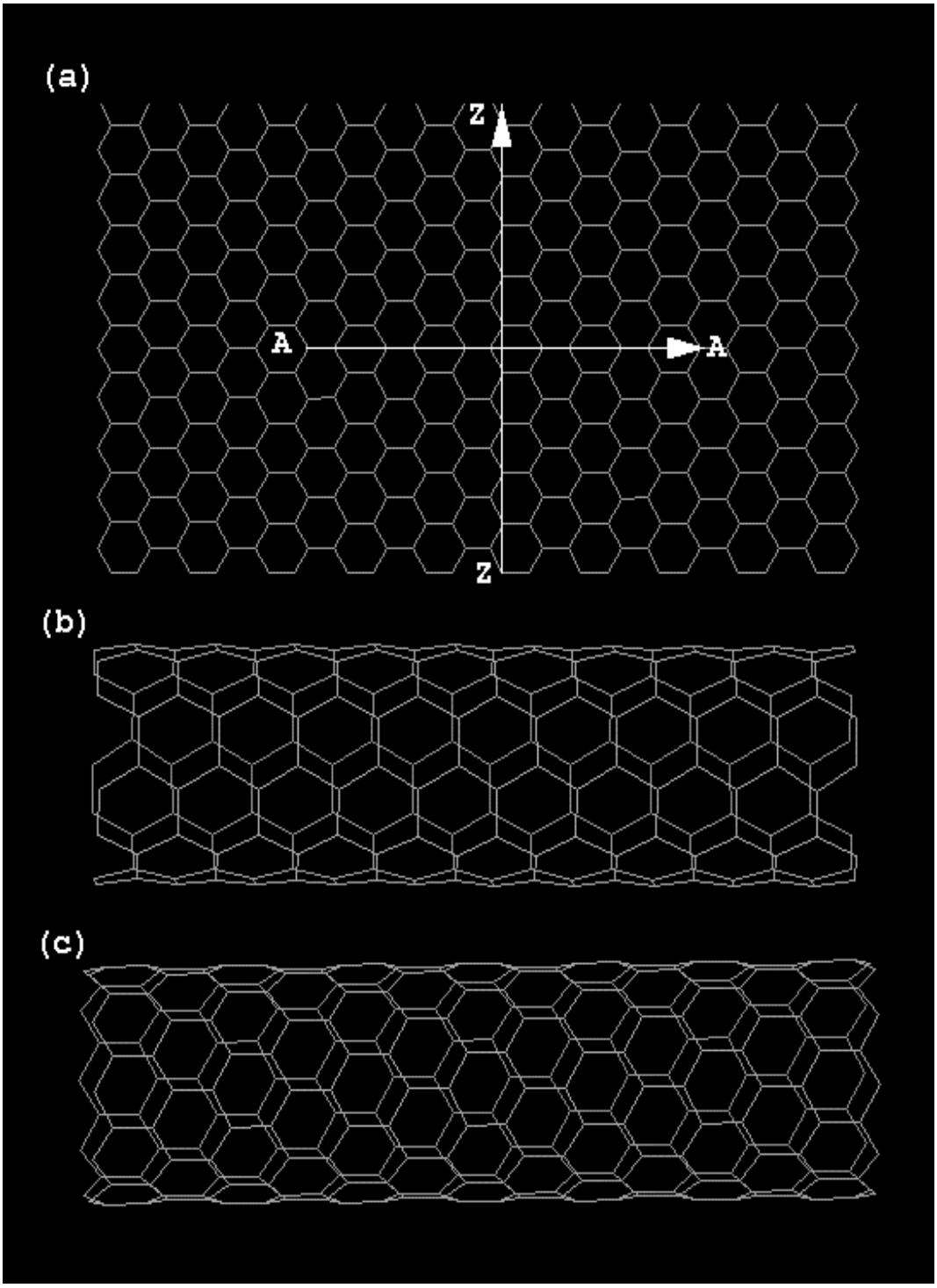

Figure 2.1.1: CNTs made of graphene sheet of C atoms

CNTs form bundles of highly complex network. They can have electrical conductivity based on the arrangement of the hexagonal rings along the tubular surface; CNTs can become metallic or semiconducting. Due to their extraordinary properties, such as large geometric aspect ratio, nanocavities, and electrical conductivity, CNTs can be considered as attractive candidates in many nanotechnological applications, including the water treatment. One drawback with CNTs is the fact that they lack solubility in solvents and this in turn has imposed great limitations to the use of CNTs in industry [14]. Alternatively, CNTs can be dispersed in some solvents by sonication or though some chemical reactions that add some functional groups to make them soluble into inorganic and organic solutions.

2.1.2 Types of Carbon Nanotubes

Nanotubes can be categorized into two types: single-walled carbon nanotubes (SWCNTs) and multi-walled carbon nanotubes (MWCNTs). SWCNTs have a diameter close to 1 nanometer with a tube length that usually in micrometers but can reach few centimeters to 18 centimeters in length (as reported by Wang) [12]. As explained on Figure 2.1.1, the structure of a SWCNT can be conceptualized as a rolled-up tubular shell of graphene sheet to form seamless cylinder. This way, the graphene sheet can produce one of the following three types of SWCNTs [2]:

(a) Zig-Zag Single-Walled Nanotube.

(b) Chiral Single-Walled Nanotube.

(c) Armchair Single-Walled Nanotube.

As illustrated in Figure 2.1.2, a single nanotube is usually characterized by its diameter d_t and the chiral angle θ ($0 \leq |\theta| \leq 30°$). The chiral vector C_h is defined by

two integers (n, m) and they are the basis vectors of the graphene sheet [2, 4, 15]:

$$C_h = n*a_1 + m*a_2 \quad (1.1)$$

where a_1 and a_2 are unit vectors in the two-dimensional hexagonal lattice.

Another important parameter is the chiral angle, which is the angle between C_h and a [16]. When m = 0, the zig-zag pattern around circumference is obtained; whereas Chiral SWCNTs are formed by twisting of hexagons around tubule body. And finally, the armchair SWCNTs are chair-like pattern around circumference and it is formed when n = m.

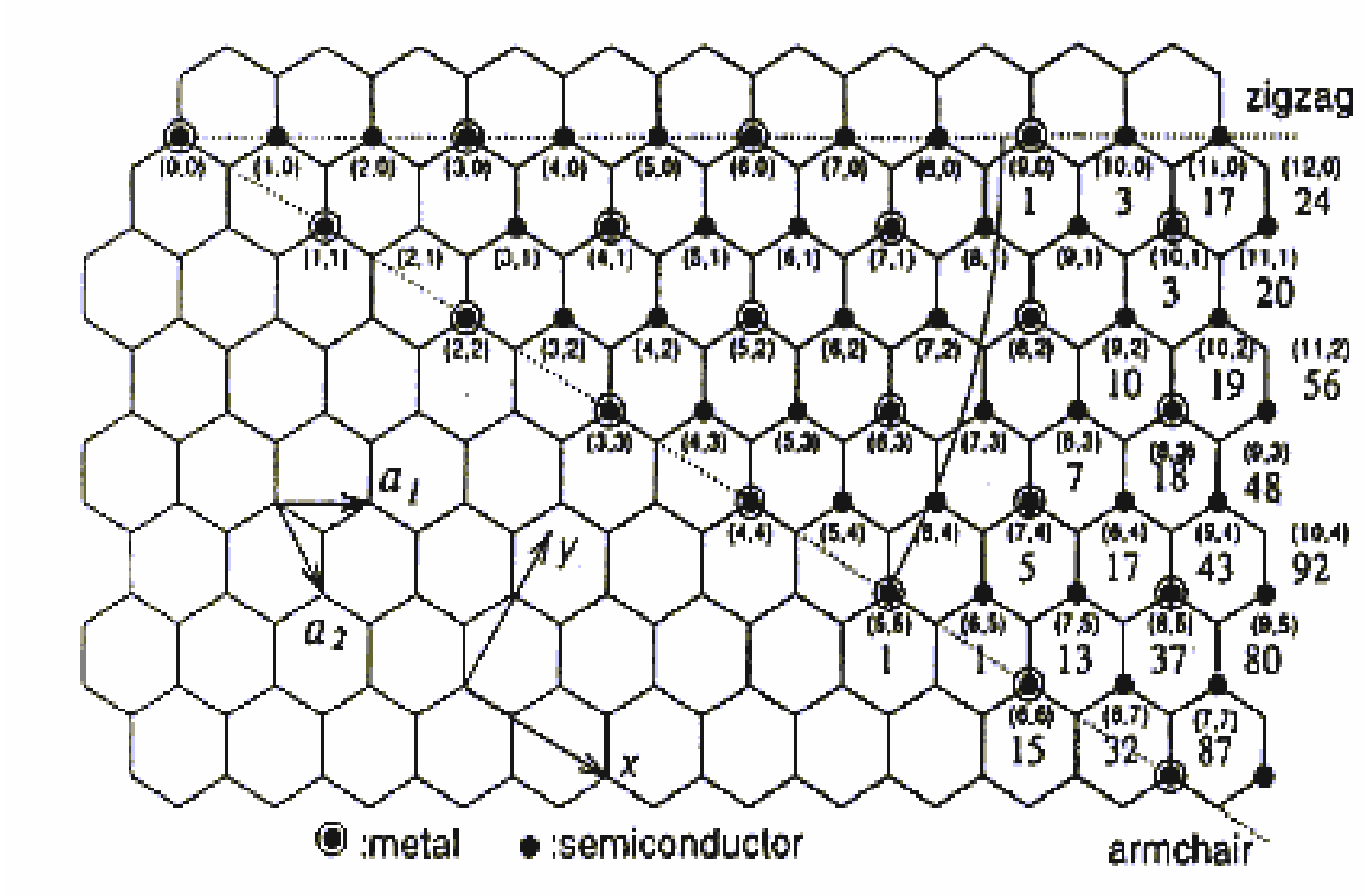

Figure 2.1.2: Diagram showing rolling direction of nanotube [4].

Using Figure 2.1.2, the carbon nanotube diameter and chiral angle can be determined by the following equations:

$$d_t = \frac{1}{\pi}\sqrt{n^2 + m^2 + nm}, \qquad \sin\theta = \frac{\sqrt{3}m}{2\sqrt{n^2 + m^2 + nm}}$$

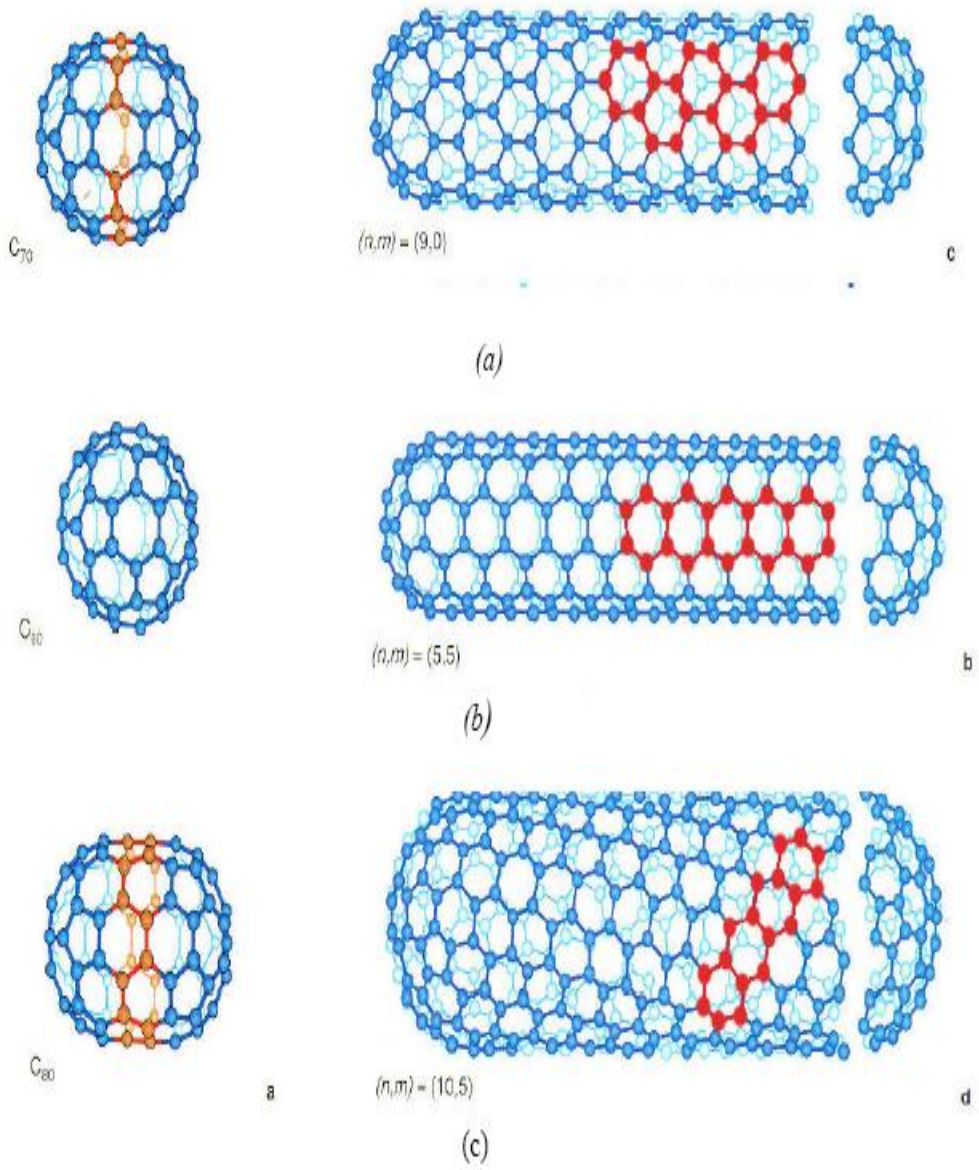

Figure 2.1.3: Types of CNT:
(a) Zig-Zag Single-Walled Nanotube. (b) Chiral Single-Walled Nanotube. (c) Armchair Single-Walled Nanotube. [2].

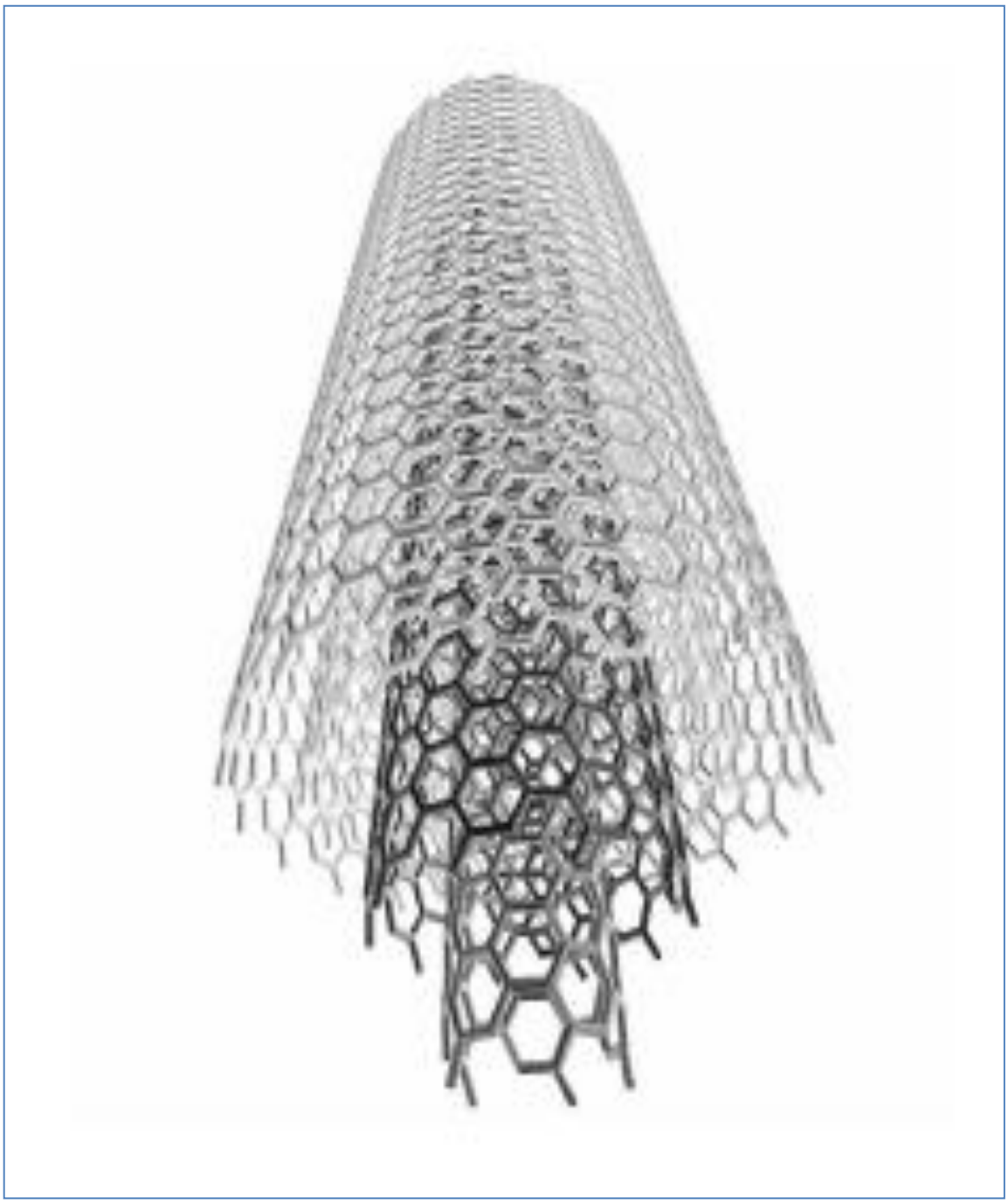

Figure 2.1.4: Schematic theoretical model for multi-walled 3 carbon nanotubes. [12]

Multi walled carbon nanotubes (MWCNTs) are a collection of concentric SWCNTs with different diameters. They can be looked as more than one graphene cylinder inserted one into another (Figure 2.1.4). The length and diameter of these structures

differ a lot from those of SWCNTs and their properties are also very different. The first production of (MWCNTs) was developed in 1992 by Ebbesen and Ajayan [17]. By using image of TEM with high resolution, the spacing of intershell was found to be approximately 0.34 nm [17]. Based on TEM images, the interlayer separation of d = 3.4 Å is commonly reported for MWCNT.

2.1.3 Properties of Carbon Nanotubes

The carbon nanotubes properties can be divided into the following:

Mechanical Properties: Due to the covalent sp^2 bonds formed between the individual carbon atoms, CNTs are considered the strongest and stiffest materials on earth, in terms of tensile strength and elastic modulus respectively. Experimental and theoretical results have shown that CNTs has an elastic modulus of greater than 1 Tpa, which is 10–100 times higher than the steel at a fraction of the weight [18]. Table 2.1.1 shows a comparison between CNTs and some materials that are known to have strong elastic modulus:

Thermal properties: carbon nanotubes are reported to have good thermal conductivity measured from 4 to 300 K [19] similar to that of graphite. Similar behavior was also observed in the measurements of the temperature-dependent thermal conductivity of bundles of SWCNTs from 8 to 350 K [20].

Table 2.1.1 : Mechanical properties of carbon nanotubes

Material	Young's modulus (GPa)	Tensile strength (GPa)	Density (g/cm3)
SWCNT	1054	150	2.6
MWCNT	1200	150	2.6
Steel	208	0.4	7.8
Epoxy	3.5	0.005	1.25
Wood	16	0.008	0.6

Electrical properties: As shown in Figure 2.1.3, above, based on the carbon nanotubes structure, zig-zag, chiral, or armchair, the CNTs can be metallic or semiconducting. When they are produced as electrically conductive, they exhibit superior and unique electrical properties. Conductive CNTs are found to carry electric current 1000 times higher than copper wires [21]. For a given (n,m) nanotube, if the difference between n and m is a multiple of 3, then the nanotube is metallic, otherwise the nanotube is a semiconductor. As explained above, all armchair (n=m) nanotubes are metallic, and nanotubes with n-m greater than 3 are semi-conducting .

Chemical reactivity: Carbon nanotubes can undergo chemical reactions that make them more soluble in inorganic, organic, and biological solutions. CNTs reactivity is directly related to the π-orbital mismatch caused by an increased curvature. Therefore, a distinction must be made between the sidewall and the end caps of a nanotube. For the same reason, a smaller nanotube diameter results in increased reactivity. Covalent chemical modification of either sidewalls or end caps has shown to be possible [22].

According to Dimitrios, the modification of CNTS is categoriesed in to three classes [14]:

(a) Covalent attachment of chemical groups through reactions onto the π-conjugated skeleton of CNTs;

(b) Noncovalent adsorption of various functional molecules

(c) The endohedral filling of their inner empty cavity.

Some of the CNTs reactivity includes:

1. *Sidewall Halogenation of CNTs*:

   Dimitrios reported that CNTs grown by the arc-discharge or laser ablation methods have been fluorinated by elemental fluorine (Figure 2.1.5). Accordingly, the sidewall carbon atoms on which F atoms are attached are tetrahedrally coordinated and adopt sp3 hybridization. This reaction destroys the electronic band structure and turn CNTs to become insulating material [14]. In addition, fluorinated nanotubes were reported to have a moderate solubility of approximately 1 mg/mL in alcoholic solvents [23]. However, the fluorination reaction can be used to facilitate further substitution, whereby different functional groups, such as alkyl groups, could replace the fluorine atoms and turn the CNTs soluble in organic solvents [24-26]. Similar reaction can be also performed to turn CNTs soluble in aqueous solutions.

2. *Hydrogenation of CNTs*:

Hydrogenated CNTs were found to have a stoichiometry of $C_{11}H$. This low ratio of hydrogen was found to reduce CNTs stability to 400 °C and causes disorder of the nanotube walls.

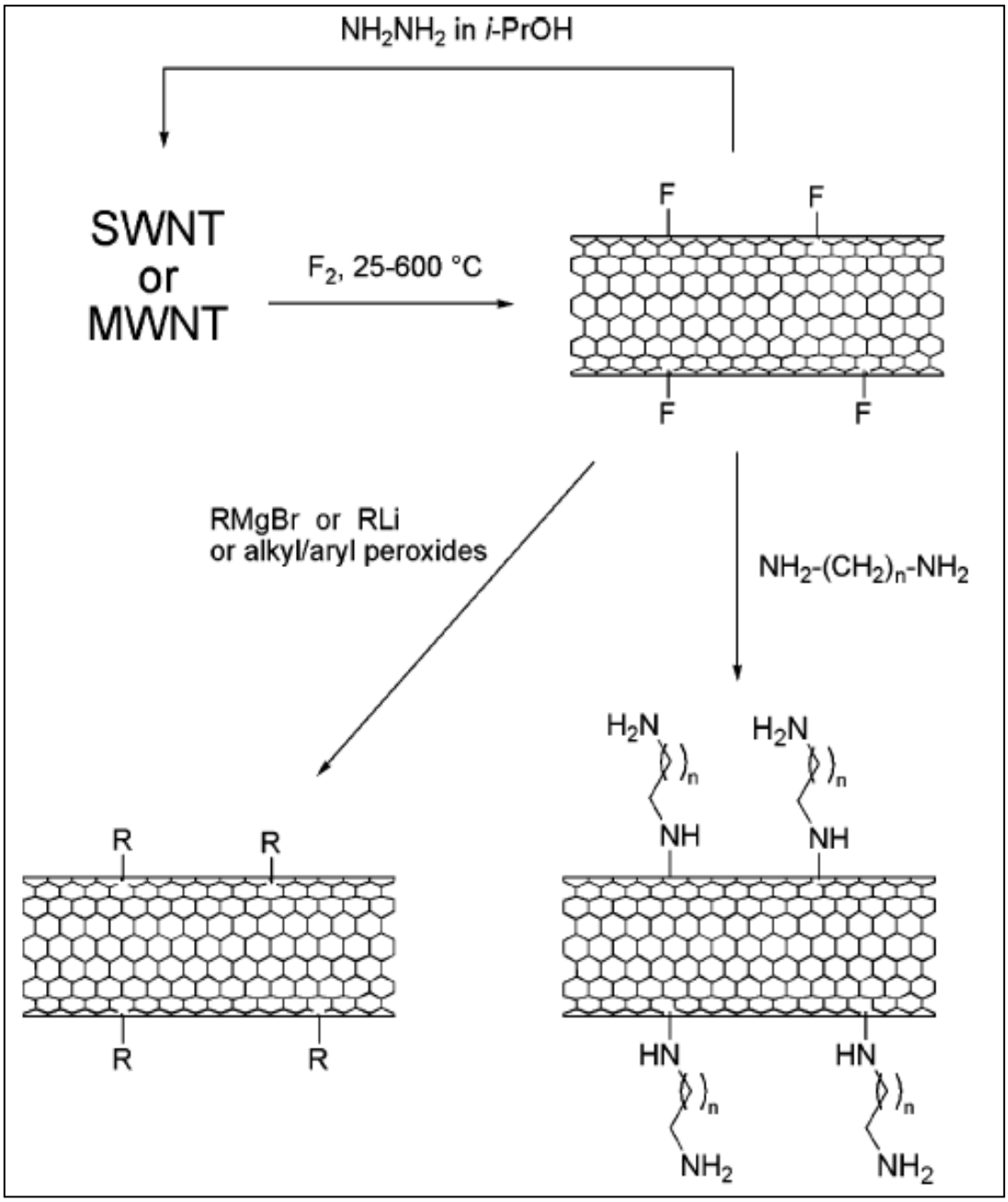

Figure 2.1.5: Reaction scheme for fluorination of nanotubes, defunctionalization, and further derivatization[14].

3. *Ozonolysis of CNT*:

Ozonolysis is well-known chemical process whereby ozone is used to break the carbon-carbon double and triple bonds in alkene and alkyne to form organic compounds in which the multiple carbon-carbon bonds is replaced by a double bond to oxygen [27]. The outcome of the reaction depends on the type of multiple bonds being oxidized by ozone and the chemical process conditions. For CNTs, when subjected to ozonolysis reaction at -78 °C and at room temperature, the products were found to be CNT-ozonides [14]. CNTs also react with hydrogen peroxide or sodium borohydride, through similar ozonolysis process, to produce a high proportion of carboxylic acid/ester, ketone/aldeyde, and alcohol groups on the nanotube surface [14]. This process increases the chemical reactivity of the carbon nanostructures due to the availability of carboxylic groups on the sidewalls and tips of the carbon nanotubes. Banerjee et al. [28] found that smaller diameter nanotubes will have greater strain energy per carbon atom due to increased curvature and higher rehybridization energy.

4. *Acid Oxidation of CNT*:

Ivanov et al. [29] reported that acid oxidation induces the opening of the carbon nanotube caps as well as the formation of holes in the sidewalls to produce nanotube fragments with lengths below 1 μm. The new fragments are short CNTs with ends and sidewalls are decorated by oxygenated functionalities, mainly carbonyl and carboxylic groups. This modification is of interest to this work of research. The chemical reactivity and properties of

oxidized CNTs have been studied by many researchers as will be shown throughout this work of research.

5. *Grafting of Polymers*:

   Grafting of polymers is a process by which a side chain is introduced to the main polymer chain. The covalent reaction of CNTs with polymers is an important process because adding polymer chains to many different substances, such as CNTs in this case, helps dissolving these substances into a wide range of solvents. In polymer industries, there are two main methodologies for the covalent attachment of polymeric substances to the surface of CNTs: grafting-to and grafting-from. In the first method, the polymer is first synthesized with a specific molecular weight followed by end group transformation; then, this polymer chain is attached to the wall-side of the CNTs. In contrast, the second method is based on attaching the polymer precursors on the surface of the nanotubes and then the subsequent propagation of the polymerization in the presence of monomeric species starts [14]. Each method produces different grafted polymers with different properties.

Based on above discussed properties, CNTs and modified CNTs are extremely promising for future applications including environment protection, materials science, medicinal chemistry, and many others.

2.1.4 Production of Carbon Nanotubes

There are many techniques to produce carbon nanotubes; however, the three widely used today are:

1. *Arc Discharge Method*

   Arc Discharge method produces CNTs in low pressure of He gas or any other neutral atmosphere [20]. This method is the method in which carbon nanotubes were first discovered by Ijima in 1991. Figure 2.1.6 illustrates the Arc Discharge method.

   This is the most common, simplest, and perhaps easiest way to produce carbon nanotubes; however, it produces a mixture of nanotubes, soot and the catalytic metals present in the crude product and require purification to obtain clean CNTs. Arc Discharge method produces nanotubes through arc-vaporisation of two carbon rods separated by approximately 1mm in an enclosure that is usually filled with inert gas, such as helium or argon, at pressure range of 50 to 700 mbar [17].

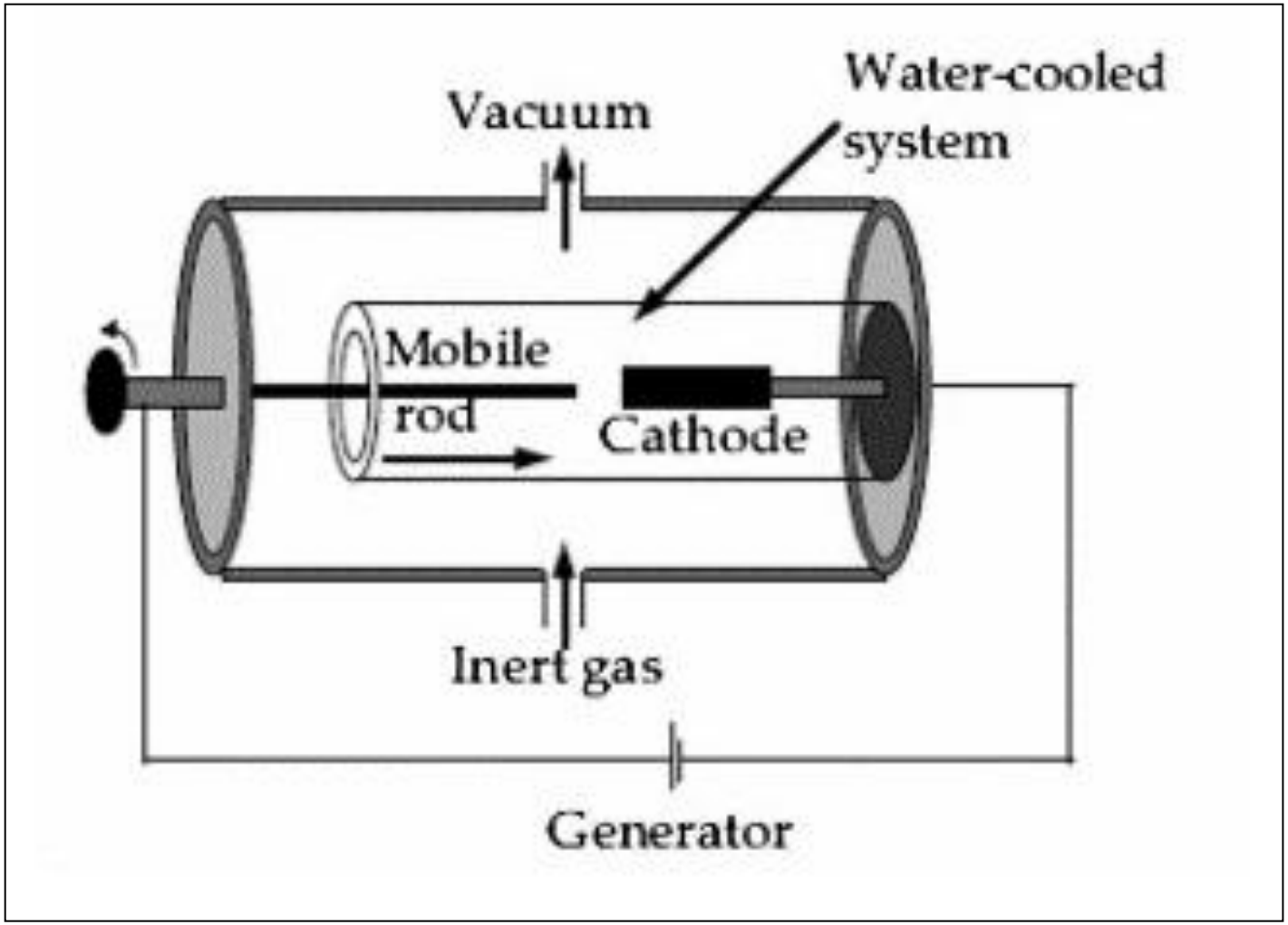

Figure 2.1.6: Experimental setup of an arc discharge apparatus [20]

1. *Laser Ablation Method*

In 1995, Richard Smalley and co-workers at Rice University reported the synthesis of carbon nanotubes by lasers group vaporisation. Richard used laser beams to vaporise a graphite target in an oven at 1200 °C [30]. Currently there are two types of laser method: continuous and pulse. The main difference between the two methods is that the pulsed laser demands a much higher light intensity of 100 kW/cm2 compared to 12 kW/cm2 for the continuous laser method.

The nanotubes produce by Laser Ablation Method is collected on the cooler surfaces of the reactor as the vaporized carbon condenses. This method produces MWCNTs when pure graphite electrodes are used. However, when nanoparticals catalyst, such as Co, Ni, Fe, are added SWNTs are formed (Journet and Bernier, 1998). An illustration for this method is shown in Figure 2.1.7

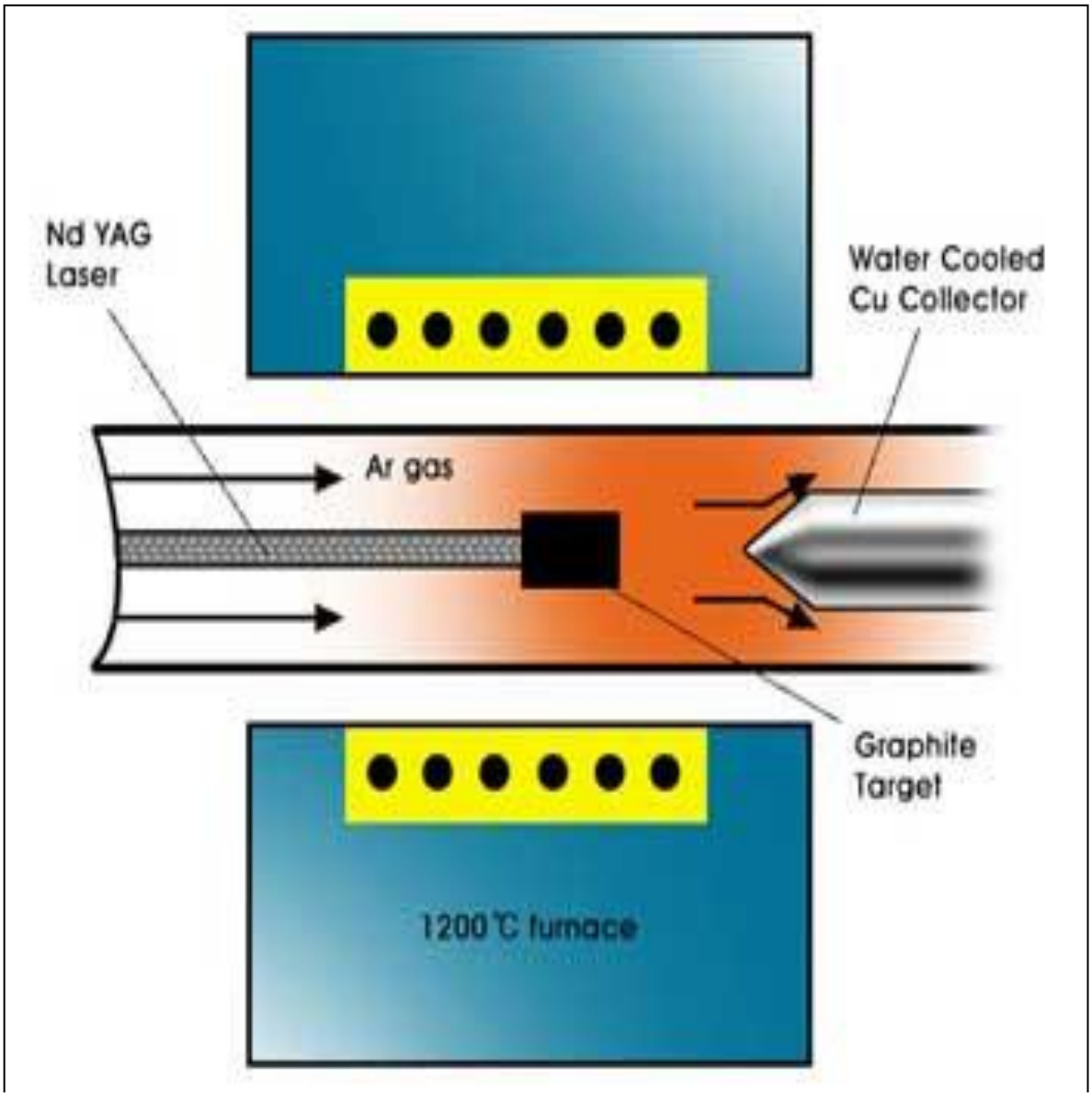

Figure 2.1.7: Schematic drawing of a laser ablation apparatus

2. *Chemical Vapor Deposition (CVD)*

Chemical Vapor Deposition method is a simple process and is believed to be the easiest method to scale up to industrial production. It has many variables that provide the producer with enough controlling parameters to produce the desired CNTs quality. CVD is essentially a two-step process consisting of a catalyst preparation step followed by the actual synthesis of the carbon nanotubes.

A carbon source in gaseous phase, such as methane and carbon monoxide, passes over an energy source to crack the molecule into reactive atomic carbons. Then, these active carbon atoms diffuse over substrate, which is heated and coated with a catalyst, to produce the CNTs. The process takes place at high temperature range of 500 to 1000 ^{o}C. Therefore, this process involves dissociation of hydrocarbon molecules to form active carbon atoms, then these active atoms are catalyzed by the transition metal to achieve the required saturation of carbon atoms in the metal nanoparticle [32]. Figure 2.1.8 shows the simplest CVD process.

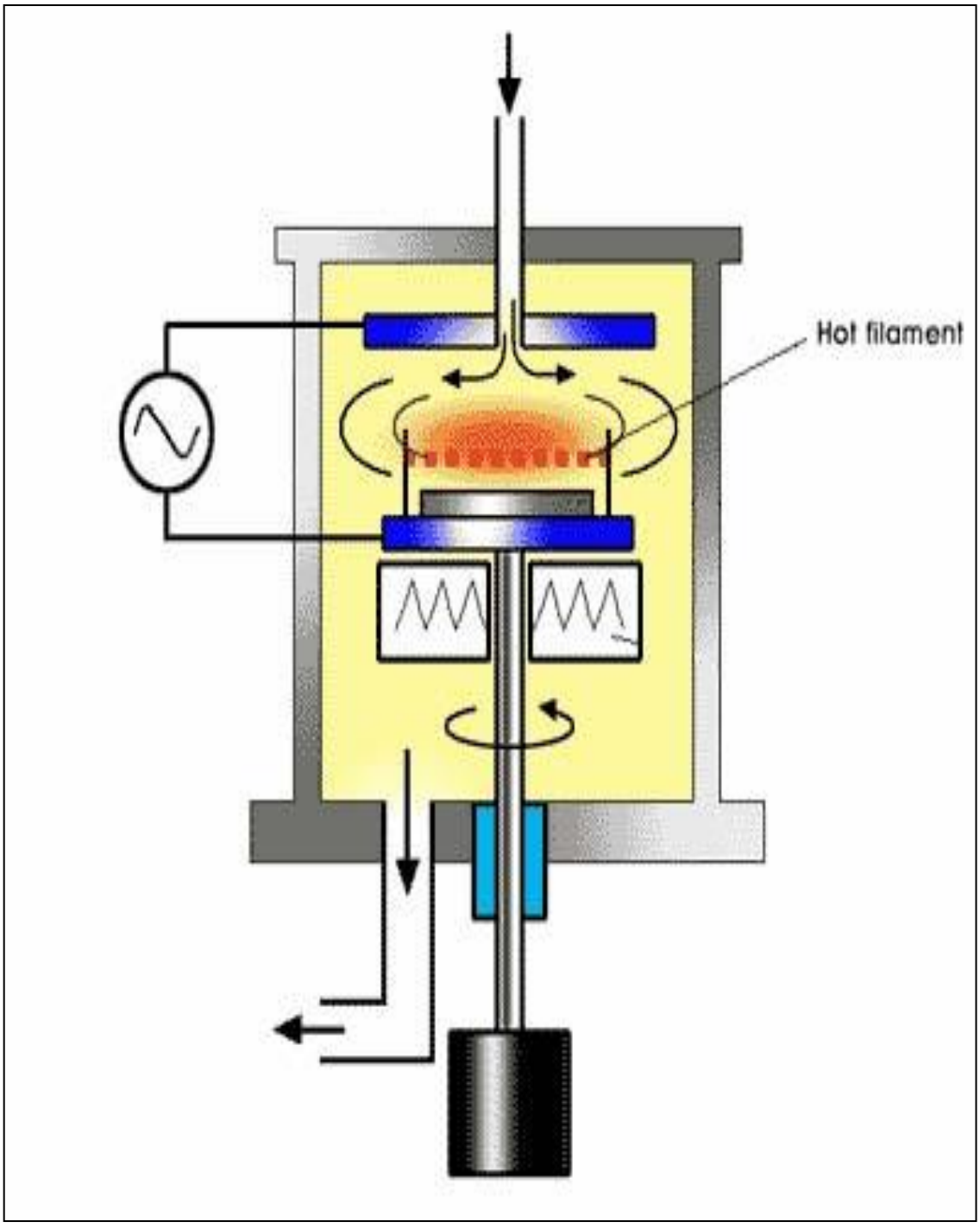

Figure 2.1.8: A schematic diagram of a plasma CVD apparatus

Table 2.1.2 compares the three methods in term of CNTs production efficiency, type of CNTs produced, and the current drawback of each technology.

Table 2.1.2: A summary of the major production methods and their efficiency

Technology	Arc discharge method	Chemical vapor deposition	Laser ablation (vaporization)
Typical yield	30 to 90%	20 to 100%	Up to 70%
SENT	Short tubes Diameters: 0.6 to 1.4nm	Long tubes Diameters: 0.6 to 4 nm	Long bundles of tubes Diameters:1 to 2 nm
MINT	Short tubes Inner diameter:1 to 3nm Outer diameter: ~10 nm	Long tubes with Diameters:10 to 240 nm	Not suitable Too expensive
Concerns	Short Tubes with random sizes and directions. Needs purification.	Nets are usually Mints and often riddled with defects.	Costly due to expensive lasers and high power requirement.

2.2 Carbon Nanofibers

2.2.1 What is Carbon Nanofibers

Carbon nanofiber is another allotropes of carbon family. Carbon nanofibers (CNFs), or sometimes called vapor grown carbon fibers (VGCFs) or vapor grown carbon nanofibers (VGCNFs), are cylindrical shaped nanostructures of graphene layers arranged in one of the following geometric forms: stacked cones, cups or plates. In

1950, the first carbon nanofibers were reported by two Soviet scientists, Radushkevich and Lukyanovich, who succeeded to show hollow graphitic carbon fibers with 50 nanometers in diameter [33]. Early in the 1970s, Koyama and Endo succeeded in the manufacturing of VGCF with a diameter of 1 μm and length of above 1 mm [34].

However, the start of commercialized production of CNFs was attempted by the Japanese company Nikosso in 1991 [35], which is the same year Ijima reported the discovery of Carbon Nanotubes (CNTs) [5]. Today, several companies produces CNFs, in a commercial scale production, and many research centers are involved in finding new engineering applications for these materials intensively. One of the Carbon Nanotubes recent interested applications is the use as a porous composite for oil spill remediation [36].

2.2.2 Types of Carbon Nanotubes

Nanofibers consist of the graphite sheet completely arranged in various orientations with 5 to several hundred microns on length and between 100- 300 nm in diameter [37]. There is currently no distinguished definition for the different type of carbon nanofibers produced; however, carbon nanofibers can be described by defining the sequence of the events leading to the formation of carbon nanofibers on hand. With the use of electronic microscopy studies, it is possible to identify these sequences. Figure 2.2.1 shows two possible ways to arrange the graphite platelets. In Figure 2.2.1 (a), the graphite platelets are aligned in directions perpendicular to the fiber axis; whereas in the second arrangement, Figure 2.2.1 (b), they are arranged parallel to the fiber axis. Parameters such as the choice of the catalyst, the ratio of the

carbon source to hydrogen gas, and all other reaction conditions, influence the morphological qualities, the degree of crystalline and the orientation of the precipitated graphite crystallites with regard to the fiber axis. One more factor that can change the type of CNFs is the distance between graphite. In regular CNFs, the separation space between CNFs layers is 0.34 nm. By introducing selected functional groups between the CNFs' layers, the spacing between layers can be increased generating new types of sophisticated molecular sieves. This pacing process is known as "intercalation" and it produces numerous numbers of new materials [38].

2.2.3 Properties of Carbon Nanofibers

The chemical reactions applied to CNTs are expected to have similar behavior when applied to CNFs due to the availability of the π-orbital. However since the CNFs are considerably flat sheet of graphene. The reactivity of CNFs is expected to be less than the chemical reactivity of CNTs due to the lack of π-orbital mismatch caused by an increased curvature in the CNTs case. Unlike CNTs, CNFs have no caps and all reactions are on the sidewall.

Similar to CNTs, the modification of CNFs is categoriesed into three classes [14]:

(a) Covalent attachment of chemical groups through reactions onto the π-conjugated skeleton of CNTs;

(b) Noncovalent adsorption of various functional molecules

(c) The endohedral filling of their inner empty cavity.

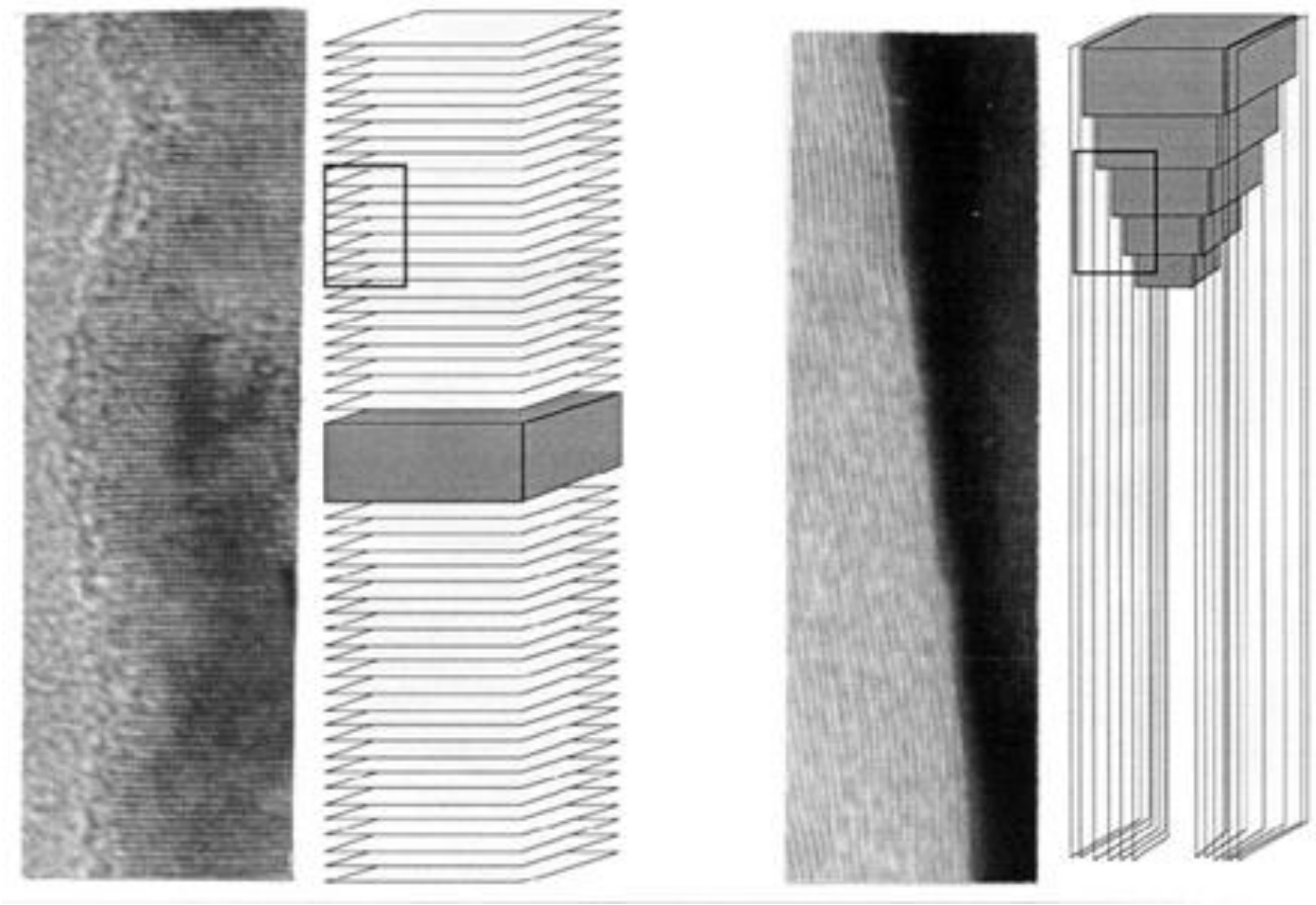

(a) (b)

Figure 2.2.1: High resolution electron micrographs of CNFs: (a) "perpendicular" and (b) "parallel" to the fiber axis

One more feature of CNFs reactions, is the possibility to control the spacing between the CNFs layers by the intercalation process, as explained earlier, to produce selective of new materials with sophisticated molecular sieves that can be used in different applications [38].

2.2.4 Production of Carbon Nanofibers

The production methods described under CNTs production can also be applied to produce CNFs with exception all reactions are catalytic reactions. Chemical Vapor Deposition could be considered the most suitable production process, since this process involves catalyst preparation stage and carbon source is required to form the required CNFs quality.

CNFs production mechanism can be explained by the sequences shown in Figure 2.2.2. The first step starts by absorption of the hydrocarbon on the catalytic metal surface, shown as (A). When the required conditions for the scission of a carbon-carbon bond exist, carbon molecules are formed. In the next step, the atomic species dissolve in the particle (B) and diffuse to the rear faces. Next, these species precipitate at the interface (C) to form a carbon nanostructure. The produced CNFs (D) depends on the composition of the reactant gases and the reaction temperature.

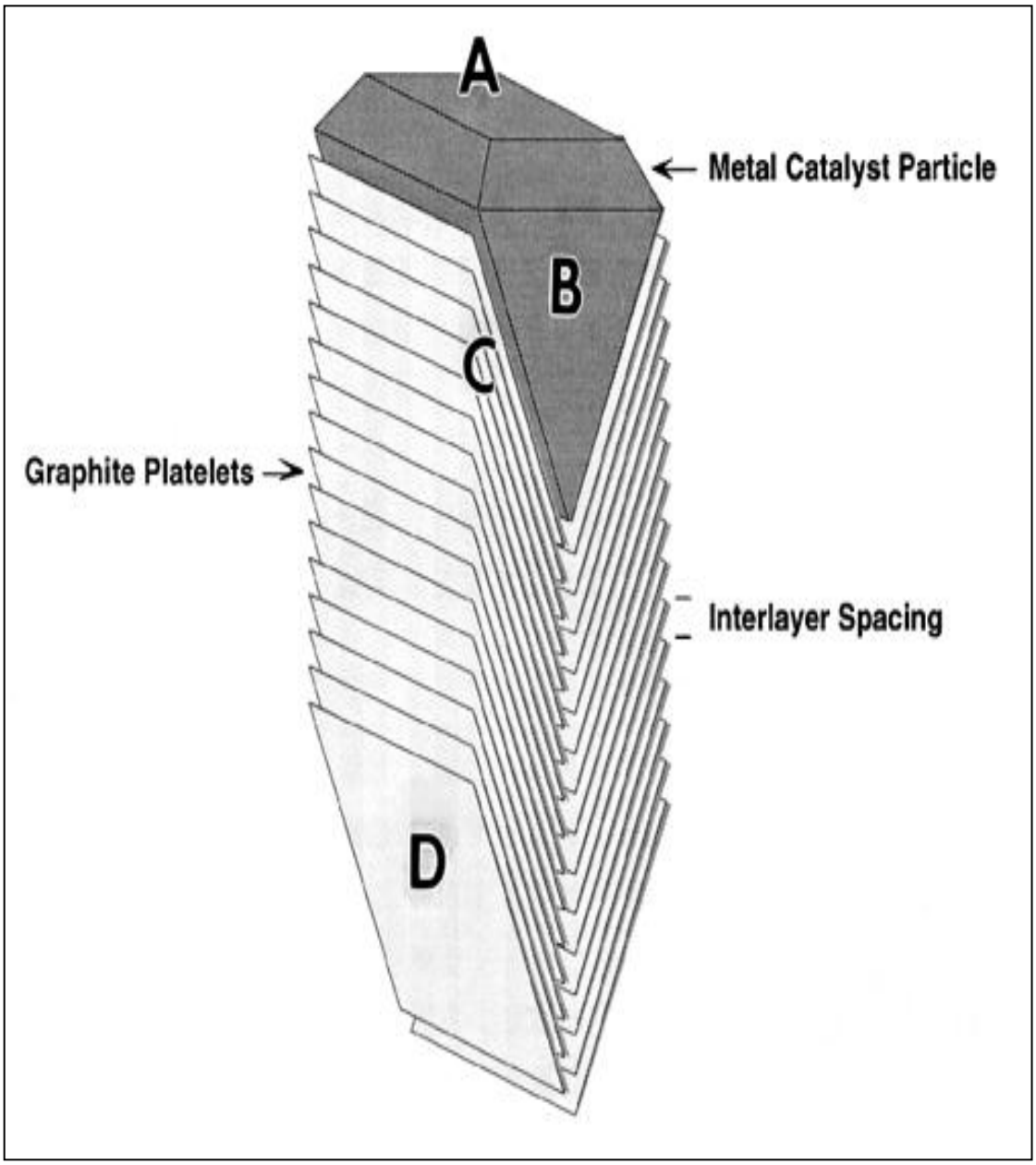

Figure 2.2.2: Schematic diagram of a catalytically grown carbon nanofibers

2.3 Activated Carbon

2.3.1 What is Activated Carbon

Activated carbon is another allotropes of carbon family. It is a pure carbon in graphite form with amorphous and highly porous structure. Activated carbons contain wide range of different pore sizes starting from visible cracks to slits of molecular dimensions [39]. The powdered activated carbon was first produced commercially from wood, as a raw material, in the early 19th century. The use of activated carbon for water taste and odor control was first reported in 1930 [40]. Today, active carbon is produced from many different raw materials including: coconut shells, wood, refineries coke, carbon black, rice hulls, sugar, and from almost all organic materials. The high surface area is the major feature of activated carbons that makes theses material good for adsorption processes. Other factors that give activated carbons the adsorptive properties are their micro-porous structure and the fact that activated carbons have high degree of surface reactivity.

2.3.2 Types of Activated Carbons

Activated carbon can be classified based on their properties, which they obtained during the activation process. Therefore, we may classify activated carbon based on the activation process to the following two main categories:

1. Physical or thermal activation: this activation process involves carbonization at raw materials at temperature of 500 ^{o}C to 600 ^{o}C [41].

2. Chemical activation: this type of activation involves the addition of some

inorganic additives, such as metallic chlorides, to activated carbons surfaces [42].

Steenberg [43] suggested another classification, which classify activated carbon as acidic and basic activated carbons. According to Steenberg:

1. Carbon activated at low temperature range of 200 ^{o}C to 400 ^{o}C develops acidic surface oxides that lower pH value of the solution. These types of activated carbons are usually adsorbing basic or hydrophilic species and exhibit a negative zeta potential.

2. In contrast, carbons activated at high temperature range of 800 ^{o} to 1000 ^{o}C develop basic surface oxides and they increase the pH value of the solution. In this case, these activated carbons adsorb acids and exhibit a positive zeta potential.

In commercial basis, the activated can be classified as [44]:

1. Powdered activated carbon (PAC): These are powders or fine granules less than 1.0 mm in size with an average diameter between .15 and .25 mm.

2. Granular activated carbon (GAC): Good for gases adsorption and comes with different sizes.

3. Extruded activated carbon (EAC): Combines powdered activated carbon with a binder into a cylindrical shaped activated carbon block with diameters from 0.8 to 130 mm. These are mainly used for gas phase applications.

4. Impregnated carbon: This type of activated carbon is porous carbons impregnated with different inorganic ions.

5. Polymer coated carbon: this type of activated carbon has application in medical fields

2.3.3 Properties of Carbon Nanotubes

Activated carbon is another form of graphene sheets (Figure 2.2.3) connected together through numerous networks of benzene rings. Therefore, the existing of π-orbital in carbons rings enable activated carbon to accept many modifications.

For instances, the positive zeta potential for the basic activated carbons can be altered to negative value by cooling the activated carbons in presence of oxygen due to the formation of acidic surface oxides.

Activated carbon used for years in adsorption processes. Today, it is rarely to find an industry without activated carbon is used in the filtration and purification treatment. In water treatment for instances, activated carbons are used to control taste and odor and to adsorb undesired suspended metals [40].

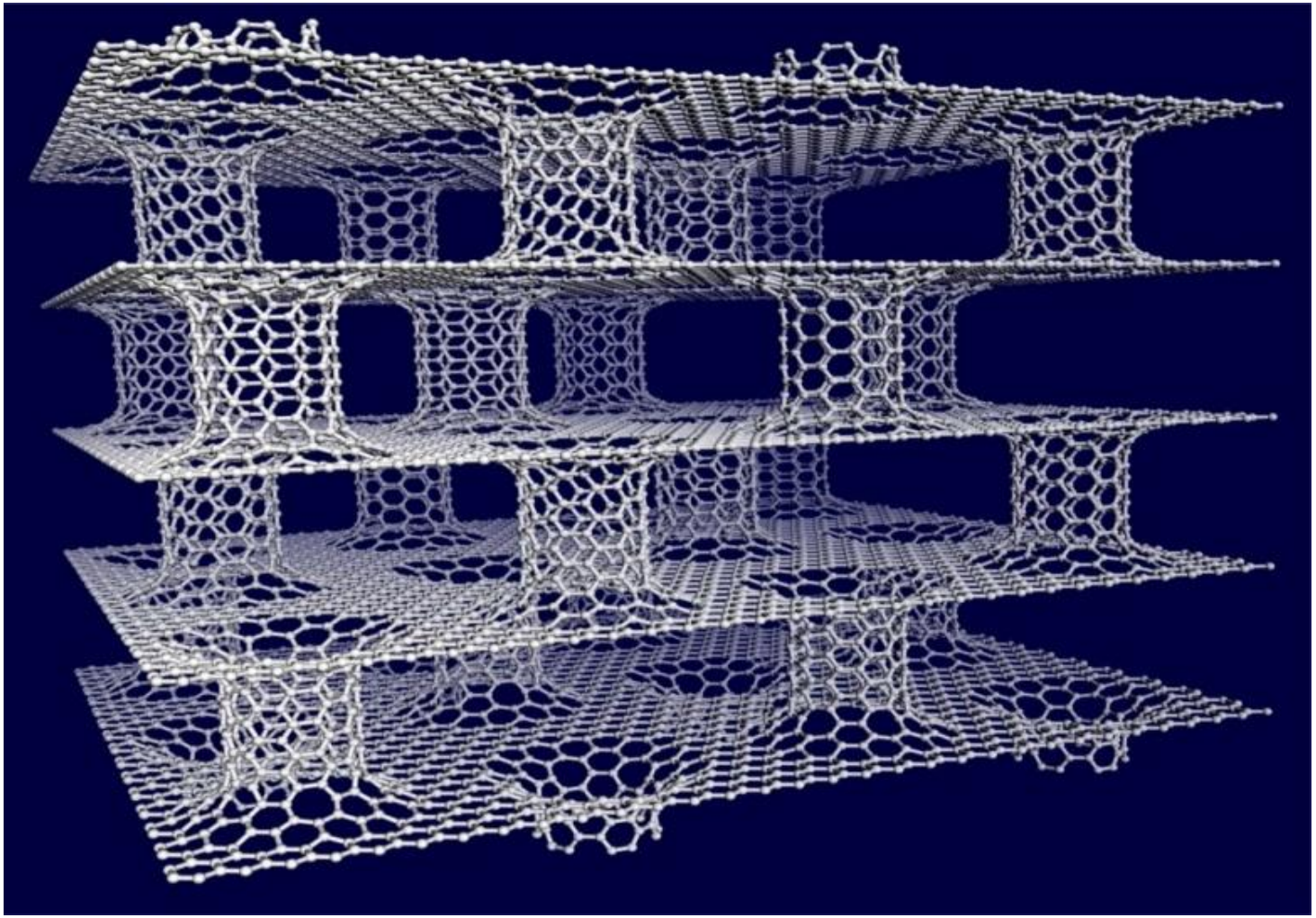

Figure 2.2.3: Schematic diagram of a catalytically grown carbon nanofibers

In general, the activated carbon properties can be determined by the starting material used for the activation process and the activation method used. Such properties include the determination of the surface functional groups. Therefore, the activated carbon surface chemistry, and hence the adsorption behavior, depends upon the activation conditions and temperatures employed. Activation also play major role in refining the pore structure that can yield large surface areas up to 2000m^2/g [41, 45].

2.3.4 Production of Activated Carbons

As stated earlier, active carbon is produced from many different raw materials reach with hydrocarbons, such coconut shells, wood, refineries coke, carbon black, rice hulls, sugar, and many almost from all organic materials. Activation carbons are produced by one of the following methods:

1. Physical or thermal activation: This activation process involves carbonization at raw materials at temperature of 500 ^{o}C to 600 ^{o}C to eliminate all volatile content of the raw materials. The carbonized material is partially processed in gasification process to develop the desired porosity and surface area. For gasification to take place, an oxidizing gas such as CO2, steam or fuel gas at temperature of 800 ^{o}C to1000 ^{o}C, is required [41].

2. Chemical activation: this type of activation involves the addition of some inorganic additives, such as metallic chlorides, before the carbonization process. This process can help improving microporous structure of the activated carbon produced [42].

2.4 Fly Ashes

2.4.1 What is Fly Ash

Another member of carbon family, with a potential application for heavy metal removal from water, is fly ashes. Fly ash is one of the residues generated in the combustion process of coal and liquid fuels, and represents the fine particles that rise with the flue gases. The primary objective of using fly ash in construction and civil engineering application, as an additive to Portland cements, is to find an application for the fly ash as environmental application for waste management [8].

Depending on fuel source, fly ashes may include one or more of the following toxic materials: arsenic, beryllium, boron, cadmium, chromium, chromium (VI), cobalt, lead, manganese, mercury, molybdenum, selenium, strontium, thallium, vanadium, and many others [46, 47]. However, many recent reports describe fly ashes as a good adsorbent for heavy metal removal from water. Two different Turkish fly ashes, Afsin-Elbistan and Seyitomer, as adsorbents were evaluated for the removal of Cd (II) from an aqueous solution [9]. Both fly ashes were found to have high adsorption capacity for Cd(II) when allowed to reach to the required equilibrium time of two hours. The reported adsorption capacities are 98.43% and 65.24% for Afsin-Elbistan fly ash and Seyitomer fly ash, respectively, at pH 7.0 and 100 rpm agitation speed [9]. Belgin compared the adsorption effectiveness of the two types of the fly ashes with activated carbon (untreated powder, 0.150–0.038 mm) derived from charcoal (Sigma, catalogue no. C 3345) and found both type of fly ashes are as effective as activated carbon for the removal of Cd(II) [9].

2.4.2 Types of Fly Ashes

Fly ashes can be classified based on their properties and the source of fuel used to generate these ashes. Basically, the fly ashes generated by hydrocarbon fuel burning can have three different products in term of fly ashes:

1. Fuel Gas is clean fuel and produces no ashes
2. Liquid Fuel, such as heavy fuel oil, produces fly ashes with relatively high percentage of carbon content.
3. Coal burning produces fly ashes with low content of unburned carbon

The fly ashes produced by coal combustion can be divided into two classes, Class F and Class C, based on particle size [48]. In large power plants, fly ash is collected in electrostatic precipitators or bughouses, then classified by precise particle size requirements to ensure a uniform quality product for application in civil field. There is one more class of coal fly ashes is called Class N, which refers to natural fly ash. The three classes are defined as:

- Class F fly ash: generally low in lime (≤ 15%) with higher percentage of silica, alumina and iron (≥ 70%)

- Class C fly ash: generally high in lime (≥ 15%) and could be as a high as 30%.

- Class N fly ash: generally low in lime (≤ 10%) with much higher percentage of silica, alumina and iron.

The fly ash used for this study is produced by burning heavy fuel oils in one of Saudi Arabia main power plants and the produced ash contains high percentage of unburned carbon and some other metals.

2.4.3 Properties of Fly Ashes

Some portions of the fly ashes are acidic, but most of the ashes are strongly alkaline [8]. Fly ashes contain high adsorbent-active surfaces make them highly adsorbents for water. In fact this property is one of the disadvantage of fly ashes in civil engineering application for cements production. The traditional approach to resolve the adsorbent activity of fly ashes is the use of thermal treatment to oxidize these adsorbent-active surfaces. Whellock introduced a new patented innovative treatment that reduces the adsorption capacity of fly ash at ambient temperature by acid treatment [49].

In this study, only the heavy fuel oil fly ashes were studied since this type is more related to Saudi Arabia industry. Daous studied the fly ash produced from burning heavy fuel oil in the power generation plant of the Saudi Consolidated Electric Company in Rabigh. According Daous, the unburned carbon content in the fly ash from this power plant was calculated to be as high as 90% by weight [7].

The FA used in this was work of research was collected from one of Saudi industry and was analyzed by the Energy Dispersive X-ray (EDX) analysis to identify the elemental composition of this FA. The EDX analysis for the FA indicated that the FA contains 67.56% weight carbon elements beside many other different metals as shown in the EDX spectrum (Table-2.3.1):

Spectrum	Sum
C	67.56
O	23.73
Na	0.12
Mg	2.04
S	4.98
V	0.76
Fe	0.12
Ni	0.25
Cu	0.25
Zn	0.19
Total	100.0

Table 2.3.1: The Energy Dispersive X-ray analysis for FA

2.4.4 Production of Fly Ashes

As stated earlier, Fly ash is one of the residues generated in the combustion process of coal and liquid fuels, and represents the fine particles that rise with the flue gases. Therefore, the production process involves the collection and processing of fly ashes from different size power plants and other plants involve combustion of solid and liquid fuels. The primary driver of the collection and uses of fly ashes in different applications is to find an application for the combustion waste material, i.e. fly ash, as environmental application for waste management [8].

Fly ashes from the combustion process in a power plant are captured by electrostatic precipitators upstream the power plant chimney. Some of the ashes, called bottom ashes, are collected from the bottom of the furnace. The electrostatic precipitator is a particulate collection device that removes particles from the flue gas using induced electrostatic charge [50].

2.5 Hexavalent-Chromium and its toxicity

Chromium is a metal found in natural deposits as ores containing other elements such as ferric chromite ($FeCr_2O_4$), crocoite ($PbCrO_4$), and chrome ochre (Cr_2O_3). Chromium is considered one of the earth crust's most abundant elements and it is estimated to be the sixth most abundant transition metal [51]. The chromium was first discovered by, Louis Nicolas Vauquelin, 1797 and it was initially named "hroma" meaning 'color' in Greek. This name was given to chromium due to its ability to from different compounds, which are usually very colorful [52]. Chromium can take different oxidation form with ability to form numerous different compounds. Its compounds are found naturally in air, water, and soil.

It is a well-known highly toxic metal in drinking water. The World Health Organization guideline for chromium in drinking water is 0.05 mg/L [1]. This stringent limit of chromium in potable water, by WHO, is due to its severe toxicity to human body. Chromium naturally found in different oxidation states ranging from 2+, 3+ and 6+, with the trivalent Cr(III) and hexavalent Cr(VI) are the most stable forms in nature. Cr(III) is much less toxic than Cr(VI) and it is an essential element in human bodies. In contrast, Cr(VI) is extremely toxic and found in various industrial

waste water effluents and can cause liver and kidney damage, pulmonary congestions, vomiting, and severe diarrhea [52-54].

Chromium metal is used in metal finishing, leather tanning, electroplating, textile industries, and chromate preparation [55]. Therefore, the potential source of chromium to drinking water contamination is industrial wastewater discharge to environment. The industrial sources include cooling tower blowdown, electroplating, metal plating and coating operations, and many other chemical industries.

Cr(VI) is primarily present in the form of chromate ($CrO4_2^-$) and dichromate ($Cr_2O_7^{2-}$) ions. Depending on solution pH, Cr(VI) can exists in water as dichromate ($Cr_2O_7^{2-}$) ions, chromic acid (H_2CrO_4), hydrogen chromate ion ($HCrO_4^-$) and chromate ion (CrO_4^{2-}) [56].

Figure-2.5.1 shows the Cr (VI) ions distribution in water as a function of pH and concentration. This work of research is carried out for water with initial Cr(VI) of 1 ppm and pH range of 2 to 8; therefore the predominate species is expected to be hydrogen chromate ion ($HCrO_4^-$) and at the pH higher than 6.5 it converts to chromate ion (CrO_4^{2-}).

Despite the wide range of chromium in soil and plants, it is rarely found in natural water above the concentration of the natural background, amounting to 1 μg/l [32]. Higher concentrations are indicators of antropogenic pollution.

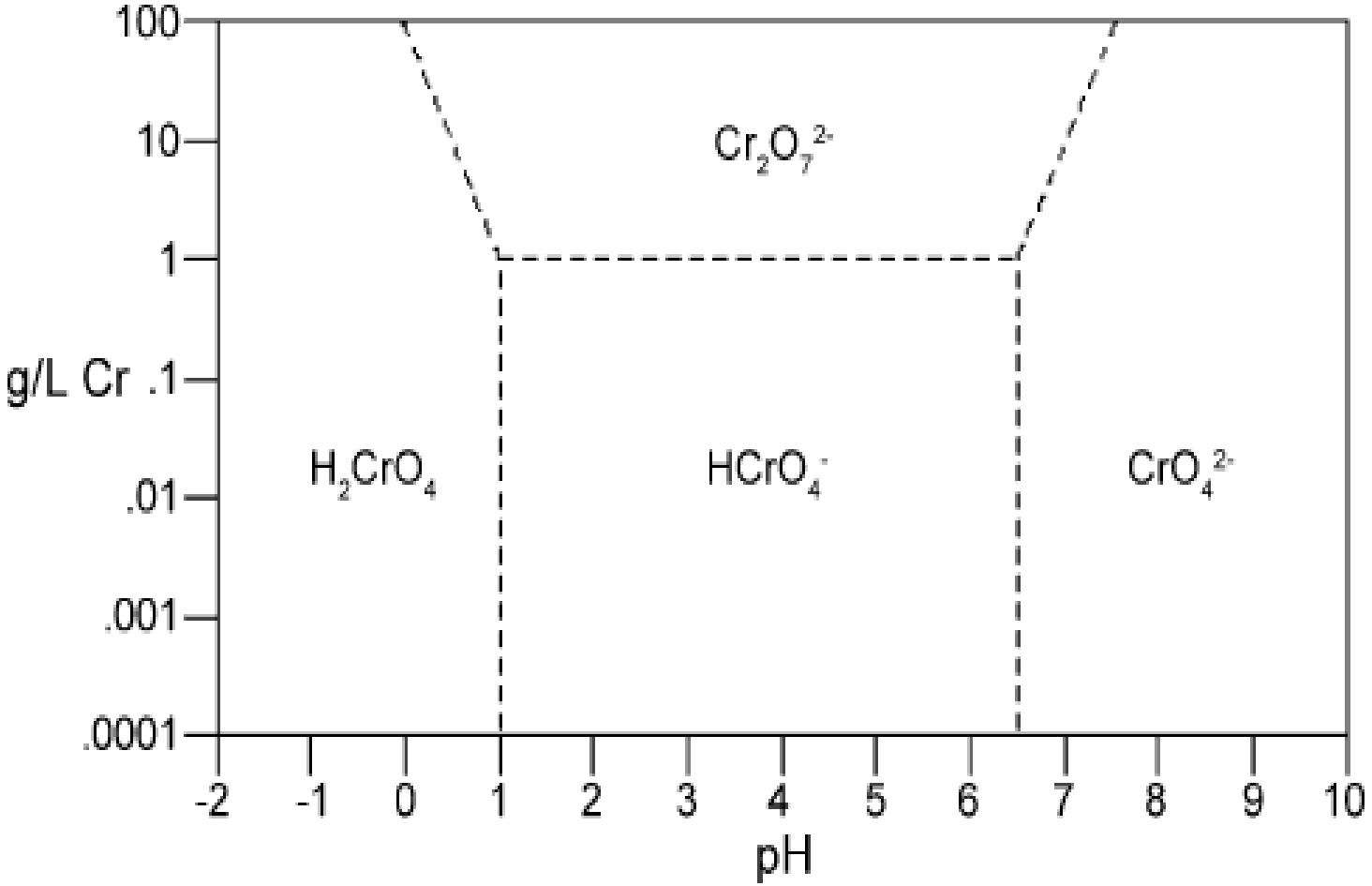

Figure 2.5.1: Distribution of Cr(VI) species in water as a function of pH and Cr(VI) concentration [56].

2.6 Cadmium (II) and its toxicity

Cadmium is one of the naturally occurring components in the earth's crust and water, and present almost everywhere in our environment. Cadmium was first discovered. as a by-product of the zinc refining process, in Germany in 1817. Its name is derived from the ancient Latin word "cadmia" and the Greek word "kadmeia" used at that time for "calamine" or zinc oxide [57].

Cadmium is a metal found in natural deposits as ores containing other elements. It is a well-known highly toxic metal in drinking water and considered as one of the major priority pollutant. The World Health Organization guideline for Cd(II) in water is 0.003 mg/L [1]. This stringent limit of Cadmium in potable water, by WHO, is due to its severe toxicity to human body. Cadmium was found to accumulate primarily in the kidneys and has a relatively long biological half-life in human bodies of 10 to 35 years [1]. As a drinking water pollutant, kidney is the main target organ for cadmium toxicity.

Cadmium metal is used in the steel industry and in plastics. Therefore, the potential sources of cadmium to drinking water contamination are industrial wastewater discharges to environment. The industrial sources include cooling tower blowdown, electroplating, metal plating and coating operations, etc. It is also used in nickel-cadmium and solar batteries and in pigments. One more major source for non-industrial sourced cadmium contamination in drinking-water is possibly caused by impurities in the zinc of galvanized pipes and some metal fittings [58].

2.7 Removal of Heavy Metals from Wastewater

There are various treatments to remove toxic heavy metals from water and wastewater. The treatments alternatives include:

2.7.1 Reverse Osmosis

Reverse Osmosis is a membranes water treatment technology used mainly to produce potable water from high saline water by applying high pressure at the saline water end. High concentration ions from water at higher concentration (saline water) tend to move toward the water at lower concentration to reduce the difference in concentrations at both solutions. When a membrane, permeable for water molecule only, placed between the salty water and the distilled water, distilled water starts flowing toward the salty water to reduce the concentration difference between the two compartments. As the distilled water moves, the water level in the salty compartment start raising, while the water level in distilled side start declining. This process will continue till the static pressure difference equals the osmotic pressure caused by the difference in concentrations between the two sides of the semi-permeable membrane.

Therefore, if a pressure is applied in the saline water side that overcomes the osmotic pressure caused by the difference in concentrations, the distilled water will start flowing back to the other side of the membrane. This process is called reverse osmosis water treatment.

Treatment by Reverse Osmosis (RO) technology is achieved by applying high pressure enough to overcome the osmotic pressure caused by the difference in

concentration at both sides of the RO membranes. This process is very affective to remove monvalent salts from water and by default all higher valent ions are removed. The treatment is very effective; however, it is extremely expensive when used for the treatment of water with low initial concentration of heavy metal [59].

2.7.2 Electrodialysis

Electrodialysis (ED) is another membrane water treatment technology used in water desalination. The difference between this technology and RO is the driving force. In RO technology, the driving force is the pressure and moving part is the permeable water. In ED, two different types of membranes are used. In this process, the ionic components (heavy metals) are separated through the use of semi-permeable ion-selective membranes. Application of an electrical potential between the two electrodes causes a migration of cations and anions towards respective electrodes. Because of the alternate spacing of cation and anion permeable membranes, cells of concentrated and dilute salts are formed. Similar to RO, this process is very affective to remove monvalent salts from water and by default all higher valent ions are removed. This treatment is very effective; however, it is again extremely expensive when used for low initial concentration of heavy metal removal [59].

2.7.3 Ultrafiltration

In principle ultrafiltration (UF) technology are very similar to RO technology with the exception that the membranes are of lager porosity and, hence, requires much lesser pressure. They are very effective for removal of divalent and higher valent ions. In

many application, UF is used upstream the RO plant to improve the RO plant productivity. This process is another affective technology to heavy metals from water, but it is another expensive technology to use for low initial concentration of heavy metal removal [59].

2.7.4 Ion Exchange

Ion exchange is a process through which ions, such as heavy metals ions, dissolved in water are transferred to a solid resin which, in turn releases ions of a different type but of the same polarity. The released ions could be H^+ or Na^+. In other words, the ions in water are replaced by different ions originally present in the ion-exchanger beds. Once the resin of the ion-exchanger bed reach saturation with the replaced ions, the resin is regenerated by subjecting the ion-exchanger resin to concentrated ions of H^+ or Na^+.

In this process is effective for removing metal ions from dilute solutions by exchange of ions held by electrostatics forces on the exchange resin. The main disadvantage of this technology is its high cost and its partial removal of certain ions [59].

2.7.5 Chemical Precipitation

Chemical precipitation is another treatment technology for impurities removal from water. It is a process used in general for the removal of suspended solid in water. Precipitation of heavy metals is achieved by the addition of certain coagulants such as alum, lime, iron salts or some organic polymers. The disadvantages of this technology is the large amounts of sludge containing toxic compounds produced during this

process and it is inefficient to treat water with low initial concentrations of heavy metals [59].

2.7.6 Applications of Carbon Based Absorbents in Water Treatment

The most common method applied for chromate control is the reduction of Cr(VI) to its trivalent form in acid (pH 2.0) and subsequent hydroxide precipitation of Cr(III) by increasing the pH to 9.0 or 10.0 using lime. Till today, less attention has been given to adsorption process as a treatment technology for Cr (VI) removal from water. According to the few available studies for Cr(VI) removal by carbon based adsorbents, the dominating mechanism for Cr(VI) removal is carried out into two steps. The first step involves surface reduction of Cr(VI) ions to Cr(III) followed by the second step of the adsorption of Cr(III) ions by these adsorbents [45].

In this research the four based carbon adsorbents were used to study the effect of these materials on the removal the low initial concentration of chromium (VI) and cadmium (II) from water. The process parameters such as pH, dosage of adsorbent, agitation speed and contact time were investigated in order to maximize the removal of chromium. In addition, these adsorbents were oxidized by acid treatment to produce various oxygen-containing groups (mainly carboxyl groups) on the surfaces. The removal efficiencies of the modified forms were compared against the regular carbon based adsorbents to study the effect of this modification on removal efficiency.

These four adsorbents were used by many other researchers for heavy metal removal and chromium (VI) and cadmium (II) metals in particular. Some of the previously reported works includes:

1. CNTs for Chromium (VI) and Cadmium (II) Removal:

   Carbon nanotubes have demonstrated excellent adsorption capacity for chromium (VI) and cadmium (II) in addition for many other heavy metals. The removal of Cd(II) by CNTs in addition to two other heavy metals, Cu^{2+} and Pb^{2+}, were studied by Li et al.. The study focused on the effects of solution pH, ionic strength and CNT dosage on the competitive adsorption of Pb^{2+} , Cu^{2+} and Cd^{2+} ions. According to Li et al., the affinity of the three metal ions adsorbed by CNTs is in the order: $Pb^{2+} > Cu^{2+} > Cd^{2+}$ [60].

   From Figure-2.7.1, Li et al. showed that Cd (II) removal by CNTs is a function of pH and CNTs dosage rate. Li et al. showed that other ions, Cu^{2+} and Pb^{2+}, reach a maximum removal at pH 7, while the Cd removal continue exponentially increasing beyond pH 7. In this work CNTs were modified, by oxidation of CNTs with H_2O_2, $KMnO_4$ and HNO_3, for oxygen group addition, and the results (Figure-2.7.2) showed that cadmium (II) adsorption capacities for three kinds of oxidized CNTs increased further. The increase in removal was explained by the availability of the functional groups.

   Another study by Tofighy et al. for the effect of CNTs oxidation on the removal efficiency of different divalent heavy metals (Pb^{2+}, Co^{2+},Cu^{2+}, Cd^{2+} , Zn^{2+}) from water reported similar effect.

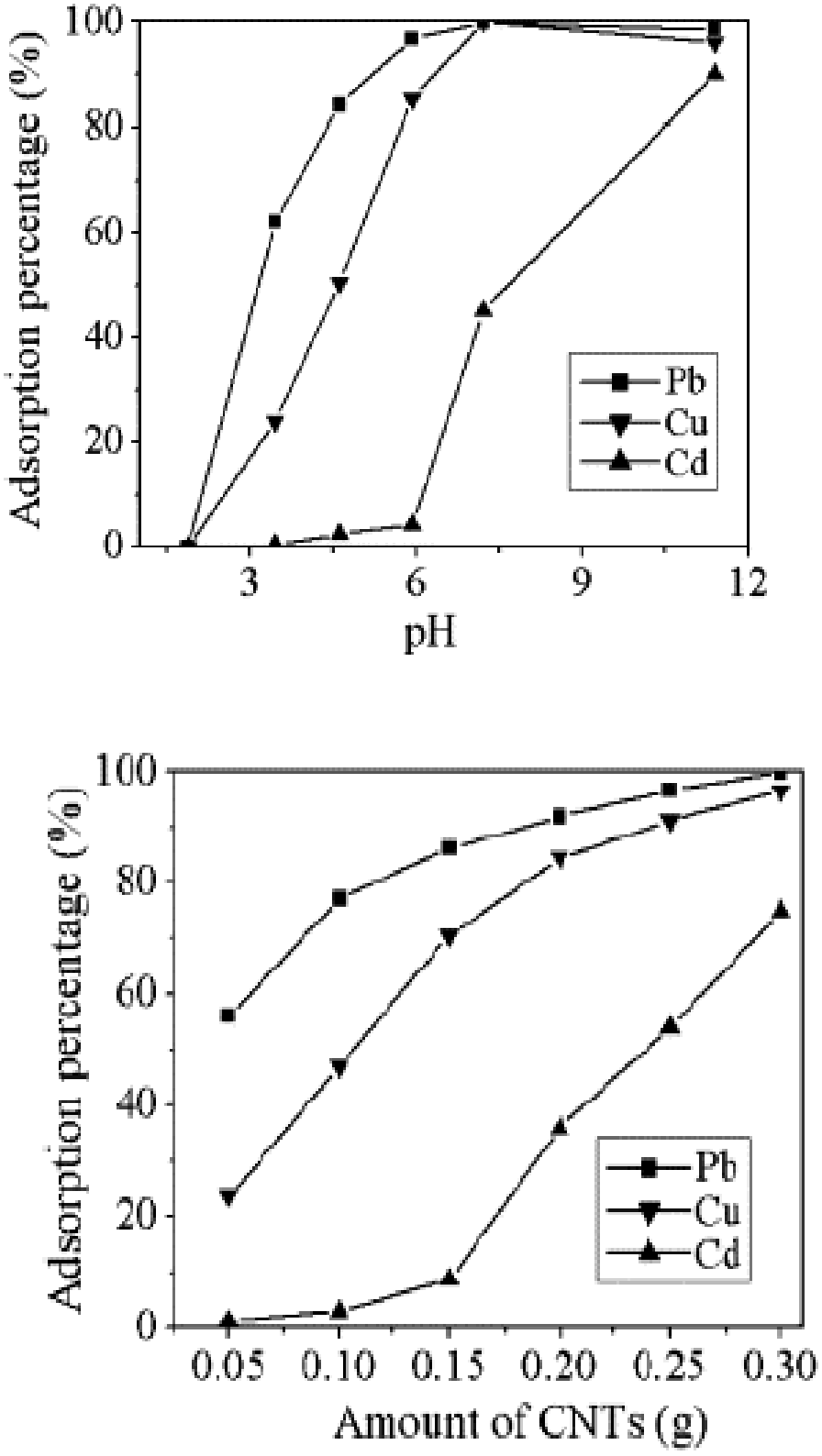

Figure 2.7.1: Competitive adsorption for three ions of Pb^{2+} Cu^{2+} and Cd^{2+} by CNTs [60]

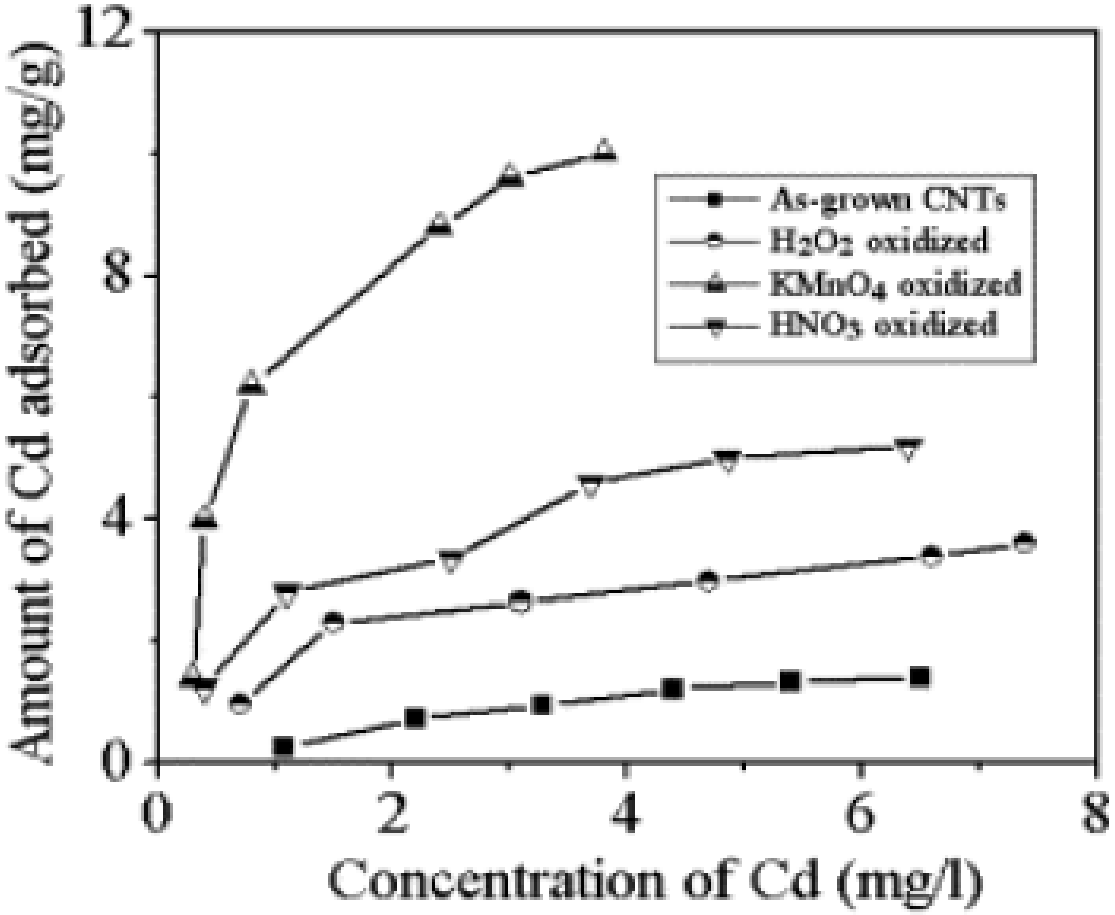

Figure 2.7.2: Adsorption isotherms of Cd (II) adsorbed by CNTs [60]

For all the five metals studied, the modified CNTs showed much higher removal, almost double, when compared to regular (as-synthesized) CNTs. The results of Tofighy et al. work are shown in Figure 2.7.3. This study showed that among the five different metal ions, cadmium comes the second highest removed heavy metal by CNTs and modified (oxidized) CNTs from water [61].

Another study for the cadmium removal from water by CNTs was conducted by Goran et al. [62]. Goran et al. studied the cadmium removal rate from water by CNTs and the effect of CNTs modification on the removal rate [62]. According to this study, the removal efficiency was found to be negligible at pH values lower than 4. The low removal at low pH was explained by the low dissociation of the carboxylic groups and competition between H^+ and Cd^{2+} ions for the same sorption site [62].

The adsorption properties of raw CNTs for divalent heavy metals removal from water ions were significantly improved by the CNTs surface modification for oxidation-functionalization. The functionalized CNTs for oxygen containing groups and amine groups were found to have maximum removal at pH 8 with removal capacity almost 100 times higher than the as received CNTs. This is clearly shown in Figure 2.7.4. This suggests that modified CNTs could effectively be used for the removal of heavy metals from industrial waters.

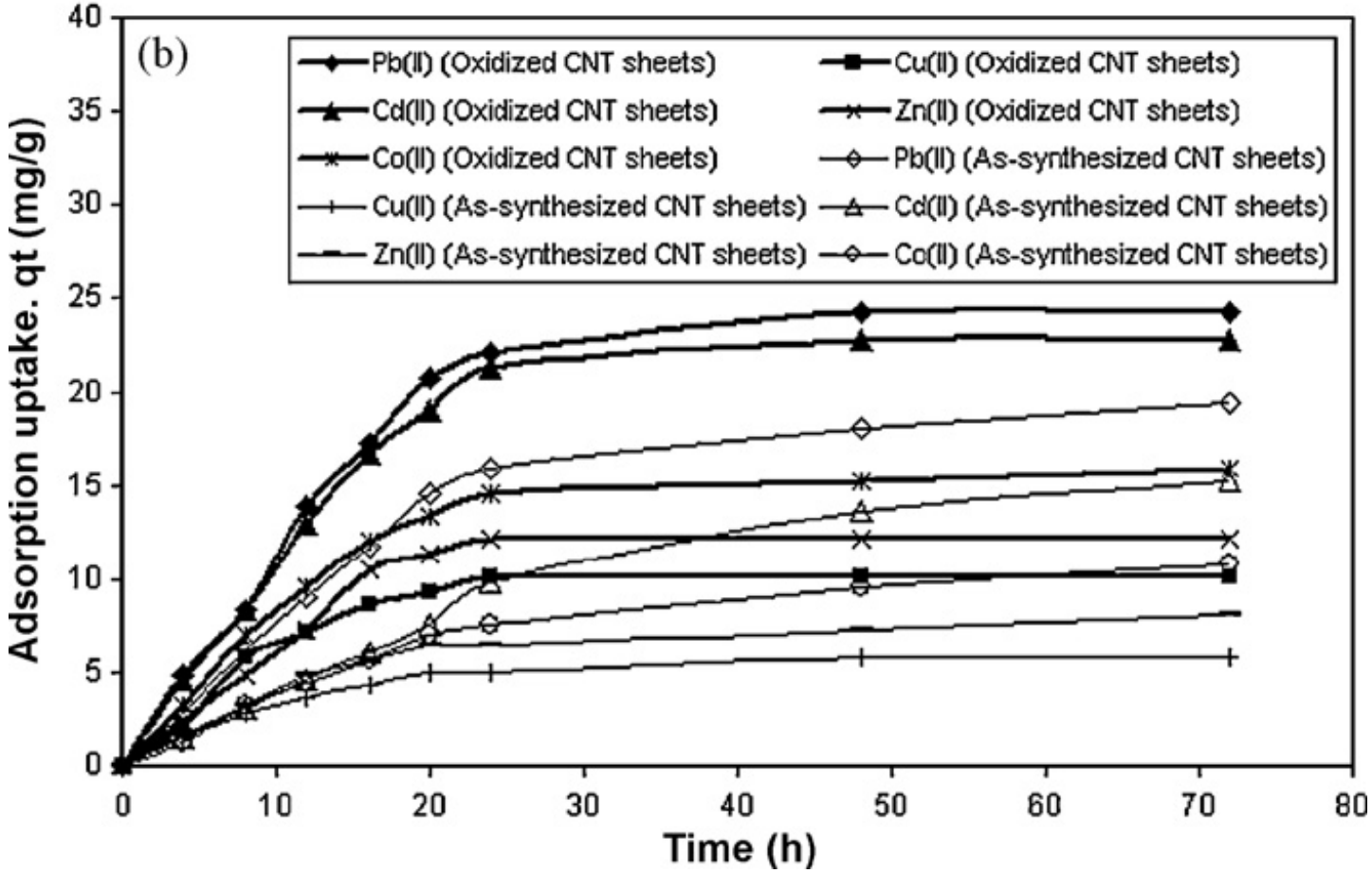

Figure 2.7.3: Effect of adsorption time on adsorption uptake of heavy metal ions [61]

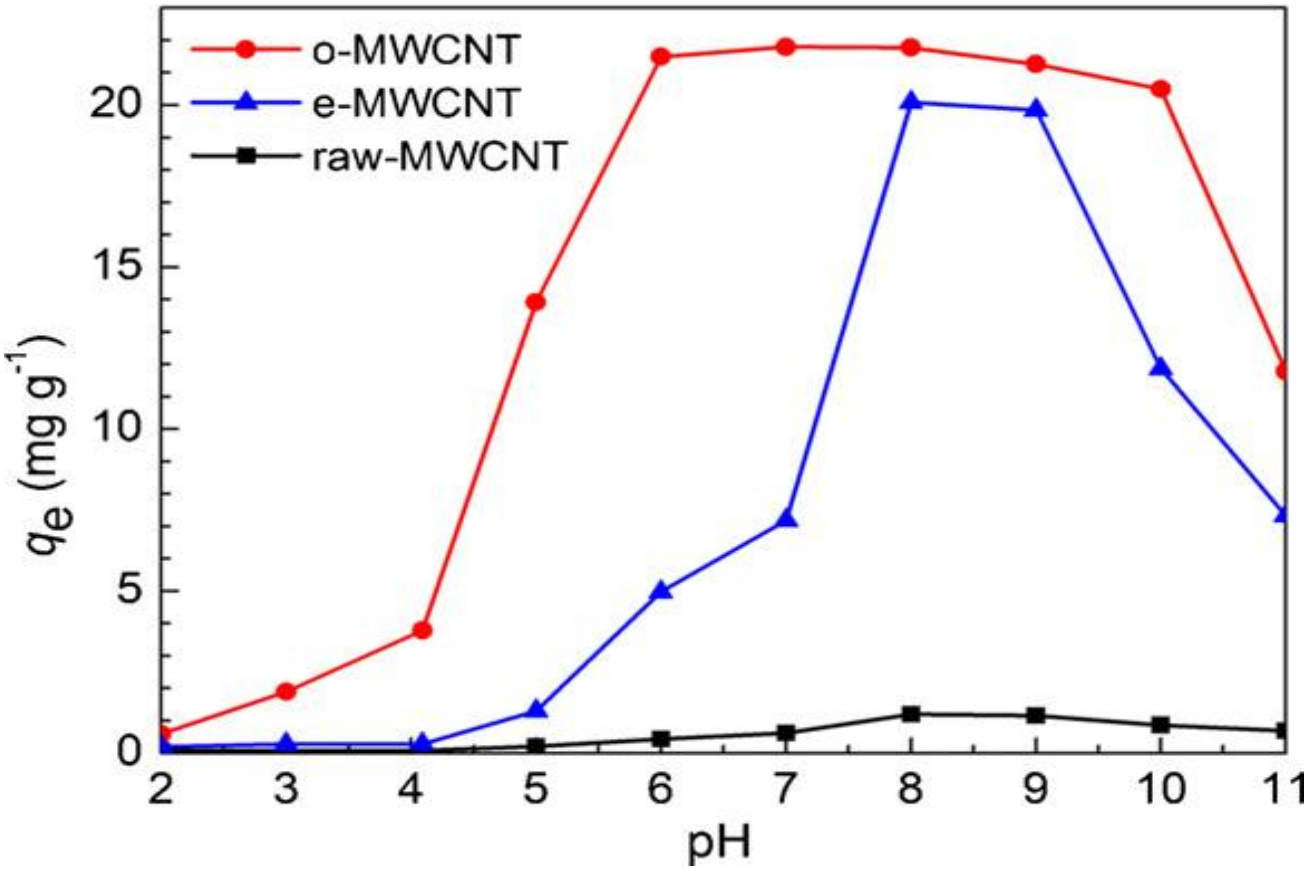

Figure 2.7.4: Effect of pH on Cr(VI) Removal by CNTs and Modified CNTS [62]

Unlike divalent ions hexavalent chromium (Cr(VI)) exist in aqueous solutions in complex ion forms carrying negative charge, such as chromate ($CrO4_2^-$) and dichromate ($Cr_2O_7^{2-}$) ions. According to Jun et al. the adsorption of Cr(VI) ions by CNTs as a function of adsorbent dosage rate, Cr(VI) concentration, contact time, and pH is still limited [10]. Jun et al. studied the adsorption kinetics of Cr(VI) to oxidized MWCNTs as a function of pH, oxidized MWCNTs content, and Cr(VI) concentration. The study concluded that the complication between metal ions and functional groups are considered the main adsorption mechanism of metal ions to carbon nanotubes.

The adsorption rate was found highly dependent on pH valve with higher removal at low pH values. Figure 2.7.5 show the removal percentage by oxidized CNTs as a function of initial Cr(VI) concentration in water for pH range from 2.05 to 4.28. This figure shows that at lower pH, higher removal was achieved.

From figure 2.7.5, it can be concluded that at low initial concentration of Cr (VI) the pH, within this narrow range, has no major effect on the percentage removal. However, at high initial concentration of Cr (VI) the pH, within this narrow range, has significant effect on the percentage removal of Cr (VI) ions from water.

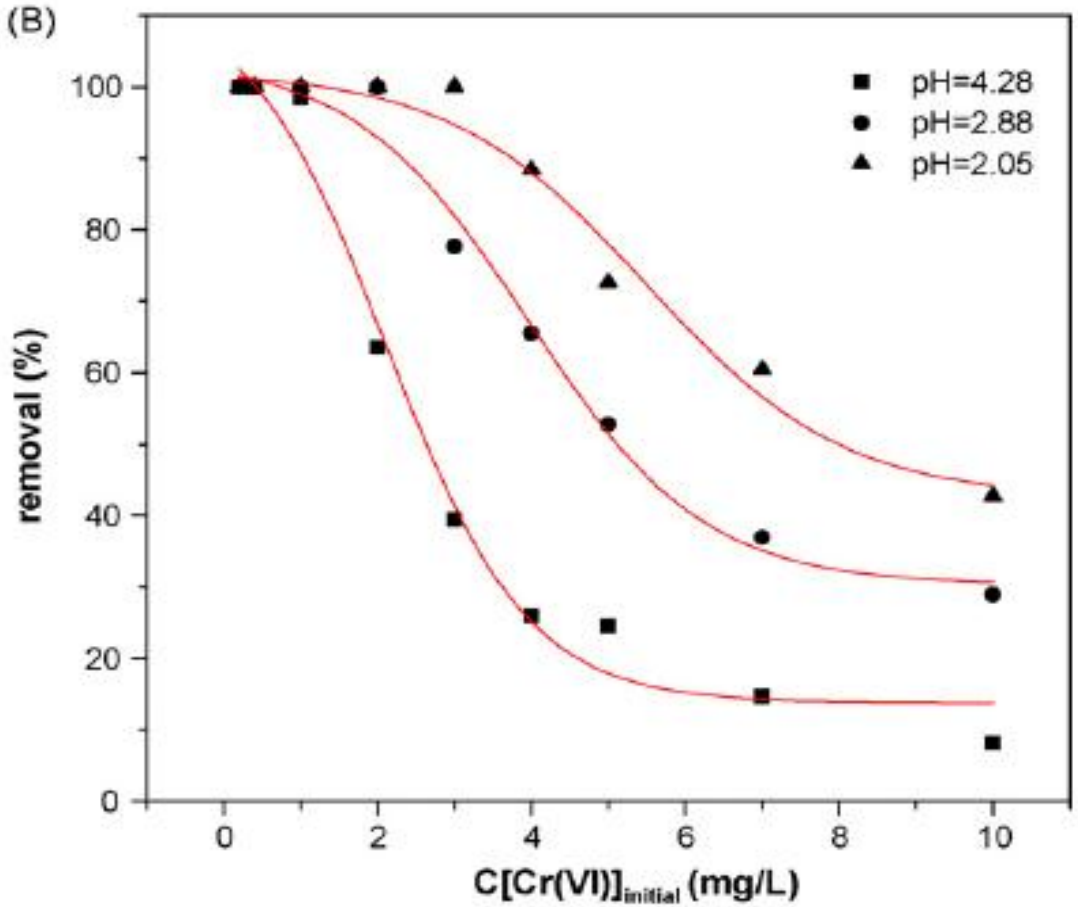

Figure 2.7.5: Effect of pH on Cr(VI) Removal for Different Initial Concentration [10]

2. CNFs for Chromium (VI) and Cadmium (II) Removal:

   Due to the hydrophobicity of CNF surface, it is difficult to disperse CNF in water. Therefore, CNF oxidation shall modify the CNFs surfaces to produce CNF that is highly dispersed.

3. Activated Carbon for Chromium (VI) and Cadmium (II) Removal:

   Activated carbon is one of the oldest adsorbents used for the removal of undesired heavy metals from water. The activated carbons, both regular and modified for carboxylic groups, were studied by many researchers for the removal of chromium (VI) from water. One of these studies is the recent study reported by Attia et al. for the use two different sources activated carbon activated carbon modified for carboxylic groups.

   These two activated carbon types are acid treated activated carbon produced from olive stones (OS-S) and acid treated commercial activated carbon (CAC-S). Both were studied for the removal of Cr(VI) from aqueous solution with high initial concentration ranging from 4 to 50 mg/L [63]. The removal efficiency of both modified forms were compared against the regular activated carbon studied by other researchers.

   Figure 2.7.6. shows the percentage removal as a function of pH for three different adsorbent rates. For both AC types and at three levels of adsorbent dosage rates, the maximum Cr (VI) removal was found at low pH value of 1.5.

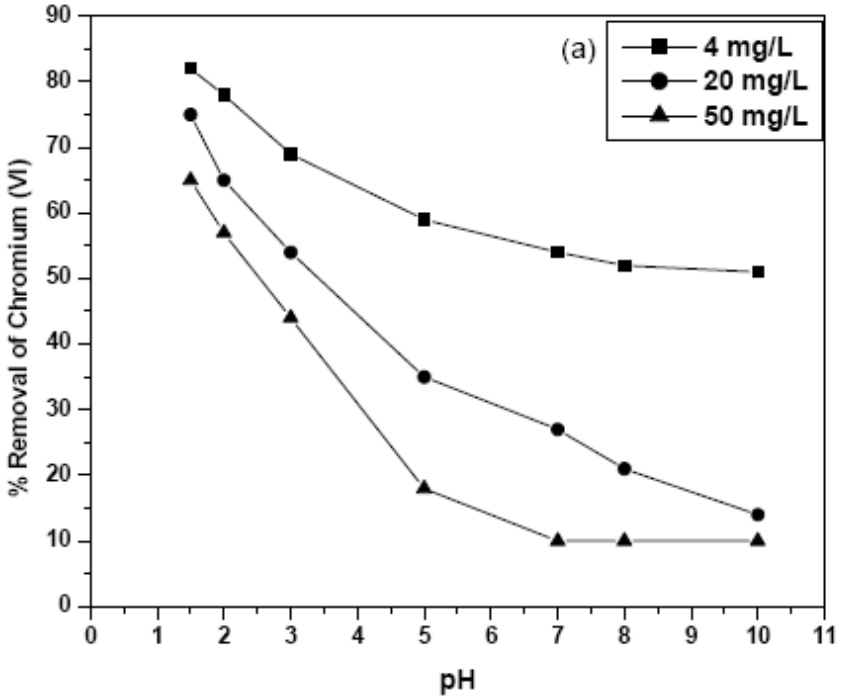

(a) OS-S Activated Carbon

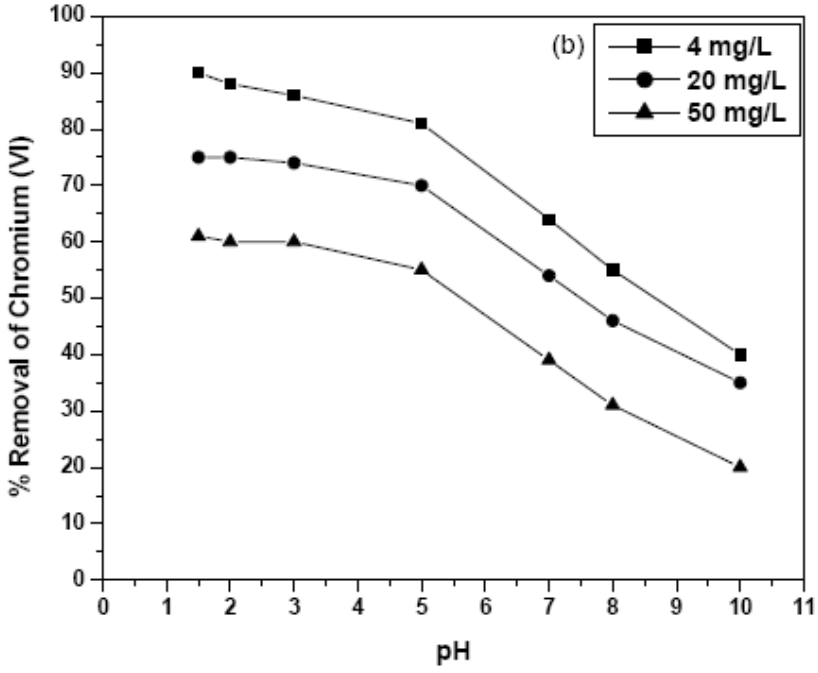

(b) CAC-S

Figure 2.7.6: Effect of pH on Cr(VI) Removal for Different Initial Concentration [63]

The table below summarizes the results obtained by Attia et al. study.

Adsorbent	Initial pH	Langmuir Constants			Freundlich Constants		
		Q_o	K_L	R^2	K_F	n	R^2
CAC-S	1.5	71.4	0.041	0.981	5.01	31.3	0.920
OS-S	1.5	25.6	0.195	0.980	4.7	43.5	0.818

The adsorption capacities of the modified forms are significantly improved when compared to unmodified CAC of 4.72 mg/g as reported by Badu and Gupta [64].

4. Fly Ashes for Chromium (VI) and Cadmium (II) Removal:

Belgin studied the removal of Cadmium and Chromium (VI) from water by two different Turkish fly ashes: Afsin-Elbistan and Seyitomer [9]. These fly ashes were found to have a higher adsorption capacity for Cd(II) as compared to Cr(VI). The adsorption of Cr(VI) was highest at pH 4.0 for Afsin-Elbistan fly ash with removal of 25.46% and highest at pH 3.0 for Seyitomer fly ash with removal of 30.91%. Cd(II) shows much higher removal with 98.43% for Afsin-Elbistan fly ash and 65.24% for Seyitomer fly ash both at pH 7.0 [9].

Figures 2.7.8 and 2.7.9 show the removal rate for Cr(VI) and Cd(II), respectively, for both fly ashes as a function of solution pH. From Figure-2.7.8, the pH dependance of Cr (VI) removal is significant. In contrast, Figure-2.7.9 shows clear pH dependency for Cadmium removal from water. The two figures compare also the removal efficiency of the fly ashes with activated carbons. As can be seen, FAs are comparable in performance to AC for cadmium removal; however, they are not good adsorbents for Cr (VI) when compared to AC.

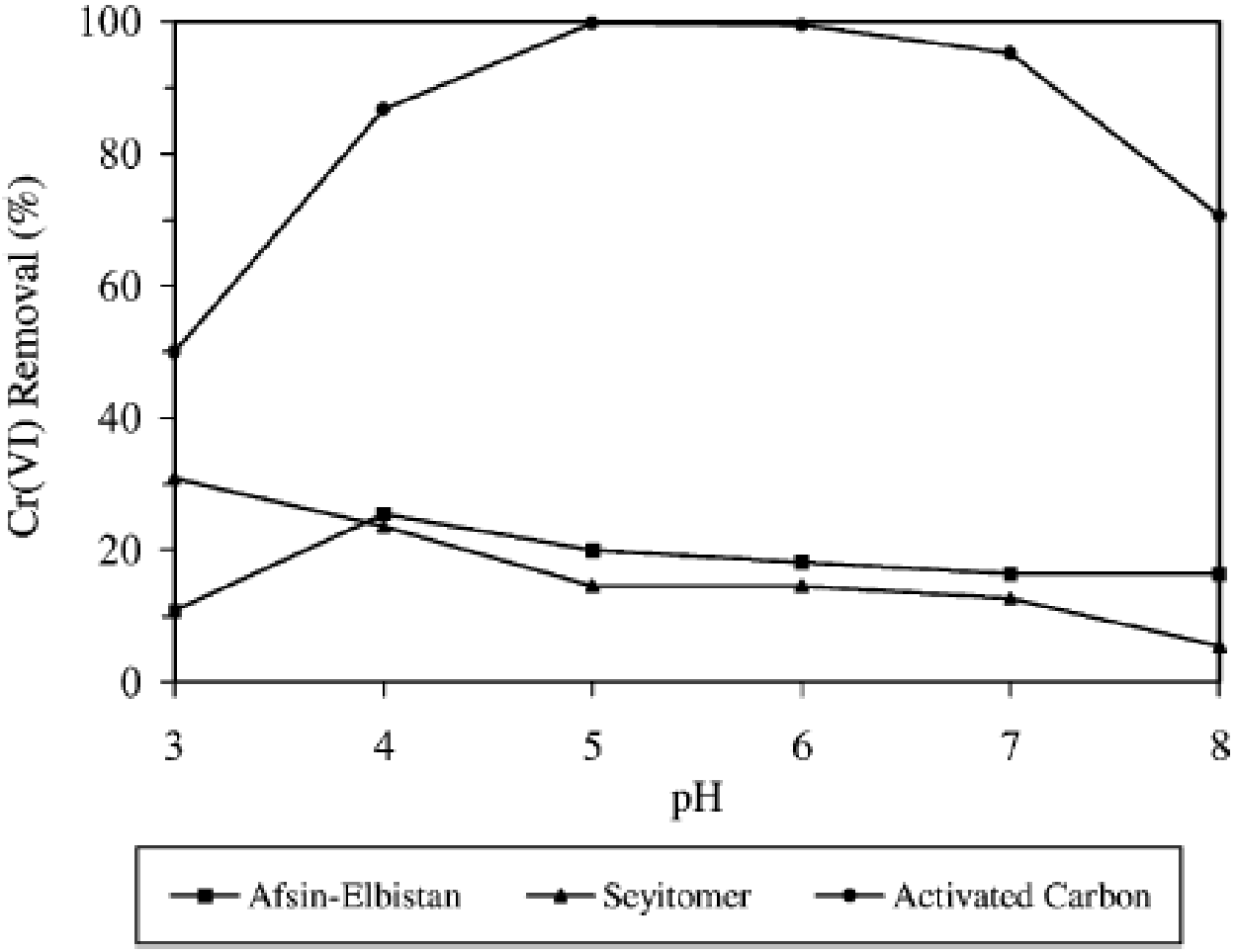

Figure 2.5.8: Effect of pH on Cr(VI) Removal by Two Turkish Fly Ashes for [9]

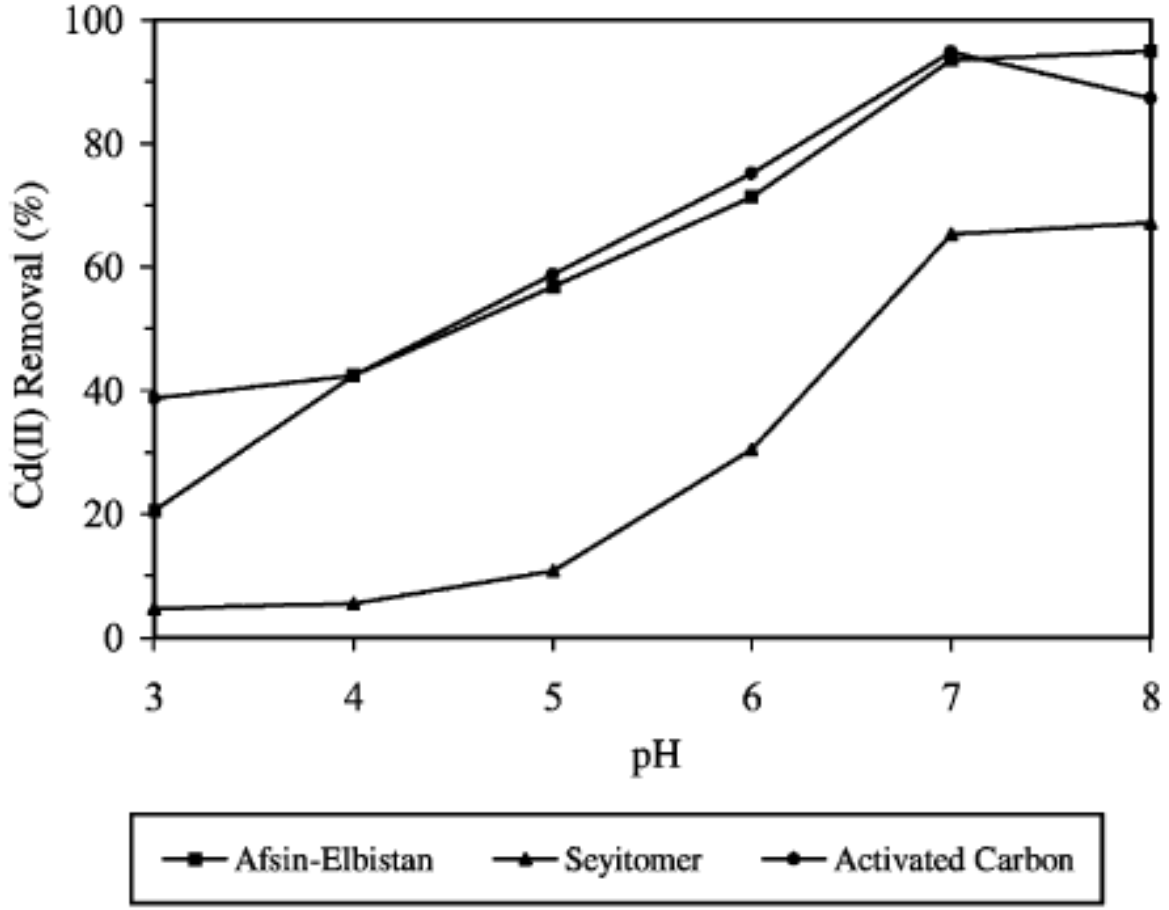

Figure 2.5.9: Effect of pH on Cd(II) Removal by Two Turkish Fly Ashes for [9]

2.8 Sorption Mechanism

The mechanisms by which the metal ions are adsorbed onto each of these four carbon based adsorbents and their modified forms are very complicated and appear attributable to electrostatic attraction, sorption–precipitation and chemical interaction between the metal ions and the surface functional groups in case of modified carbon based adsorbents. In the case of modified CNTs, it has been suggested that the chemical interaction between the metal ions and the surface functional groups of CNTs is the major sorption mechanism [65].

For chromium adsorption from water, it has been reported that Cr (III) adsorption on oxidized carbons increase, while, adsorption of Cr(VI) ions decreases on oxidized carbons. The increase of Cr(III) and the decrease of Cr(VI) on oxidized carbons were due to existence of acidic groups on the carbon surface (Figure 2.8.1). Acidic surface groups enhanced the Cr(III) adsorption and suppressed Cr(VI) adsorption.

The literature survey revealed that chromic ions exist in aqueous solutions as $[Cr(H_2O)_6]^{3+}$; therefore, these associated water molecules are exchanged with the hydroxyl ions and the amount exchanged depends on the pH of the solution. As a result, these changes in the surface negative charge resulting from oxidation and the changes in the positive charge on positive heavy metal ion such as Cr(III) and Cd(II) ions in solution favor the adsorption of Cr(III) and Cd (II) ions because of the attractive electrostatic interactions between the carbon surface and the metal positive charged ions present in the solution [45].

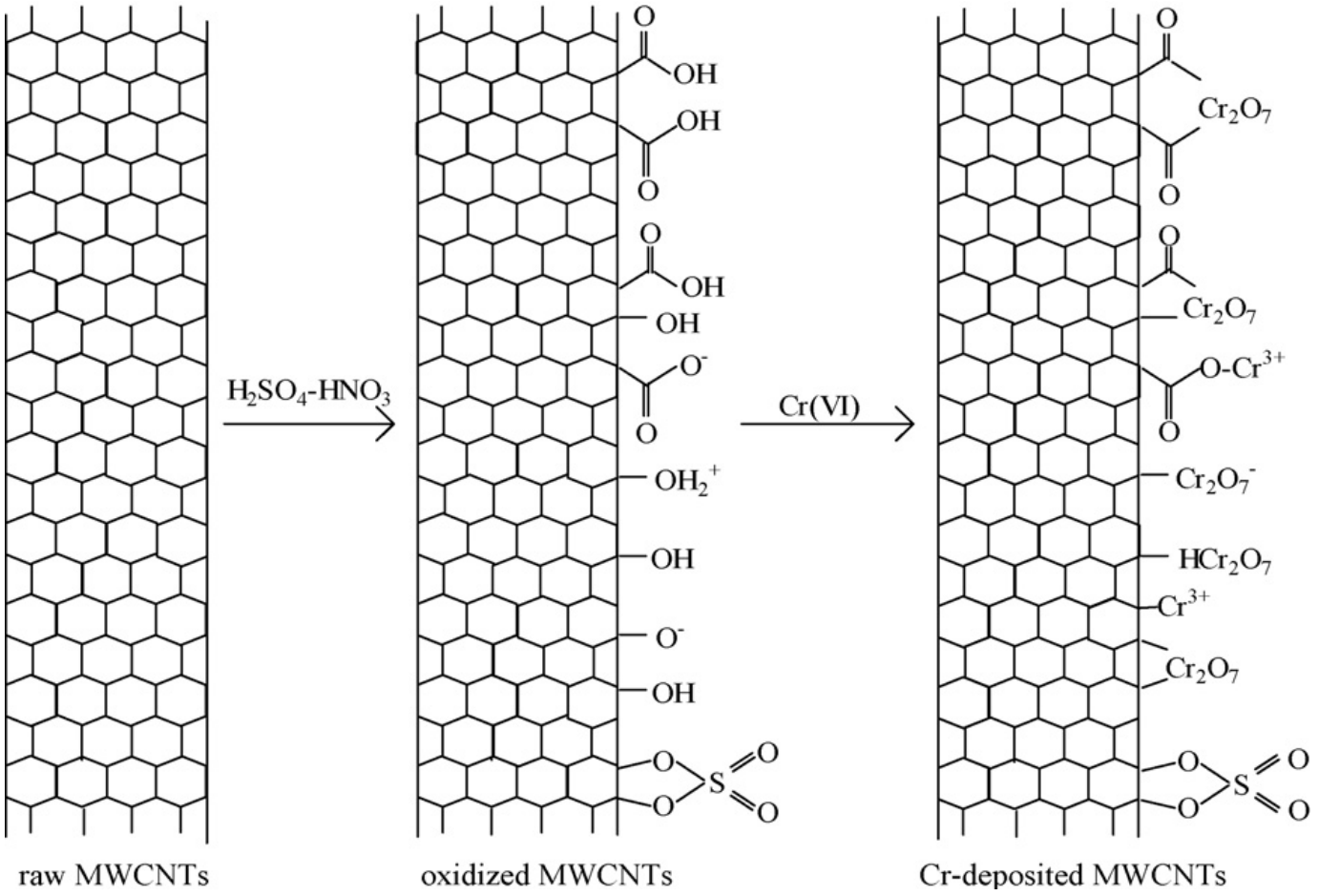

Figure 2.8.1: Schematic diagram of the major mechanism for sorption of divalent metal ions onto CNT surface

Table 2.8.1, as reported by D. Mohan, lists the isotherms model used by many researchers to describe the adsorption isotherm for AC and other low cost carbon based adsorbents [45]. As can be seen, Lungmuir is the mostly used isotherm to describe the adsorption by the many adsorbents reported.

The kinetic data of the sorption on all the investigated MWCNTs were well fitted with the pseudo-second-order kinetic model, suggesting that the rate-limiting step was chemical sorption rather than diffusion. The sorption of cadmium onto the studied MWCNTs is a rather complex process, the mechanism of which may include both of physisorption and chemisorptions mechanisms. The metal ion sorption capacity and affinity of MWCNTs (raw and modified) strongly depended more on their surface groups, pH and temperature than on their surface area, pore volume and pore diameter.

Table 2.8.1: Isotherms model used for AC and other carbon based adsorbents

Adsorbents	pH	Temperature (°C)	Model used to calculate adsorption capacities	Adsorption capacity (mg/g)		Refere
				Cr(VI)	Cr(III)	
	8.0	50	Langmuir	23.0	–	
Native algae (*Chlamydomonas reinhardtii*)	2.0	25	Langmuir	25.0	–	
Heat-treated algae (*Chlamydomonas reinhardtii*)	2.0	25	Langmuir	30.2	–	[288]
Acid-treated algae (*Chlamydomonas reinhardtii*)	2.0	25	Langmuir	25.6	–	
Activated carbon prepared from *Terminalia arjuna* nuts	1.0	25	Langmuir	28.4	–	[81]
Isparta–Yalvaç–Yarikkaya (YK) coal	4.5	25	Langmuir	–	16.2	[152]
Kasikara (KK) coal	4.5	25	Langmuir	–	5.4	
	2.0	10	Langmuir	25.9	–	
Agave lechuguilla biomass	2.0	22	Langmuir	34.6	–	[253]
	2.0	40	Langmuir	35.6	–	
	2.0	27	Langmuir	47.4	–	
M. hiemalis	2.0	40	Langmuir	51.0	–	[235]
	2.0	50	Langmuir	53.5	–	
B. thuringiensis (vegetative cell)	2.0	25	Langmuir	28.6	–	[247]
B. thuringiensis (spore–crystal mixture)	2.0	25	Langmuir	34.2	–	
Lewatit MP 62 anion exchange resin	5.0	25	Langmuir	21.6	–	[131]
Lewatit M 610 anion exchange resin	5.0	25	Langmuir	22.1	–	
Lentinus sajor-caju (untreated)	2.0	25	Langmuir	19.6	–	
Lentinus sajor-caju (heat-treated)	2.0	25	Langmuir	33.1	–	[230]
Lentinus sajor-caju (HCl-treated)	2.0	25	Langmuir	25.8		
Lentinus sajor-caju (NaOH-treated)	2.0	25	Langmuir	27.7		
Carrot residues	4.5	25	Langmuir	–	45.1	[116]
	4.4	25	Langmuir	5.1	–	
Ferric chloride impregnated-sponified sugar beet pul	4.4	35	Langmuir	4.9	–	[289]
	4.4	45	Langmuir	4.6	–	
Carboxymethylcellulose (CMC)	2.0	25	Langmuir	5.1	–	
Free mycelia of *Lentinus sajor-caju*	2.0	25	Langmuir	18.9	–	[212]
Immobilized mycelia (in carboxymethylcellulose (CMC)) of *Lentinus sajor-caju*	2.0	25	Langmuir	32.3	–	
Sawdust	–	–	Freundlich	1.5	–	
Rice husks	–	–	Freundlich	0.6	–	[102]
Coir pith	–	–	Freundlich	0.2	–	
Raw stevensite	3.0	25	Dubinin–Radushkevich	0.7	–	[159]
Fe-stevensite	3.0	25	Dubinin–Radushkevich	2.6	–	
Cone biomass of *Thuja oriantalis*	1.5	17	Langmuir	49	–	[256]
Quaternary chitosan salt (QCS)	4.5	25	Langmuir	68.3	–	[276]
	9.0	25	Langmuir	30.2	–	
Uncalcined hydrotalcite	2.0–2.1	25	Freundlich	4.6	–	[35]
Amberlite IR-120 resin	–	20	Langmuir	–	67.7	[129]
Pantoea sp. TEM18	3.0	25	Langmuir	204.1	–	[248]
	2.0	20	Langmuir	0.5	–	
Bauxite	2.0	35	Langmuir	0.5	–	[167]
	2.0	50	Langmuir	0.4	–	
Hydrous titanium(IV) oxide	2.0	25	Langmuir	5.0		[165]
	2.5	20	Langmuir	284.4	–	
Aeromonas caviae, a gram-negative bacteria	2.5	40	Langmuir	181.5	–	[245]
	2.5	60	Langmuir	169.1	–	
	3.7	30	Langmuir	–	56.7	
Activated carbon from co-mingled natural	3.7	35	Langmuir	–	56.2	
organic wastes	3.7	40	Langmuir	–	56.6	
	3.7	45	Langmuir	–	43.5	[95]
	3.7	22	Langmuir	–	25.6	
	3.7	30	Langmuir	–	52.5	
Norit carbon (oxidized)	3.7	40	Langmuir	–	53.0	
	3.7	50	Langmuir	–	45.9	
Beech (*Fagus orientalis* L.) sawdust	~1.0	25	Langmuir	16.1	–	[252]

Table 2.8.1: (*Continued*)

Adsorbents	pH	Temperature (°C)	Model used to calculate adsorption capacities	Adsorption capacity (mg/g)		Referenc
				Cr(VI)	Cr(III)	
Wine processing waste sludge	4.0	20	Langmuir	–	10.5	[186]
	4.0	30	Langmuir	–	13.5	
	4.0	40	Langmuir	–	15.4	
	4.0	50	Langmuir	–	16.4	
Polyacrylonitrile fibers (APANFs)	5.0	–	–	~16	~5	[137]
Peat	4.0	22–25	Extended Langmuir	–	22.4	[267]
Bio-polymeric beads of cross-linked alginate and gelatin	8.9	25	Langmuir	0.8	–	[169]
Ocimum basilicum seeds	1.5	25	Langmuir	205	–	[119]
Bagasse fly ash	5.0	30	Langmuir	–	2.5	[176]
	5.0	40	Langmuir	–	2.3	
	5.0	50	Langmuir	–	2.1	
Protonated dry alginate beads	3.5	25	Langmuir	–	57.0	[170]
	4.5	25	Langmuir	–	77	
Fe-modified steam exploded wheat straw	3.0	25	Langmuir	9.1	–	[105]
Solvent impregnated resins	4.0	25	Langmuir	50.4	–	[134]
Persimmon tannin (PT) gel	3.0	25	Langmuir	274.0	–	[172]
Distillery sludge	3.0	25	Langmuir	5.7	–	[187]
Ion exchange resin 1200H	3.8	25	Langmuir	84.0	–	[12]
Ion exchange resin 1500H	3.8	25	Langmuir	188.7	–	
Ion exchange resin IRN97H	3.8	25	Langmuir	58.1	–	
Hydrotalcite	6.0	25	Freundlich	120.0	–	[158]
Maple sawdust	6.0	25	Langmuir	5.1	–	[101]
Pitch-based activated carbon fibers, ACF30M	3.0	25	Langmuir	23.7		[138]
Pitch-based activated carbon fibers, ACF45M	3.0	25	Langmuir	24.9	–	
Activated carbon, FS-100	3.0	–	Langmuir	69.3	–	[63]
Activated carbon, GA-3	3.0	–	Langmuir	101.4	–	
Activated carbon, SHT	3.0	–	Langmuir	69.1	–	
Activated carbon, CZ-105	3.0	–	Freundlich	40.4	–	
Activated carbon, CZ-130	3.0	–	Freundlich	44.9	–	
Activated carbon, CK-22	3.0	–	Freundlich	47.4	–	
Activated carbon, CK-26	3.0	–	Freundlich	45.6	–	
Free biomass	2.0	30	Freundlich	27.6	–	[231]
Polysulfone entrapped biomass	2.0	30	Freundlich	17	–	
Polyisoprene immobilized biomass	2.0	30	Freundlich	15.6	–	
PVA immobilized biomass	2.0	30	Freundlich	13.4	–	
Calcium alginate entrapped biomass	2.0	30	Freundlich	9.6	–	
Polyacrylamide biomass	2.0	30	Freundlich	2.3	–	
SI resin prepared using HP-20	4.0	30	Langmuir	38.0	–	[133]
SI resin prepared HP-2MG	4.0	30	Langmuir	40.0	–	
Dunaliella alga (sp. 1)	2.0	25	Langmuir	111.0	–	[213]
	2.0	25	Langmuir	102.5	–	
Inorganic–organic silicon hybrid matrices	–	–	–	–	29.12	[156]
Cone biomass of *Pinus sylvestris*	1.0	25	Freundlich	38.4	–	[257]
PAC	2.0	25	Langmuir	0.03	–	[177]
Bagasse	6.0	25	Langmuir	0.0005		
Flyash	6.0	25	Langmuir	0.001		
Immobilized dried activated sludge	1.0	25	Langmuir	18.9		[197]
Granular activated carbon	1.0	25	Langmuir	147.1	–	
Wool	2.0	30	Langmuir	41.2	–	[100]
Olive cake	2.0	30	Langmuir	33.4	–	
Sawdust	2.0	30	Langmuir	15.82	–	
Pine needles	2.0	30	Langmuir	21.5	–	
Almond	2.0	30	Langmuir	10.6	–	
Coal	2.0	30	Langmuir	6.78	–	
Cactus	2.0	30	Langmuir	7.08	–	
Soya cake	<1.0	20	Langmuir	0.00028	–	[120]
Activated sludge	1.0	25	Langmuir	294.0	–	[188]
Activated sludge	4.5	25	Langmuir	95.2	–	
Cation-exchange resin, IRN77	3.5	25	Freundlich	35.4	–	[11]

Table 2.8.1: (*Continued*)

Adsorbents	pH	Temperature (°C)	Model used to calculate adsorption capacities	Adsorption capacity (mg/g)		Reference
				Cr(VI)	Cr(III)	
Untreated *R. nigricans*	2.0	30	Langmuir	123.5	–	
CTAB-treated R. nigricans	2.0	30	Langmuir	140.8	–	[232]
PET-treated *R. nigricans*	2.0	30	Langmuir	161.3		
APTS-treated *R. nigricans*	2.0	30	Langmuir	200.0		
Biomass of filamentous algae *Spirogyra* species	2.0	18	Langmuir	14.7	–	[211]
	2.0	22	Langmuir	48.1	–	
Carbonaceous adsorbent from waste tires (TAC)	2.0	30	Langmuir	55.3	–	
	2.0	38	Langmuir	58.5	–	
	2.0	22	Langmuir	1.9	–	
Carbonaceous adsorbent from sawdust (SPC)	2.0	30	Langmuir	2.2	–	[85]
	2.0	38	Langmuir	2.3	–	
	2.0	22	Langmuir	44.4	–	
Carbon, F-400	2.0	30	Langmuir	48.5	–	
	2.0	38	Langmuir	53.2	–	
IRN77 resin	3.5	25	Freundlich	–	35.4	[10]
SKN1 resin	3.5	25	Freundlich	–	46.3	
Dried anaerobic activated sludge	1.0	25	Langmuir	577.0	–	[198]
	2.0	30	Langmuir	22.7	–	
Red mud	2.0	40	Langmuir	21.6	–	[29]
	2.0	50	Langmuir	21.1	–	
Tannin gel (66% water content)	2.0	30	–	192.0	20.0	
Tannin gel (72% water content)	2.0	30	–	224.0	28.0	[173]
Tannin gel (75% water content)	2.0	30	–	235.0	38.0	
Tannin gel (77% water content)	2.0	30	–	287.0	50.0	
Cow dung carbon	3.4	30	Langmuir	10.0	–	[86]
Carbon C3	3.0	25	Langmuir	35.0	–	[92]
Carbon C4	3.0	25	Langmuir	15.0	–	
Algae, *Chlorella vulgaris*	2.0	25	Langmuir	27.3	–	[214]
Insoluble straw xanthate (ISX)	3.6–3.9	25	Langmuir	–	1.9	[118]
Alkali-treated straw (ATS)	3.6–3.9	25	Langmuir	–	3.9	
Algae, *C. vulgaris*	2.0	25	Langmuir	79.3	–	
Algae, *S. obliquus*	2.0	25	Langmuir	58.8	–	[215]
Algae, *Synechocystis* sp.	2.0	25	Langmuir	153.6	–	
Algae, *C. vulgaris*	2.0	25	Freundlich	6.0	–	[217]
Peat	2.0	25	–	30.7	–	[268]
	4.0	25	–	–	14.0	
Free biomass of *R. arrhizus*	2.0	–	Freundlich	11.0	–	[226]
Immobilized biomass of *R. arrhizus*	2.0	–	Freundlich	8.6	–	
GAC-S	–		Langmuir	–	13.3	
GAC-E	–		Langmuir	–	10.5	[65]
ACF-307	–		Langmuir	–	7.1	
ACF-310	–		Langmuir	–	3.5	
	3.0	30	Langmuir	12.2	–	
Polymer-grafted sawdust	3.0	40	Langmuir	9.4	–	[97]
	3.0	50	Langmuir	7.6	–	
	3.0	60	Langmuir	6.2	–	
Dithizone-anchored poly(EGDMA-HEMA) microbeads	5.0	25	Langmuir	–	62.2	[171]
Aspergillus biomass	5.0	28	Langmuir	23.6	15.6	[229]
R. arrhizus	2.0	25	Langmuir	58.1	–	[227]
Leaf mould	2.5	25	Column capacity	25.9	–	[107]
Activated carbon	2.5	25		75.6	–	
Biogas residual slurry	1.50	30	Langmuir	5.87	–	[193]
Peat moss	2.0	25	Column capacity	65.8	–	[269]
Irish sphagnum peat	2.5	25	Column capacity	35.5	–	[270]
	2.0	25	Column capacity	43.9	–	
	3.5	30	Langmuir	61.4	–	
Chitosan impregnated with a microemulsion	3.5	40	Langmuir	81.9	–	[277]
	3.5	50	Langmuir	85.6	–	
Lignocellulosic substrate	2.1	–	Langmuir	35.0	–	[108]
Chitosan	4.0	25	Langmuir	154	–	[278]

Table 2.8.1: (*Continued*)

Adsorbents	pH	Temperature (°C)	Model used to calculate adsorption capacities	Adsorption capacity (mg/g)		Reference
				Cr(VI)	Cr(III)	
Sargassum wightii Seaweed	3.5–3.8	25	Langmuir	35.0	–	[220]
Surface-modified jacobsite ($MnFe_2O_4$)	2.0	25	Langmuir	31.5	–	[127]
Protonated brown seaweed *Ecklonia* sp.	2.0	20–25	–	233.5	–	[294]
Aeromonas caviae biomass	2.5	20	Langmuir	284.4	–	[245]
Activated carbon, FAC	2.0	10	Langmuir	16.0	–	
Activated carbon, SAC	2.0	10	Langmuir	1.4	–	
Activated carbon, ATFAC	2.0	10	Langmuir	1.1	–	
Activated carbon, ATSAC	2.0	10	Langmuir	1.6	–	
Activated carbon fabric cloth	2.0	10	Langmuir	116.9	–	
Activated carbon, FAC	2.0	25	Langmuir	21.8	–	
Activated carbon, SAC	2.0	25	Langmuir	9.5	–	
Activated carbon, ATFAC	2.0	25	Langmuir	10	–	[2]
Activated carbon, ATSAC	2.0	25	Langmuir	11.5	–	
Activated carbon fabric cloth	2.0	25	Langmuir	96.3	–	
Activated carbon, FAC	2.0	40	Langmuir	24.1	–	
Activated carbon, SAC	2.0	40	Langmuir	32.6	–	
Activated carbon, ATFAC	2.0	40	Langmuir	15.6	–	
Activated carbon, ATSAC	2.0	40	Langmuir	16.4	–	
Activated carbon fabric cloth	2.0	40	Langmuir	42.1	–	
	5.0	10	Langmuir	–	11	
Activated carbon, ATFAC	5.0	25	Langmuir	–	12.2	
	5.0	40	Langmuir	–	16.1	[3]
	5.0	10	Langmuir	–	36.1	
Activated carbon fabric cloth	5.0	25	Langmuir	–	39.6	
	5.0	40	Langmuir	–	40.3	
Activated carbon, A	3.0	30	Langmuir	–	0.8	
Activated carbon, D	3.0	30	Langmuir	–	0.4	[84]
Activated carbon, OA	3.0	30	Langmuir	–	31.5	
Activated carbon, OD	3.0	30	Langmuir	–	26.3	
PEI-modified biomass of *P. chrysogenum*	4.6	25	Langmuir	279.2	–	[228]
Fleshing from animal hides/skins	4.0	25	Langmuir	51.0	–	[202]
Treated fleshing from animal hides/skins	4.0	25	Langmuir	9.0	–	
	2.5	30	Langmuir	24.1	–	
Carbon slurry	2.5	45	Langmuir	25.2	–	[290]
	2.5	60	Langmuir	25.6	–	
Biogas residual slurry	2.5	30	Langmuir	–	7.8	[194]
Coniferous leaves	3.0	30	Freundlich	6.3	–	[262]
	3.0	20	Langmuir	68.0	–	
London leaves	3.0	30	Langmuir	75.8	–	[261]
	3.0	40	Langmuir	83.3	–	
Brown seaweed (*Turbinaria* spp.)	3.5	30	Langmuir	–	31	[223]
Cork powder	4.0	22	Langmuir	–	6.3	[109]
Hazelnut shell activated carbon	1.0	30	Langmuir	170	–	[90]
Kendu fruit gum dust (KGD)	1.0	30	Freundlich	218	–	[110]
		30	Langmuir	24.1	–	
Carbon slurry		45	Langmuir	25.2	–	[195]
		60	Langmuir	25.6	–	
Cationic surfactant-modified yeast	4.5–5.5	20	Langmuir	94.3	–	[244]
	3.0	20	Langmuir	127.3	–	
Amine-modified polyacrylamide-grafted		30	Langmuir	123.4	–	
coconut coir pith		40	Langmuir	111.4	–	[104]
		50	Langmuir	108.4	–	
Dowex	3.0	30	Langmuir	109.3	–	
	3.0	20	Langmuir	144.2	–	
Sawdust (SD) of rubber wood (*Hevea*	3.0	30	Langmuir	153	–	
brasiliensis) was grafted with	3.0	40	Langmuir	158.7	–	[99]
polyacrylamide	3.0	50	Langmuir	166.7	–	
	3.0	60	Langmuir	172.4	–	
As received CSC	6.0	25	Langmuir	2.2	–	
CSC coated with chitosan	6.0	25	Langmuir	3.7	–	
CSC oxidized with sulfuric acid	6.0	25	Langmuir	4.1	–	[73]

Table 2.8.1: (*Continued*)

Adsorbents	pH	Temperature (°C)	Model used to calculate adsorption capacities	Adsorption capacity (mg/g)		Reference
				Cr(VI)	Cr(III)	
CSC oxidized with sulfuric acid and coated with chitosan	6.0	25	Langmuir	9	–	
CSC oxidized with nitric acid	6.0	25	Langmuir	11	–	
As received CAC	6.0	25	Langmuir	4.7	–	
CAC oxidized with sulfuric acid	6.0	25	Langmuir	8.9	–	
CAC oxidized with nitric acid	6.0	25	Langmuir	10.4	–	
Agave lechuguilla biomass	2.0	10	Langmuir	2.5	–	[259]
	2.0	22	Langmuir	3.3	–	
	2.0	40	Langmuir	3.4	–	
Fly ash	2.0	30	Langmuir	1.4		
Fly ash impregnated with aluminum	2.0	30	Langmuir	1.8	–	[179]
Fly ash impregnate with iron	2.0	30	Langmuir	1.7	–	
Japanese ceder (*Cryptomeria japonica*)	3.0	30	Langmuir	71.9	–	[263]
	3.0	40	Langmuir	80.0	–	
	3.0	50	Langmuir	90.9	–	
Larch bark	3.0	30	Langmuir	31.3	–	[264]
Fly ash-wollastonite	2.0	25	Langmuir	2.9		[291]
Sawdust	2.0	25	Langmuir	39.7	–	[292]
Sugar beet pulp	2.0	25	Langmuir	17.2	–	
Maize cob	1.5	25	Langmuir	13.8	–	
Sugarcane bagasse	2.0	25	Langmuir	13.4	–	
Dried *Chlorella vulgaris*	2.0	25	Langmuir	27.8	–	[217]
Chitosan cross-linked with epichlorohydrin	3.0	25	Langmuir	11.3	–	[293]
Chitosan coated on perlite	4.0	25	Langmuir	153.8	–	[280]
Metal ion imprinted chitosan	5.5	25	Langmuir	51.0	–	[281]
Chitosan cross-linked with epichlorohydrin	5.5	25	Langmuir	52.3	–	
Metal ion imprinted chitosan cross-linked with epichlorohydrin	5.5	25	Langmuir	51.0	–	
Chitosan cross-linked with ethylene glycol diglycidyl ether	5.5	25	Langmuir	56.8	–	
Bagasse fly ash	1.0	30	Langmuir	259.0	–	[27]
	1.0	40	Langmuir	123.7	–	
Activated carbon developed from fertilizer waste slurry	2.0	27	Langmuir	371.0	–	[78]
	2.0	45	Langmuir	173.0	–	
Blast furnace slag	1.0	30	Langmuir	1.45	–	[181]
	1.0	40	Langmuir	1.76	–	
Activated carbon obtained from black liquor lignin	7.0	25	Langmuir	40.0–56.0		[66]
	3.0	25	Langmuir	80.0–92.6		
Cement kiln dust	–	–	Langmuir	33.3	–	[204]
Activated carbon, F	6.0	25	Langmuir	7.3		[67]
Activated carbon, F10	6.0	25	Langmuir	10.7		
Activated carbon, F120	6.0	25	Langmuir	19.2		
Brown coal, YK	3.0	25	Langmuir	47.83		[153]
Brown coal, KK	3.0	25	Langmuir	50.95		

CHAPTER III

METHODOLOGY

3.1 Characterization of Adsorbents

The field emission scanning electron microscopy (FE-SEM) was used to characterize the morphology of the different adsorbents used, while the structure, wherever applicable, was characterized using the transmission electron microscopy (TEM). In addition, the thermal analyses results of Thermogravimetric (TG) and Derivative thermogravimetric (DTG) curves were obtained for the four adsorbents at heating rates (10^{o}C/min) to measure the purity of these adsorbents.

The SEM images give good results in characterizing the length and the diameter of the CNTs and CNFs; however, TEM images are required to distinguish between the structure of these nanocarbons and other nanoparticles that may exist in the samples.

3.2 Preparation of Cadmium and Chromium (VI) Stock Solutions

Stock solutions with concentration of 1 mg/L of cadmium and chromium (III) were prepared from standard solutions of 1000 mg/L of each metal. As the number of moles of cadmium or chromium in a solution does not change with the dilution

process, the required initial concentration of 1 mg/L were calculated per the following relation

$$M_c V_c = M_d V_d$$

Where, the subscript "c" refers to concentrated solutions and the subscript "d" refers to diluted solutions.

Per the above relation, the stock solutions were prepared by adding 1mL from each standard concentrated solution (1000 mg/L) into volumetric flask of 1 L, then tap up the flask with deionized water. The prepared solutions mixed gently to ensure proper mixing of these solutions. The pHs of the stock solutions were adjusted to the desired different values of pH by using Nitric Acid for decreasing the pH or NaOH for increasing the pH. Magnetic stirrer with magnetic rods was used during the pH adjustment process to ensure good mixing. Different molarities for acid and base (1.0 M, 0.1 M, and 0.05M) were prepared and used to provide smooth and gradual pH adjustments.

Initially, all laboratory glassware items used in this project were carefully washed and rinsed with 2% of Nitric Acid. This step is also repeated after each use of any glassware to ensure removal of all impurities on the glassware and to prevent further adsorption of cadmium and chromium ions on the glassware walls.

3.3 Batch Mode Adsorption Experiment

All adsorption experiments were conducted on batch mode and at room temperature. For each set of experiments one variable was allowed to change, while remaining variables were kept constants. This way, the effect of solution pH, adsorbent dosage rate, agitation speed, and contact time on the adsorption rate of Cd (II) and Cr (VI) ions were observed and studied.

At the end of each experiment the solution was vacuum-filtered through a 0.2µm pore size PTFE membrane filter, and then remaining ions concentration was determined. Each experiment was conducted in volumetric flask, with fixed volume of 100 mL, and then both initial and final concentrations of Cd (II) and Cr (VI) were analyzed and recorded by using Inductive Coupled Plasma (ICP).

3.3.1 Effect of pH

The effect of the pH of the solution on Cd (II) and Cr (VI) ions removal percentage was investigated by conducting different experiments at different pH readings, while fixing all other parameters. The fixed parameters were:

Experimental Parameter	Value
Initial Ion Concentration	1 mg/L
Solution Volume	100 mL
Adsorbent Dosage	50 mg
Agitation Speed	150 rpm
Contact Time	120 min

For this work of research, the solution pH range used during these experiments is: 2, 3, 4, 5, 7, and 8. The pH of each sample was adjusted to the desired value by sodium hydroxide and nitric acid to increase and degrease the solution pH, respectively.

3.3.2 Effect of Agitation Speed

The determined optimal pH for ions removal by each adsorbent was used to study the effect of the agitation speed on adsorption capacity of cadmium and hexavalent chromium by each of the four adsorbents. By varying the speed of agitation from 50 to 250 rpm, the effect of agitation speed on adsorption capacities of both ions was studied. The samples were shaken with mechanical shaker that is provided with digital controller to ensure accurate readings. Finally, the samples were vacuum-filtered through a 0.2µm pore size PTFE membrane filter and the concentrations of the remaining ions were analyzed by (ICP).

3.3.3 Effect of Contact Time

The third parameter that was evaluated is the effect of contact time on ions removal from water. The determined optimal pH and agitation speed, as described above, for the maximum ions removal by each adsorbent were used to study the effect of the contact time on adsorption capacity of cadmium and hexavalent chromium by each of the four adsorbents. The experimental work was carried out for the following time intervals: 10, 30, 60, 120, 240, 480, and 1440 minutes. After each experiment, the sample was vacuum-filtered through a 0.2µm pore size PTFE membrane filter and remaining ions were analyzed by (ICP).

3.3.4 Effect of Adsorbent Dosage Rate

The above described experiments shall identify the optimum pH, agitation speed, and contact time for the maximum adsorption capacity of cadmium and hexavalent chromium for each of the four adsorbents at a dosing rate of 50 mg in 100 mL solution. Therefore, one more set of experiments was conducted to study the effect of adsorbent mass on removal of these ions from solution. The experimental work was carried out for the following different adsorbent dosage rate at fixed solution volume of 100 mL: 25, 50, 75, 100, 150, 200, and 250 mg. Finally, the samples were vacuum-filtered through a 0.2µm pore size PTFE membrane filter and remaining ions were analyzed by (ICP).

3.4 Experimental Design

Table 3.4.1 below summarizes the experimental model for this research work

Table 3.4.1: Experiment parameters and its variation

Parameter	Variation						
pH	2	3	4	5	7	8	
Agitation Speed (rpm)	50	100	150	200	250		
Contact Time (min)	10	30	60	120	240	480	1440
Dosage of Adsorbent (mg)	25	50	75	100	150	200	250

3.5 Oxidation of the Adsorbents

All adsorbents were modified for oxygen-containing groups (mainly carboxyl groups) by acid treatment. Three hundred ml of a concentrated nitric acid of AnalaR (69%)

were added to 2 g of each of the four adsorbents. The mixture was refluxed for 48 hours at 120^{o}C. After cooling the acid treated adsorbents to room temperature, the reaction mixture is diluted with 500 ml of deionised water and then vacuum-filtered through a filter paper (3 μm porosity). This washing step is repeated until the pH becomes the same as the deionsed water pH and is then followed by drying in a vacuum oven at 100^{o}C. Such conditions lead to the removal of the catalysts from the carbon nanotubes and carbon nanofibers and opening the tube caps as well as the formation of holes in the sidewalls, followed by an oxidative etching along the walls with the concomitant release of carbon dioxide. This less vigorous conditions, minimized the shortening of the tubes and the chemical modification is then limited mostly to the opening of the tube caps and the formation of functional groups at defect sites along the sidewalls. The final products are nanotubes and nanofibers fragments whose ends and sidewalls are decorated with various oxygen-containing groups (mainly carboxyl groups). Figure 3.5.1 illustrates a typical modification for carbon nanotubes. Acid treatment is also expected to remove impurities from activated carbon and fly ashes as well as oxidative etching over the surfaces of these adsorbents.

Moreover, the percentage of carboxylic functions on the oxidized MWCNT surface does not exceed 4% in the best cases, which corresponds to the percentage of MWCNT structural defects [66, 67]. Due to the hydrophobicity of CNF surface, it is difficult to disperse CNF in the water. Therefore, CNF oxidation shall modify the CNFs surfaces to produce CNF that is highly dispersed.

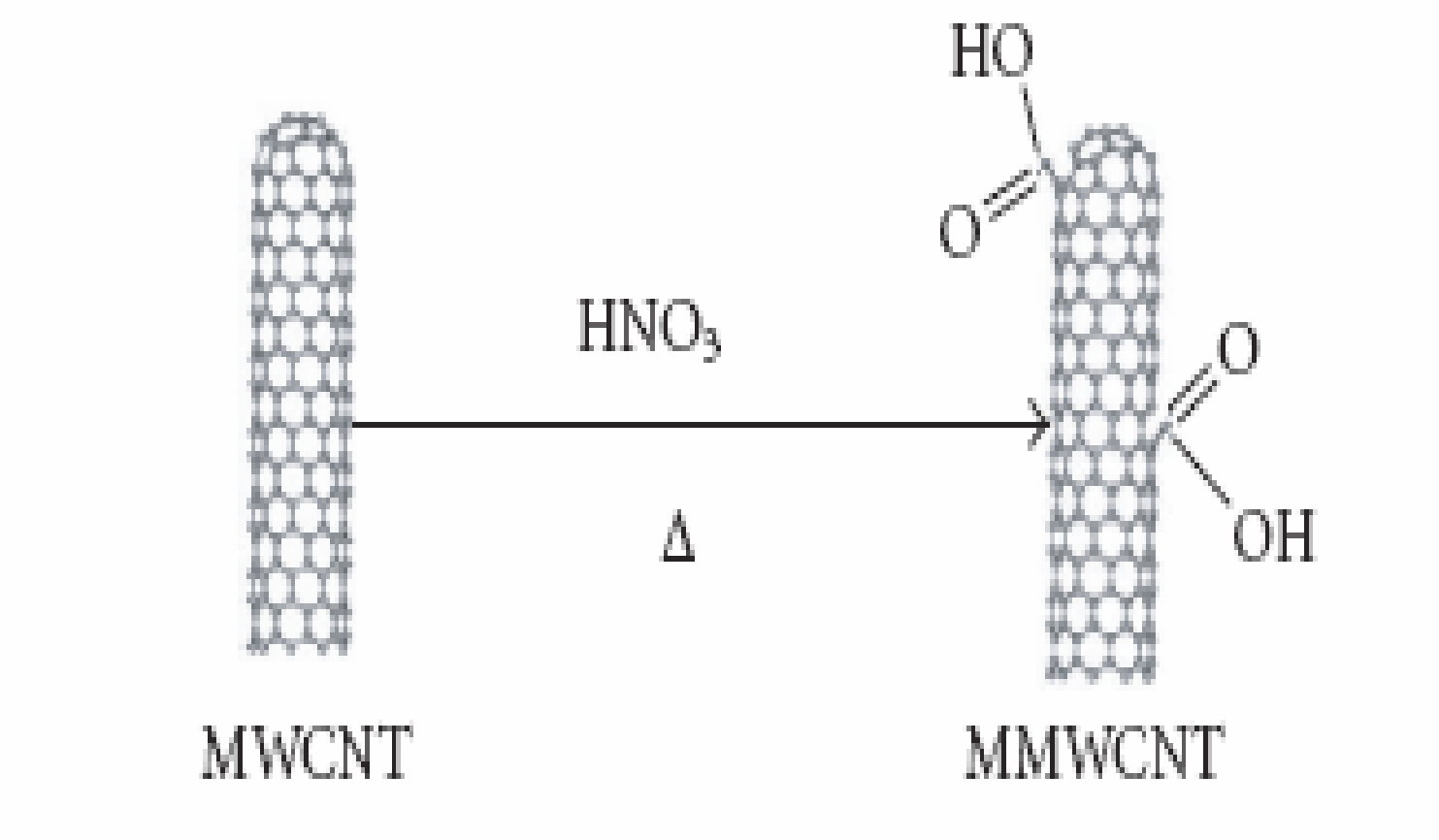

Figure 3.5.1: Chemical modification of carbon nanotubes (MWCNT) through thermal oxidation.

Oxidation of fly ash is extensively applied in civil engineering field to improve the properties of fly ash used in the production of concrete. Fly ash containing unburned carbon is considered a problem in concrete production due to the extremely high adsorbent-active surface caused by the availability of active carbon. The traditional approach to resolve the adsorbent activity of carbon in fly ash is by the use of thermal treatment. Whellock introduced a new patented innovative treatment that reduces the adsorption capacity of fly ash at ambient temperature [49]. Based on the claimed advantages for the concrete production, the modified fly ash is expected to show less adsorption capacity for heave metal removal from water when compared to as received fly ash.

In contrast the modification of activated carbon improves the removal of heavy metals from water due to the fact that metal ions have a tendency to form metalcomplexes with the negatively charged acid groups [68].

3.6 ADSORPTION ISOTHERMS MODELS

Adsorption isotherms are mathematical models that describe the distribution of the adsorbate species among liquid and adsorbent, based on a set of assumptions that are mainly related to the heterogeneity/homogeneity of adsorbents, the type of coverage, and possibility of interaction between the adsorbate species. The Langmuir model assumes that there is no interaction between the adsorbate molecules and the adsorption is localized in a monolayer. The Freundlich isotherm model is an empirical relationship describing the adsorption of solutes from a liquid to a solid surface, and assumes that different sites with several adsorption energies are involved. In order to

model the adsorption behavior and calculate the adsorption capacity for the adsorbent, the adsorption isotherms will be studied. The Langmuir adsorption isotherm is perhaps the best known of all isotherms describing adsorption and it is often expressed as:

$$Q_e = \frac{X_m K C_e}{(1 + K C_e)} \quad (4)$$

Where;

Q_e *= the adsorption density at the equilibrium solute concentration C_e (mg of adsorbate per g of adsorbent)*

C_e = *the equilibrium adsorbate concentration in solution (mg/l)*

X_m = *the maximum adsorption capacity corresponding to complete monolayer coverage (mg of solute adsorbed per g of adsorbent)*

K = *the Langmuir constant related to energy of adsorption (l of adsorbent per mg of adsorbate)*

The above equation can be rearranged to the following linear form:

$$\frac{C_e}{Q_e} = \frac{1}{X_m K} + \frac{C_e}{X_m} \quad (5)$$

The linear form can be used for linearization of experimental data by plotting C_e/Q_e against C_e. The Langmuir constants $\mathbf{X_m}$ and **K** can be evaluated from the slope and intercept of linear equation.

In addition, we can describe adsorption with Langmuir if there is a good linear fit. If not, then Freundlich Isotherm will be used to represent the adsorption isotherm. Freundlich Isotherm is often expressed as:

$$Q_e = K_F C_e^{1/n} \quad (6)$$

Where;

Q_e *is the adsorption density (mg of adsorbate per g of adsorbent)*

C_e *is the concentration of adsorbate in solution (mg/l)*

K_f *and* ***n*** *are the empirical constants dependent on several environmental factors and* ***n*** *is greater than one.*

This equation is conveniently used in the linear form by taking the logarithm of both sides as:

$$\ln Q_e = \ln K_f + 1/n \ln C_e \quad (7)$$

A plot of ln [C_e] against ln [Q_e] yielding a straight line indicates the confirmation of the Freundlich isotherm for adsorption. The constants can be determined from the slope and the intercept.

To confirm the suitability of one of these desorption isotherms for the carbon based adsorbents under the scope of this study, two more adsorption isotherms were used to fit the experimental data obtained. These two adsorption isotherms are BET adsorption isotherm and TEMKIN adsorption isotherm. These two isotherms were considered due to the following:

- BET isotherm was first developed by Stephen Brunauer, Paul Hugh Emmett, and Edward Teller. The isotherm is similar to Langmuir isotherm with the exception BET assume multilayer adsorption. In addition, BET assumes that Langmuir isotherm applies to each layer with equal energy of adsorption for each layer except for the first layer. The adsorption equation for BET isotherm is defined as:

$$q_e = \frac{K_B \cdot C_e \cdot Q_a^0}{(C_s - C_e) \cdot \{1 + (K_B - 1) \cdot (C_s / C_e)\}}$$

Whereas, C_s is the saturation concentration and K_B is a parameter related to the binding intensity for all layers

For cases where C_S is much higher than the C_e the BET isotherm approaches Langmuir isotherm.

- TEMKIN adsorption isotherm accounts for interaction between adsorbed molecules at the surface of the adsorbent. The adsorption equation for TEMKIN isotherm is defined as:

$$q_e = \frac{RT}{B_T} \ln K_T + \frac{RT}{B_T} \ln C_e$$

3.7 KINETIC MODELING

The study of sorption kinetics is applied to describe the adsorbate uptake rate and this rate evidently controls the residence time of adsorbate at solid liquid interface. In order to evaluate the mechanism of sorption for Cd (II) and Cr(VI) by each adsorbent, the first-order equation, the pseudo-second-order rate equation and the second-order rate equation were calculated by the below shown equations, respectively:

$$\log \frac{q_e - q_t}{q_e} = -\frac{K_L t}{2.303} \quad (8)$$

$$\frac{t}{q_t} = \frac{1}{2K_s q_e^2} + \frac{t}{q_e} \quad (9)$$

$$\frac{1}{q_e - q_t} = \frac{1}{q_e} + kt \quad (10)$$

Where:

q_e = *sorption capacity at equilibrium*

q_t = *sorption capacity at time (mg/g)*

K_L = *the Lagergren rate constant of adsorption (1/min)*

k = *rate constant of the pseudo second-order sorption* ($g.mg^{-1}.min^{-1}$)

t = *time (min)*

For the first-order equation, the calculated quantities of log ($q_e - q_t$) were plotted versus *t*ime variable. Similarly, for the pseudo-second-order rate equation, the calculated quantities t/q_t were plotted versus *time variable.* And for the second-order rate equation, the calculated quantities $1/(q_e - q_t)$ were plotted versus *time variable.* From the best fit for the linear equations, the representative kinetics model for each adsorbent was determined.

CHAPTER IV

Results and Discussion

4.1 Characterization and Purity of the Carbon Based Adsorbents

Under this section, the characterization of the as-received (regular) and modified carbon based adsorbents and their purity measure using thermal analyses are resented.

4.1.1 Characterization of Carbon Based Adsorbents

High purity of multi wall carbon nanotubes were produced by chemical vapor deposition (CVD) technique. The produced carbon nanotubes were observed by suing field emission scanning electron microscopy (FE-SEM) and transmission electron microscopy (TEM) [69]. The diameter of the produced carbon nanotubes varies from 20 to 40 nm with average diameter at 24 nm while the length of the CNTs was found to be up to few microns. Figure-4.1.1(a) shows the SEM image of carbon nanotubes at low magnification. Figure-4.1.1(b) shows the SEM image of carbon nanotubes at high magnification. From the SEM observation, the product is pure and only carbon nanotubes were observed.

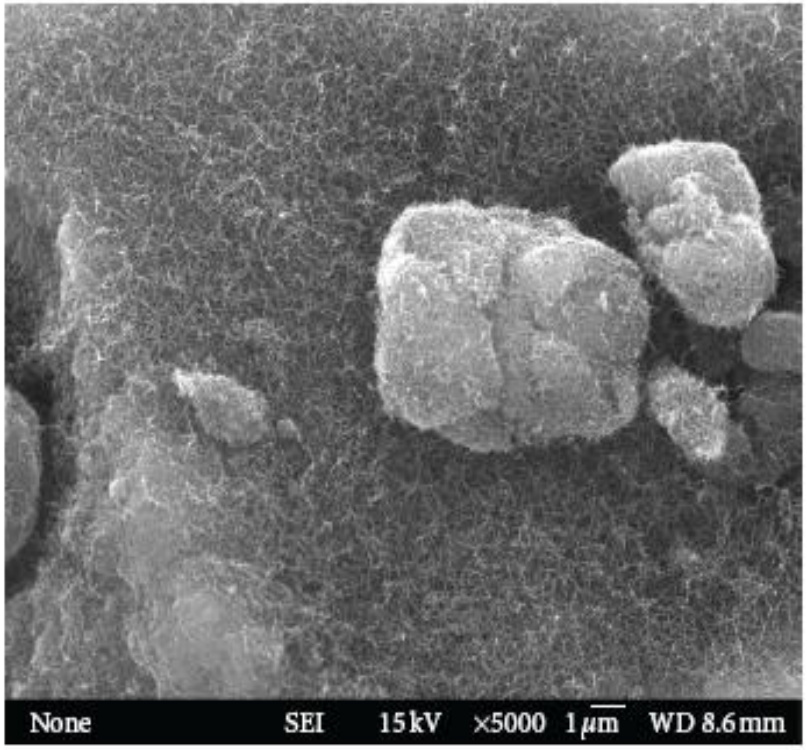

(a)

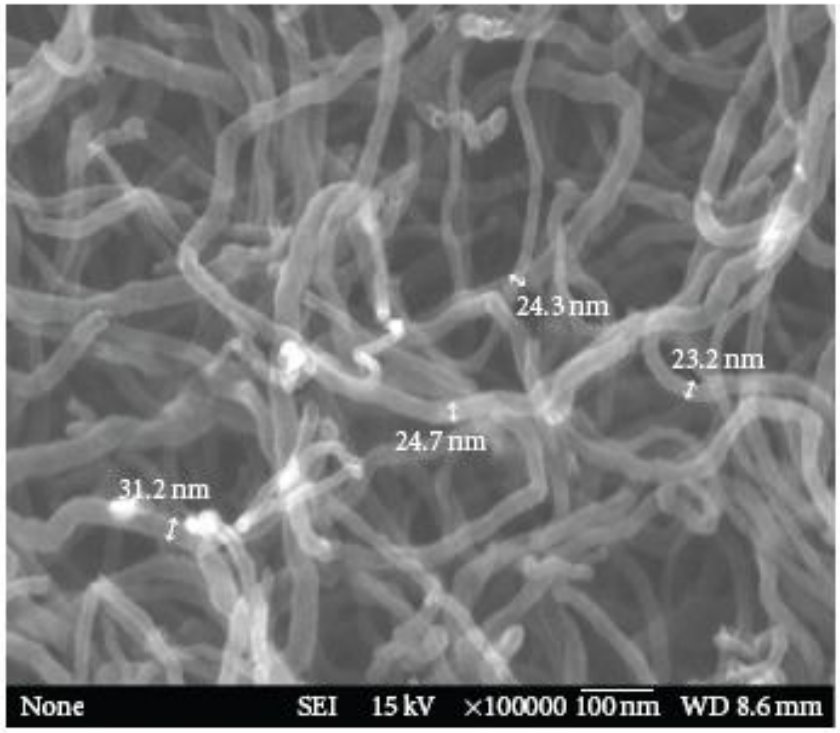

(b)

Figure 4.1.1: SEM Images of carbon nanotubes at (a) at low resolution and (b) at high resolution.

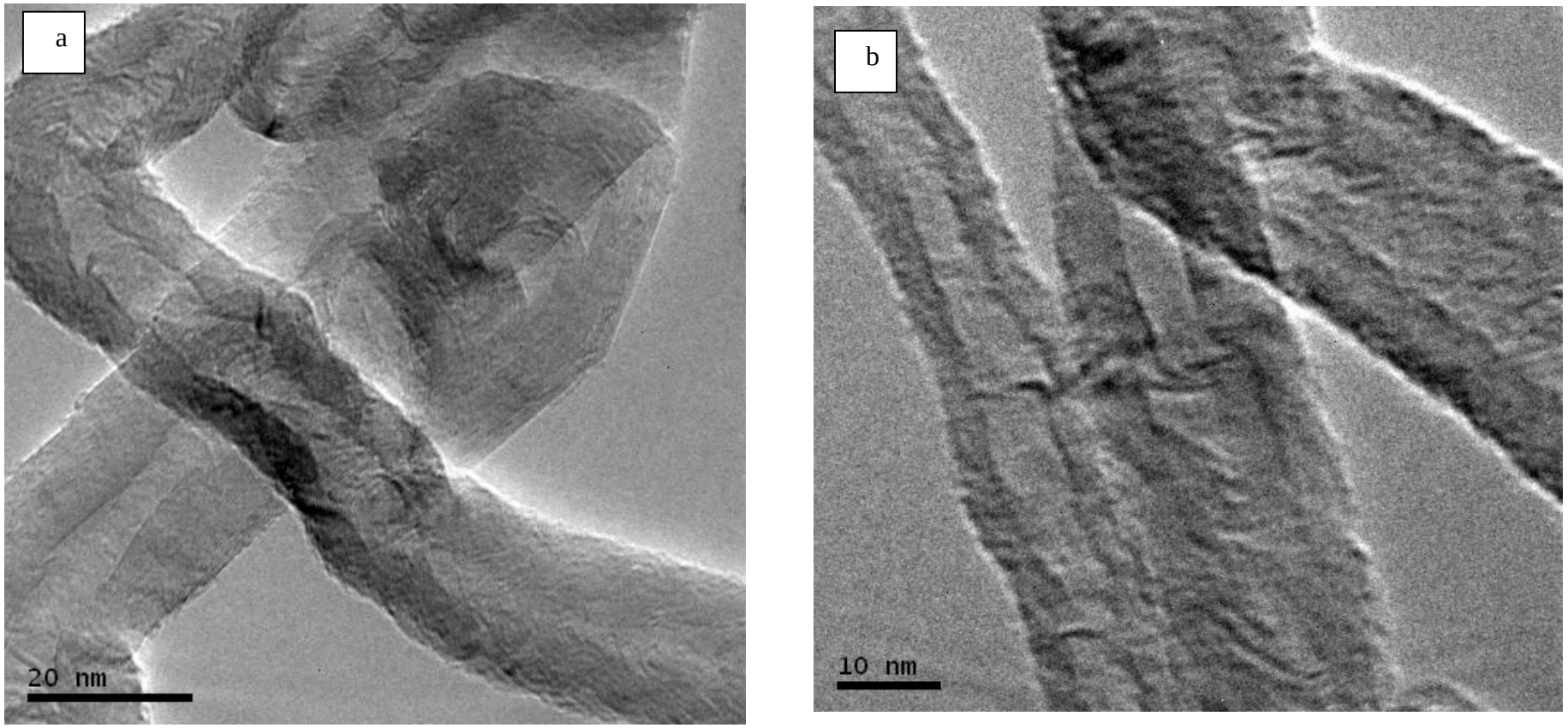

Figure 4.1.2: TEM Images of carbon nanotubes (a) at low resolution (b) at high resolution.

Moreover, TEM was carried out to characterize the structure of nanotubes (Figure-4.1.2). To prepare TEM samples, some alcohol was dropped on the nanotubes films, then these films were transferred with a pair of tweezers to a carbon-coated copper grid. It is obvious from the images that all the nanotubes are hollow and tubular in shape. In some of the images, catalyst particles can be seen inside the nanotubes. TEM images indicate that the nanotubes are of high purity, with uniform diameter distribution and contain no deformity in their structures. Figure-4.1.2(b) shows the High Resolution Transmission Electron Microscope (HRTEM) of the carbon nanotubes. Form this image, it can be concluded that a highly ordered crystalline structure of CNT is present.

Carbon nanofibers were purchased from Nanostructured & Amorphous Materials, Inc. USA. The Purity of CNF is >95%, its outside and inside diameters are 200–500nm and 1–10 nm, respectively. The length of these CNFs is 10–40 um. Figure-4.1.3 shows the Transmission Electron Microscopy (TEM) for the used CNFs [66].

The modification of CNT is expected to reduce the CNTs length. Figure-4.1.4 and Figure-4.1.5 show the SEM image for the modified CNTs and CNFs, respectively. It can be noted from Figure-4.1.1 how the crystalline of carbon in these nano forms are relatively disturbed.

The SEM image for the fly ashes (Figure-4.1.6) when compared to activated carbons (Figure-4.1.7) demonstrates the high surface area property for the FA and its suitability to be used as adsorbent.

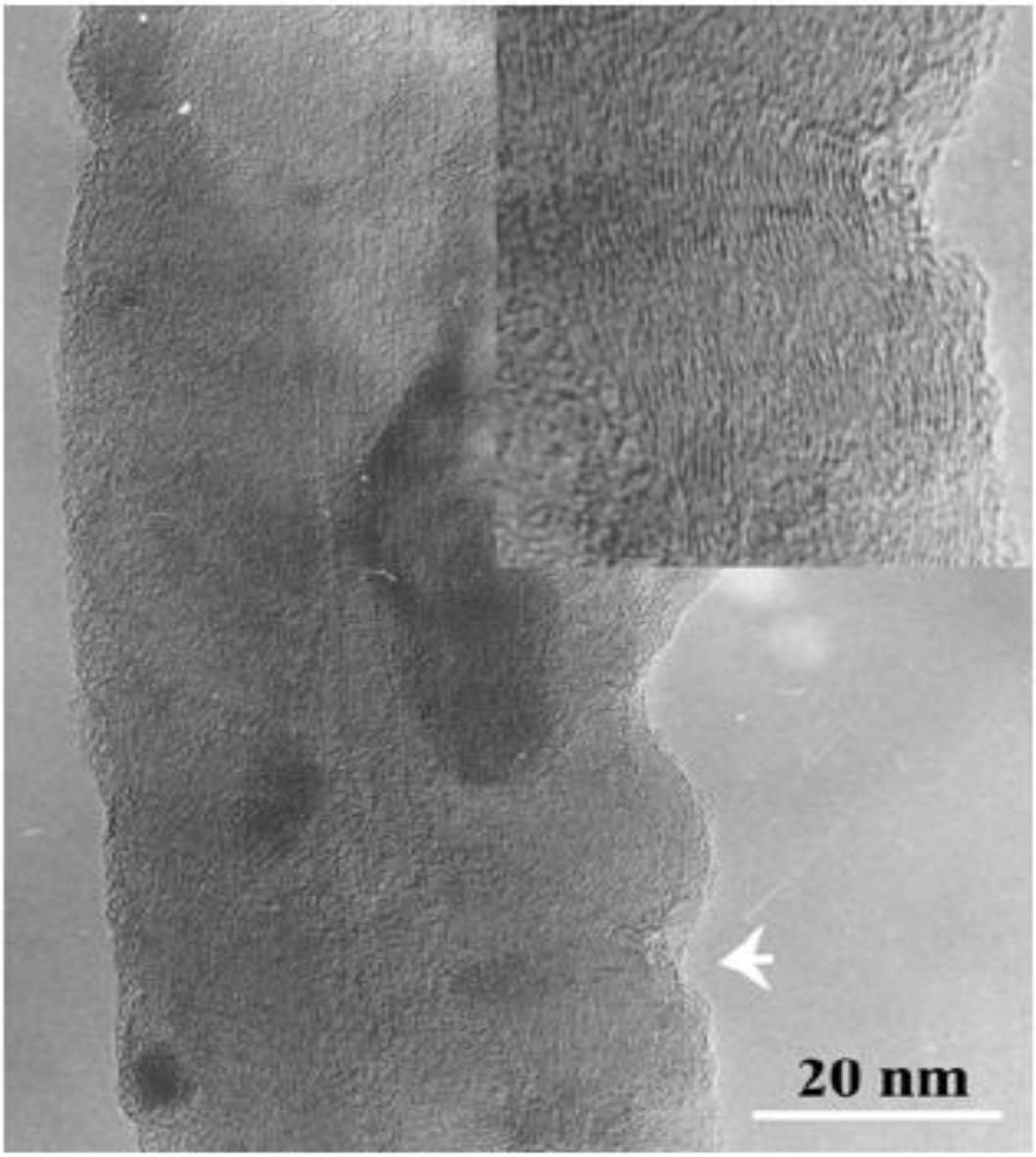

Figure 4.1.3: Transmission Electron Microscopy (TEM) for the CNFs.

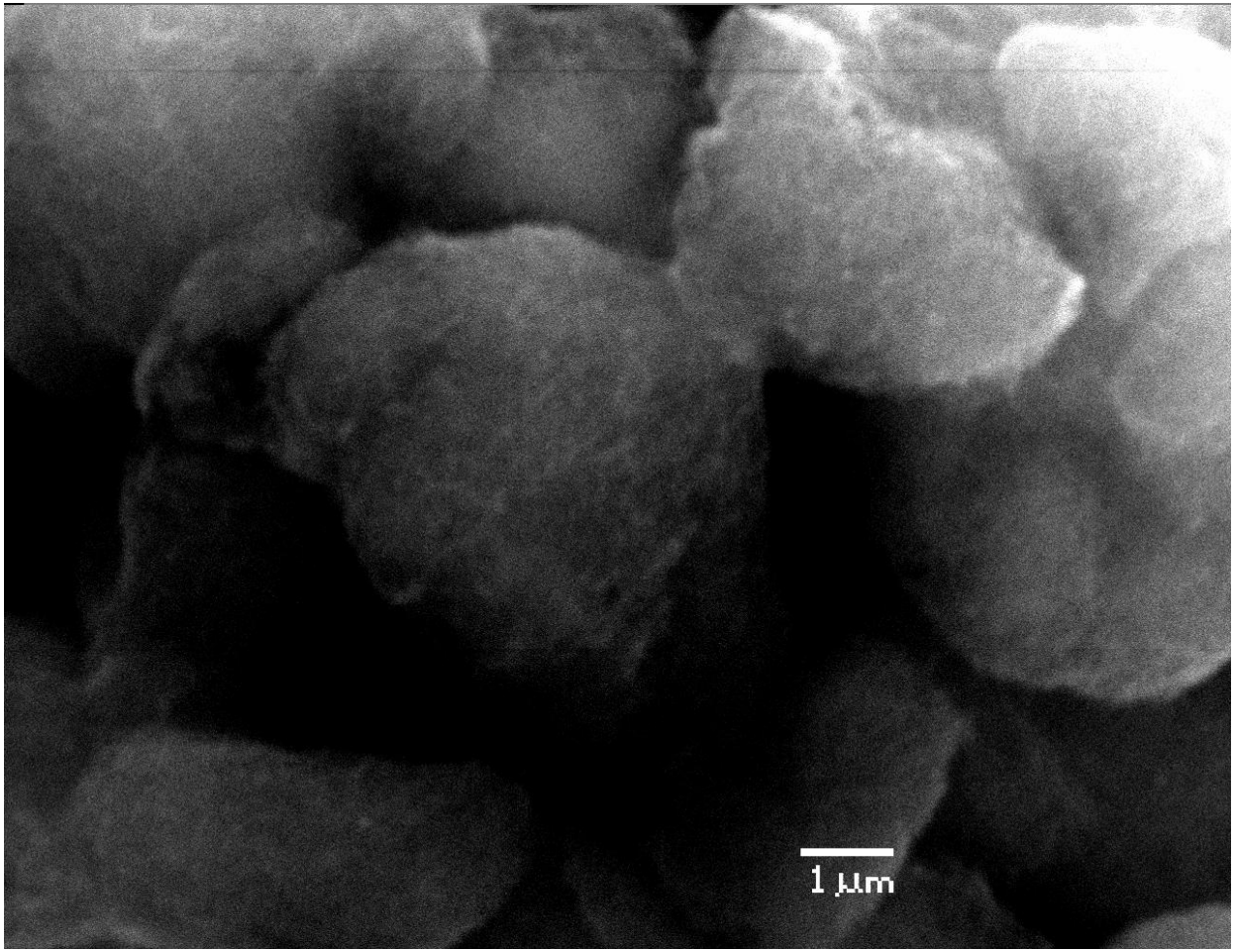

Figure 4.1.4: SEM Images of modified CNTs

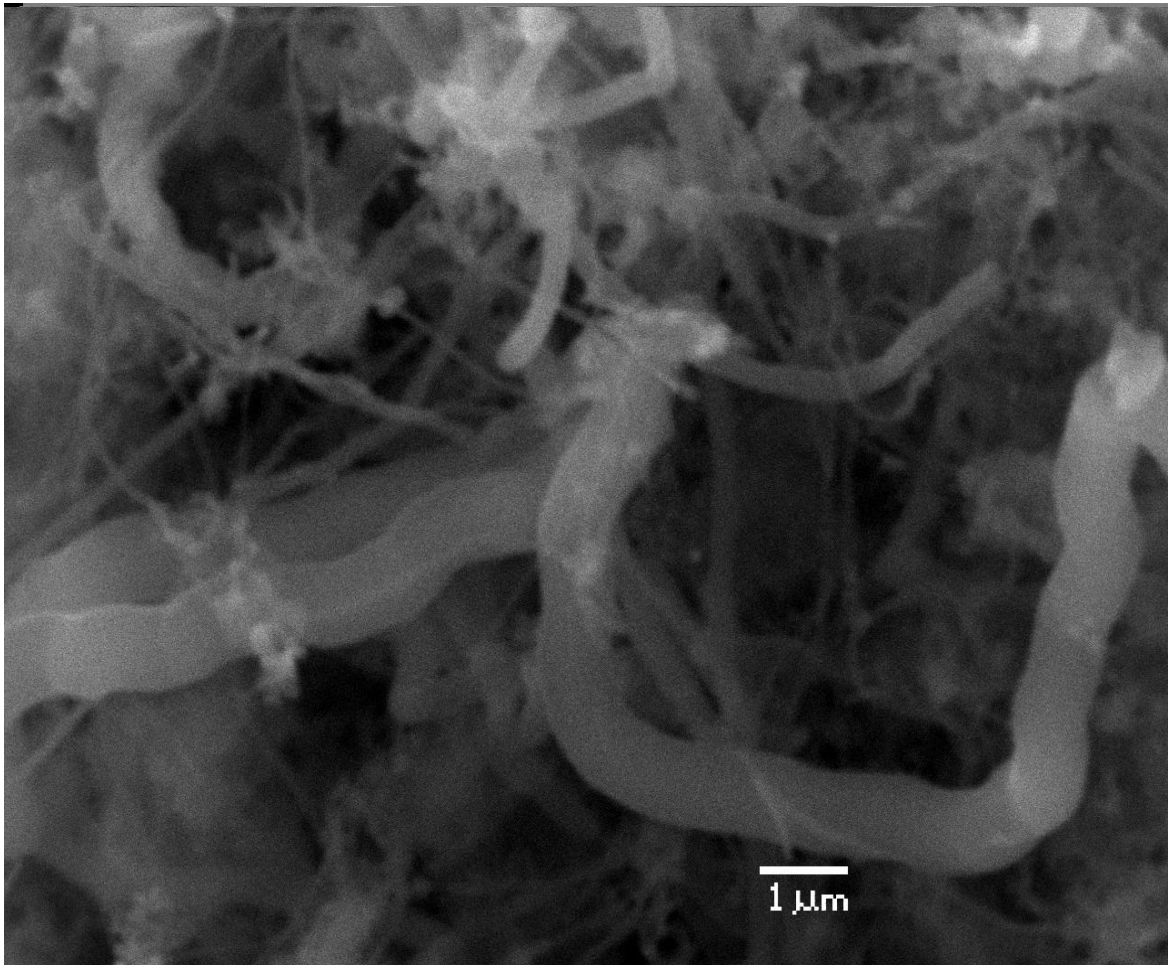

Figure 4.1.5: SEM Images of modified CNFs.

The images clearly show FA with much wider opening and higher porosity allowing higher volume of water to enter the deep inner spaces of these substances. One more advantage of FA over other carbon based adsorbents is the high content of metals which help speeding and magnifying the adsorption capacity as will be explained shortly.

Figure-4.1.8 and Figure-4.1.9 show the SEM images of the modified activated carbons and fly ashes, respectively. When these images are compared with the SEM images of regular activated carbons and fly ashes (Figure-4.1.5 and Figure-4.1.6), the effect of modification on these forms of carbons can be easily noted. In the case of fly ashes, the acid treatment exposed some of the metals surfaces as can be seen by the white spots. In addition, the acid treatment caused some damaging to the wide openings found in the regular fly ashes. This in turn reduces the fly ashes porosity. This might explain the current use of oxidation treatment for the fly ash used in the production of concrete. The oxidation process breaks the graphite sheets resulting in narrower openings and, hence, less exposed surfaces for adsorption process. The experiments as will be shown shortly support this conclusion, too.

The SEM image of the modified AC when compared to the SEM image of the regular AC (Figure-4.1.6) indicates similar observation. The regular activated carbon is reported to have approximately 40% removal of cadmium from water when the same experimental conditions applied. Therefore, the attachment of carboxyl groups to the surface of the activated carbon is expected to have some impact on the low reported adsorption capacity of regular activated carbon as will be shown shortly.

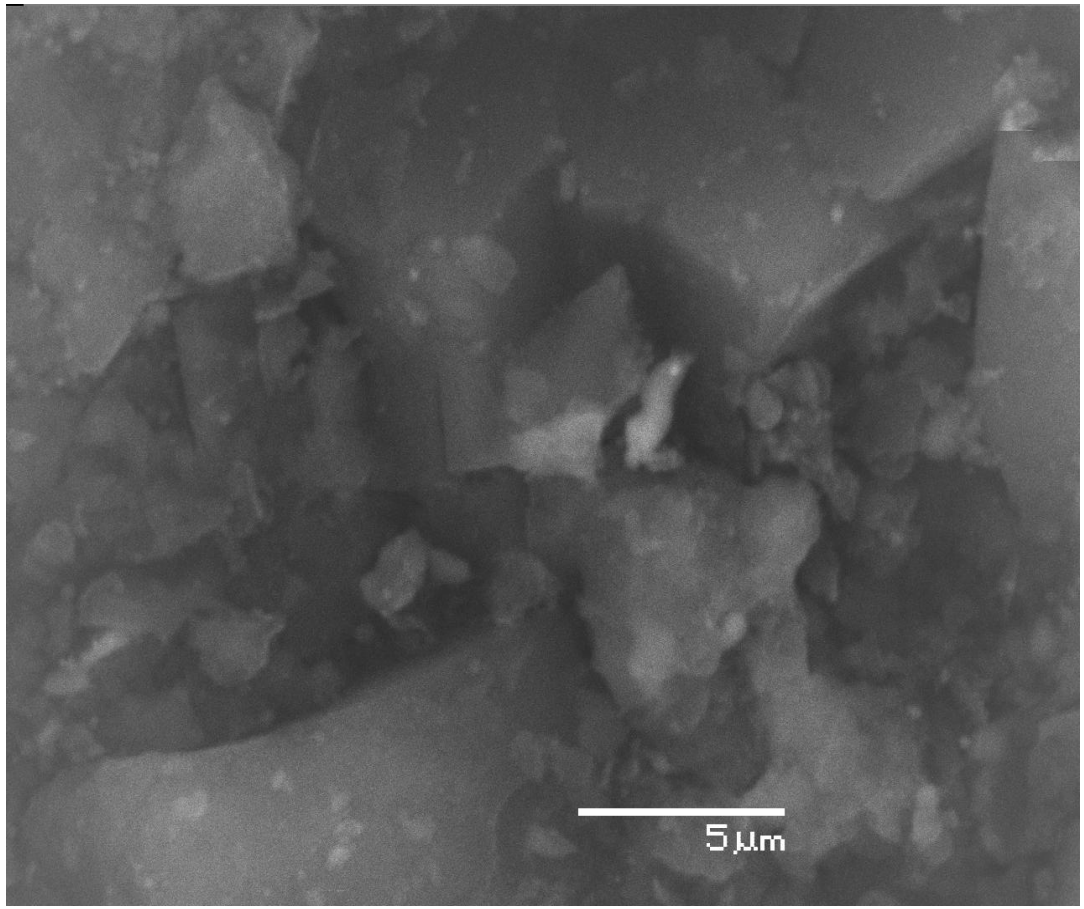

Figure 4.1.6: SEM Images of Acivated Carbon

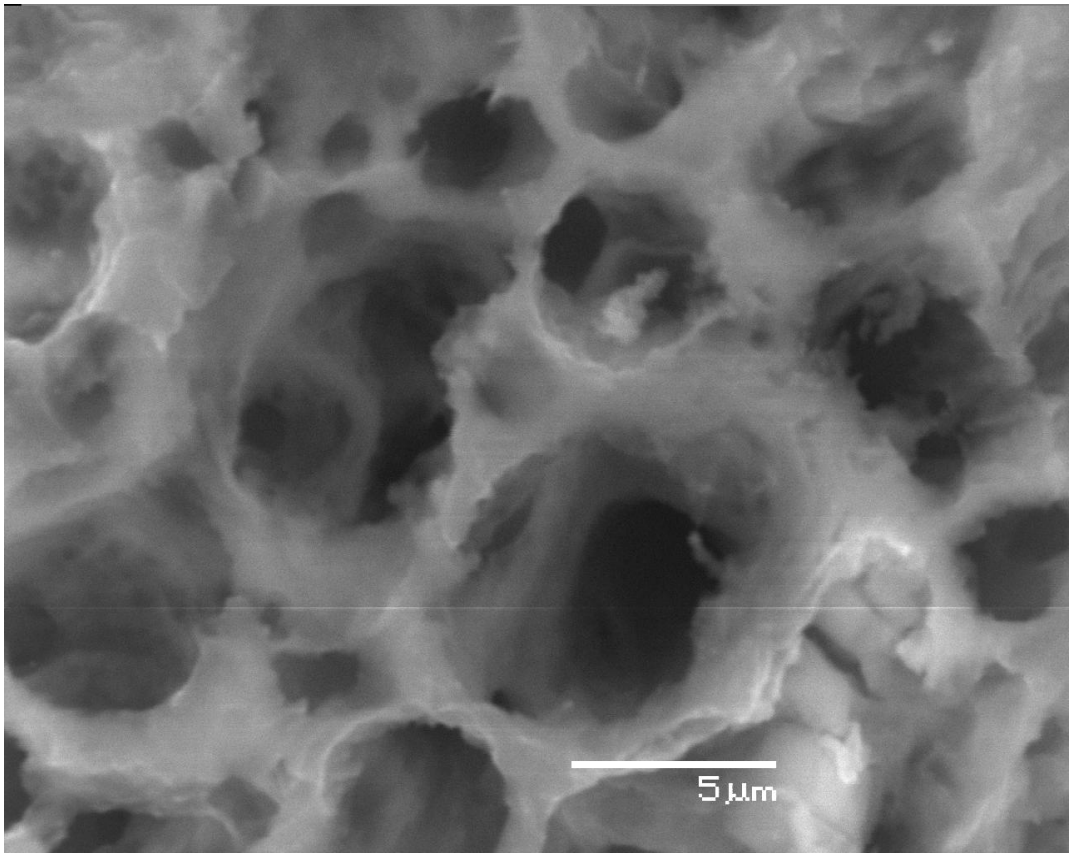

Figure 4.1.7: SEM Images of Fly Ash

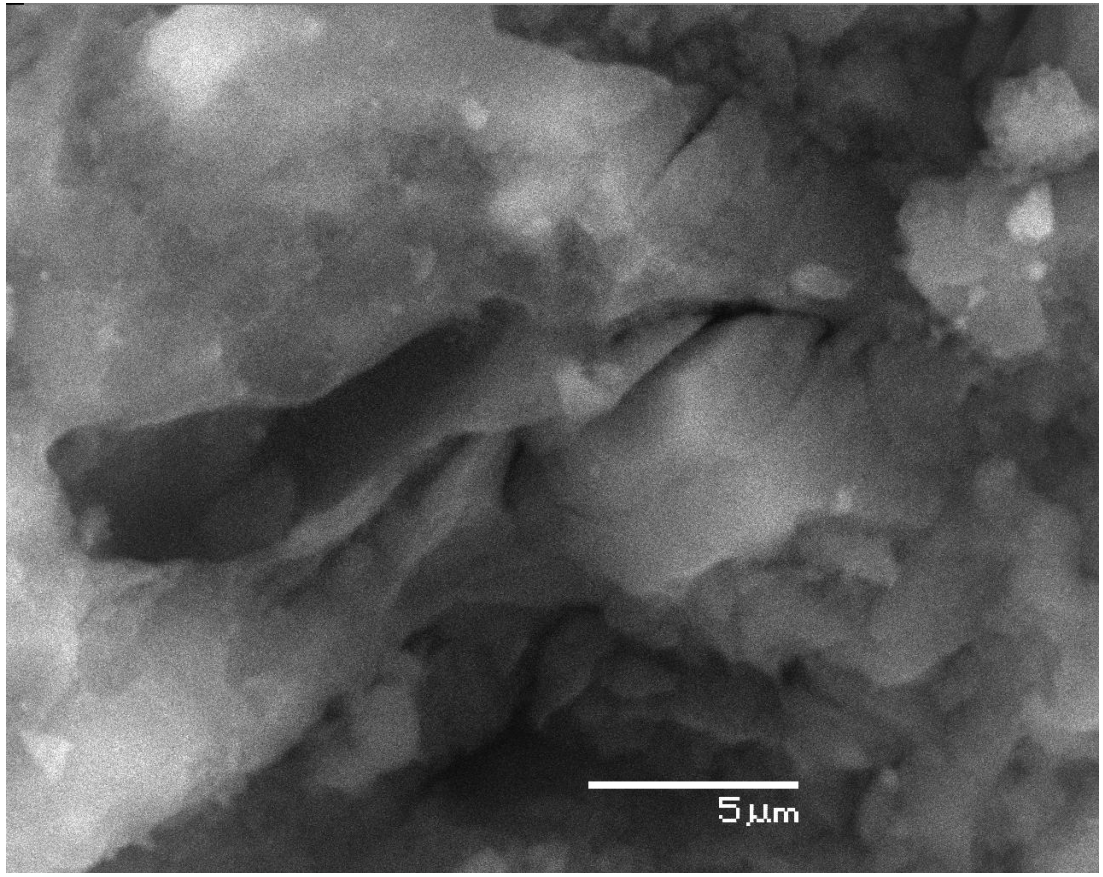

Figure 4.1.8: SEM Images of modified Activated Carbon.

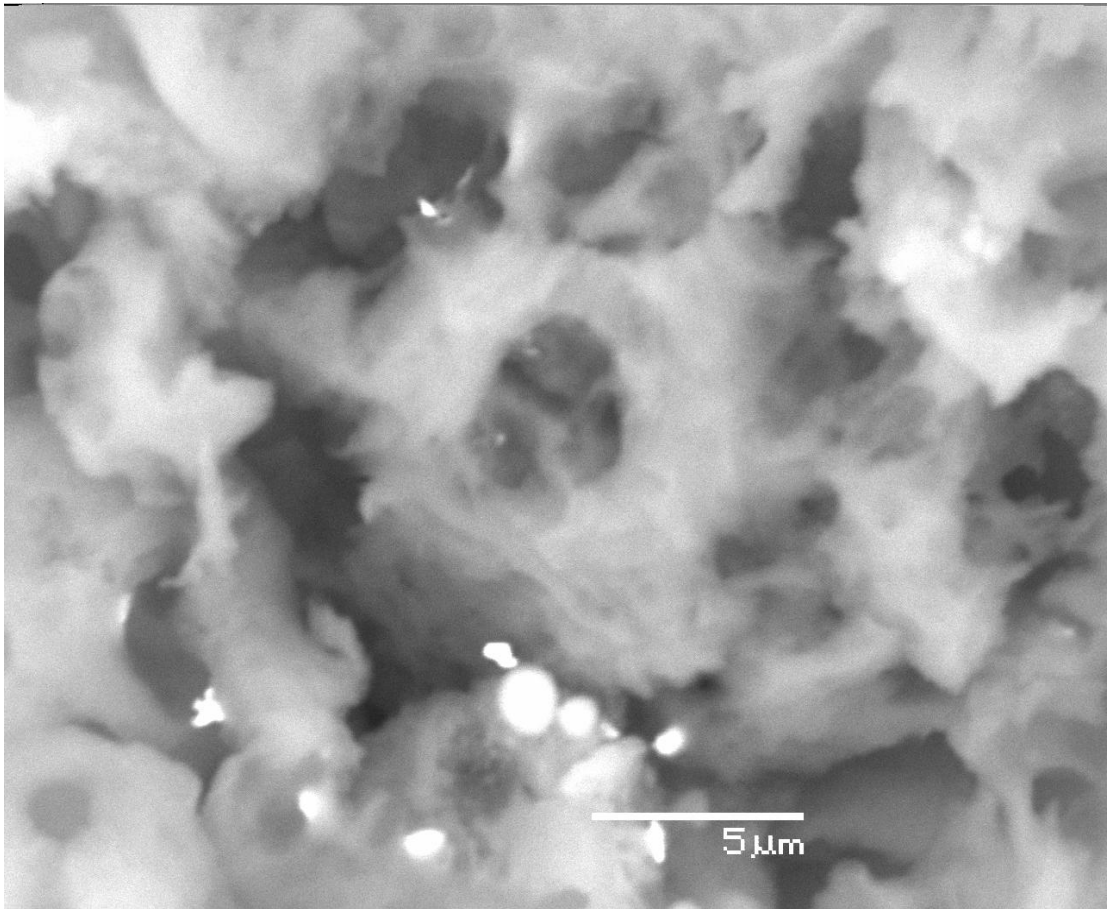

Figure 4.1.9: SEM Images of modified Fly Ash.

4.1.2 Purity Measurement of the Carbon Based Adsorbents

The thermal analyses results of Thermogravimetric (TG) and Derivative thermogravimetric (DTG) curves obtained for the four adsorbents and their modified forms at heating rates (10°C/min) are shown below. The TG thermgrams was carried out in air and it was noted that there was some residual remains of the samples, when it was heated to about 900°C.

For CNTs and CNFs, the residues appear reddish which shows that all the CNTs and CNFs were oxidized leaving only the catalyst. It can be seen that this decomposition process is a single-stage decomposition reaction where the procedural decomposition temperatures are well defined. For AC, apparently, there are volatile materials burned out during the initial heating process and impurities remain after the heating process. Figure-4.1.10 shows that the initial degradation temperature (T_i) for the CNTs was at 520°C while the maximum weight loss was at (T_m) 650°C and the final degradation temperature was at (T_f) 740°C. CNFs and AC show relatively similar behavior. However, only CNTs show one peak which indicates this CNT material is pure. The two peaks in case of CNF material makes it also practically pure. The few peaks in the case of the AC is due to the presence of approximately 8% ashes.

FA, in contrast, show a mix of different form of carbon based materials. The obtained TG thermgrams for the FA indicates that the used FA has three major components: volatile material (25% weight), carbon based material (35% weight), and other material with high temperature resistance including metals and other impurities.

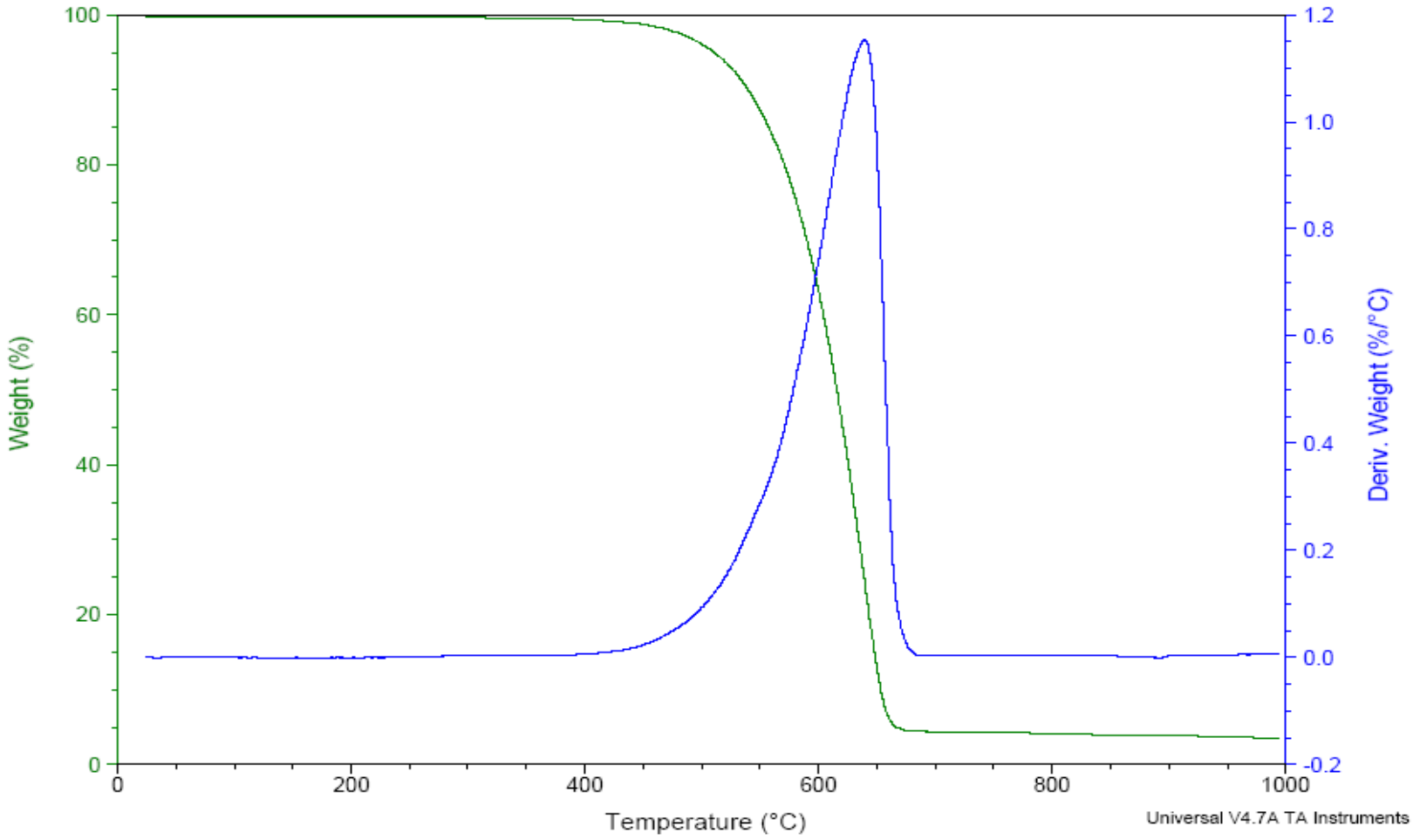

Figure 4.1.10: Thermogravimetric (TG) curve as green color Derivative thermogravimetric (DTG) curve as blue color for pure CNTs.

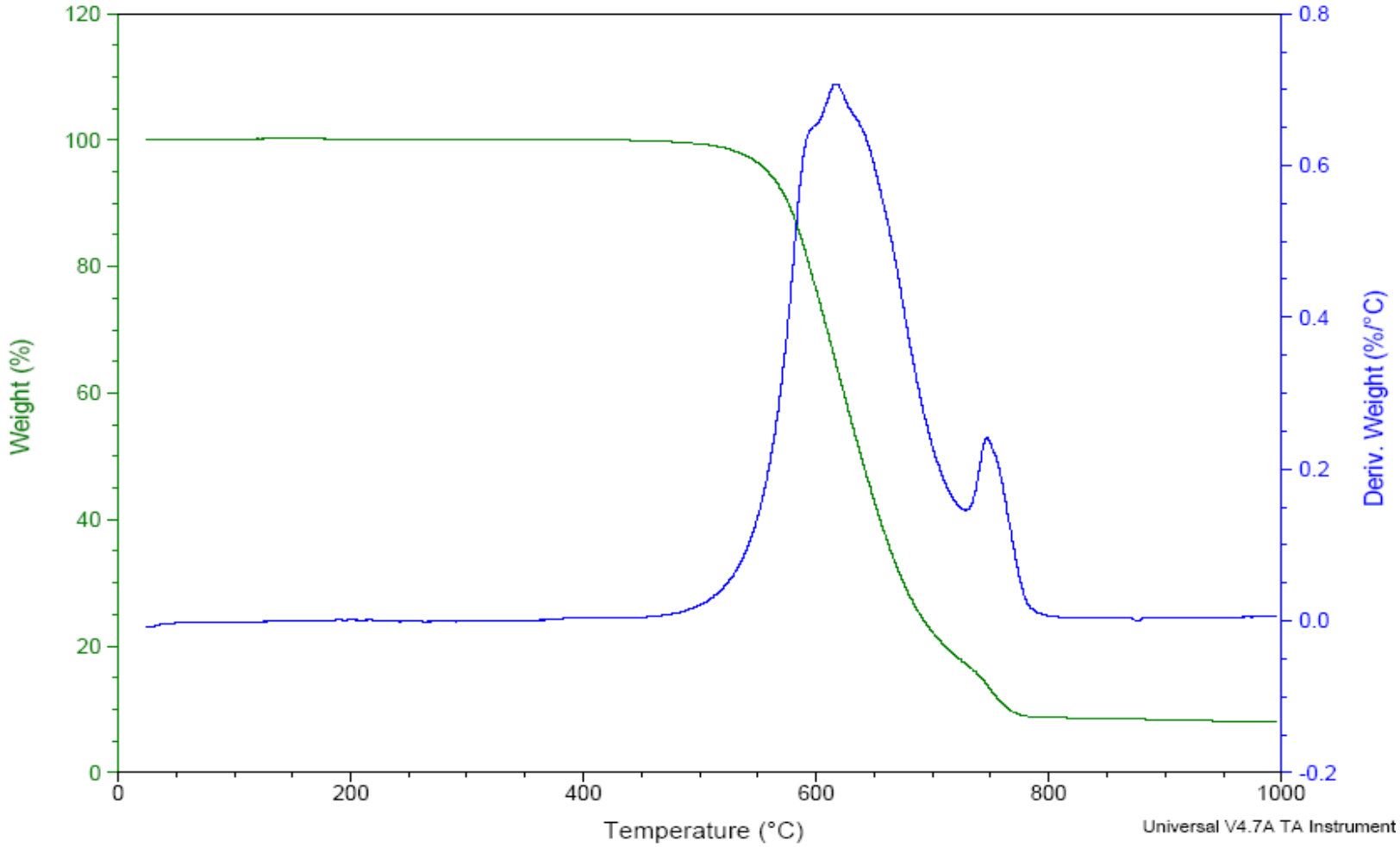

Figure 4.1.11: Thermogravimetric (TG) curve as green color Derivative thermogravimetric (DTG) curve as blue color for pure CNFs.

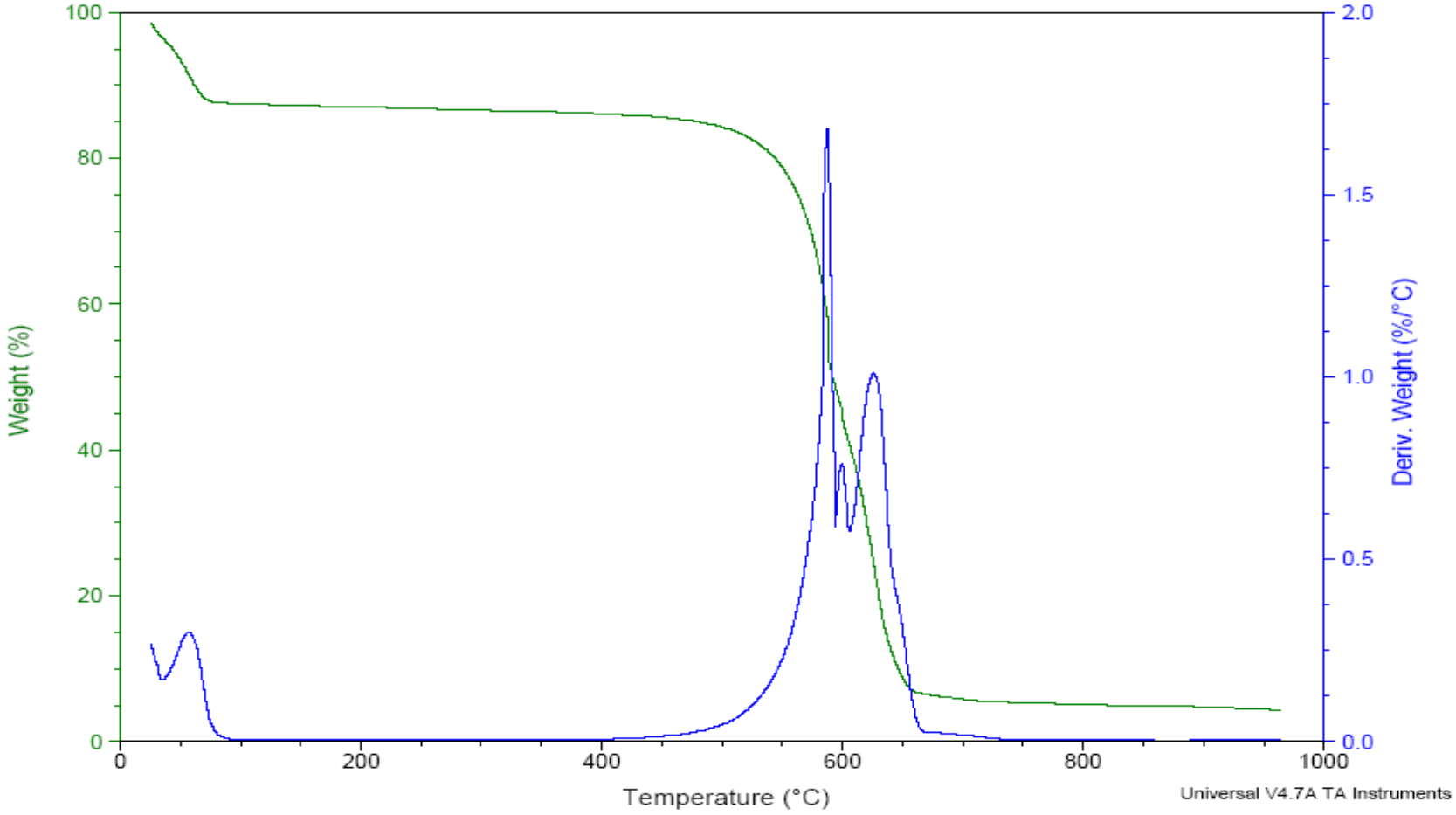

Figure 4.1.12: Thermogravimetric (TG) curve as green color Derivative thermogravimetric (DTG) curve as blue color for pure Activated Carbon.

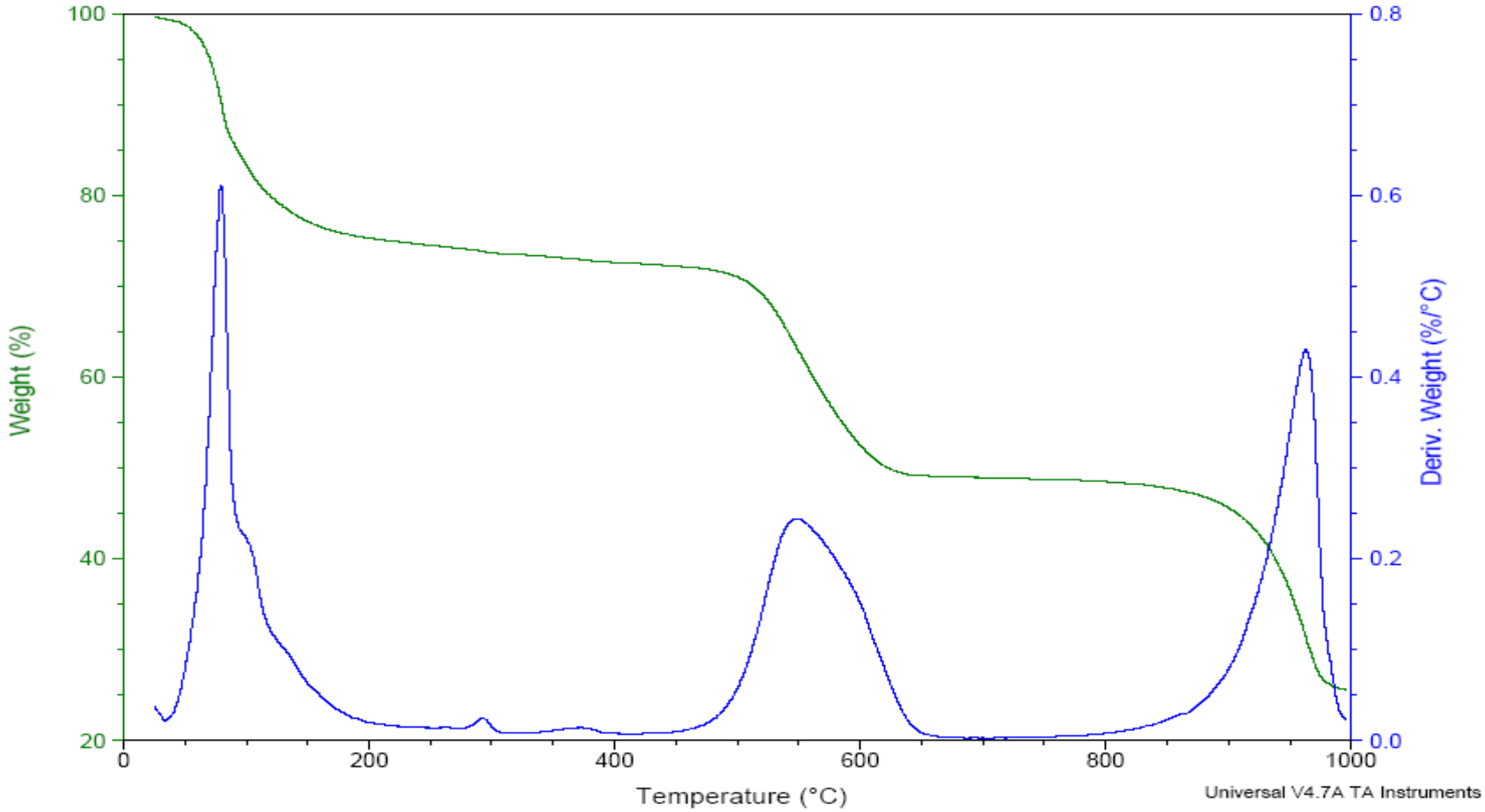

Figure 4.1.13: Thermogravimetric (TG) curve as green color Derivative thermogravimetric (DTG) curve as blue color for pure Fly Ash.

The thermal analyses results of Thermogravimetric (TG) and Derivative thermogravimetric (DTG) curves obtained for the four modified absorbents at heating rates (10°C/min) are shown in Figure-4.1.8. The TG thermgrams was carried out in air and it was noted that there was some residual remains of the samples, when it was heated to about 900°C. For modified CNTs and CNFs, the residue appears reddish which shows that all the modified CNTs and CNFs were oxidize leaving only the catalyst. It can be seen that this decomposition process is a single-stage decomposition reaction where the procedural decomposition temperatures are well defined. For the modified AC, apparently, there are volatile materials, burned out during the initial heating process, and impurities, remain after the heating process.

Figure-4.1.14 shows that the initial degradation temperature (T_i) for the modified CNTs was at 520°C while the maximum weight loss was at (T_m) 570°C and the final degradation temperature was at (T_f) 640°C. When compared to regular CNTs, the modification treatment reduced the T_m and T_f of by approximately 100°C. The modified CNFs (Figure-4.1.15) shows one peak compared to regular CNFs where two peaks are obtained. It can be noted from comparing the TG of modified AC (Figure-4.1.16) with regular AC that the acid treatment clean up the activated carbons and improve the purity. This conclusion is obtained by the single peak in case of the modified activated carbon. Similar behavior is also obviously observed for fly ashes.

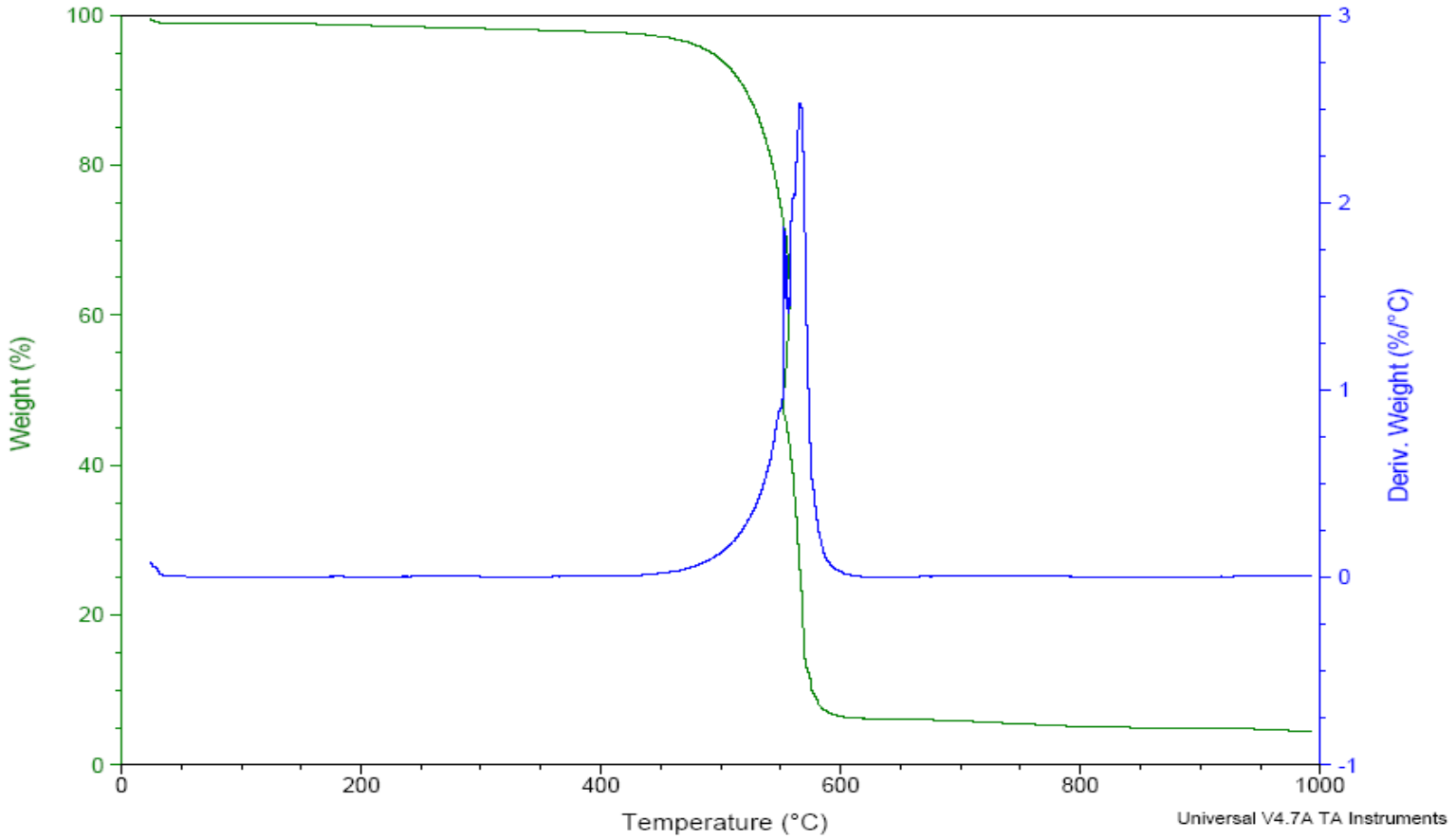

Figure 4.1.14: Thermogravimetric (TG) curve as green color Derivative thermogravimetric (DTG) curve as blue color for Modified CNTs

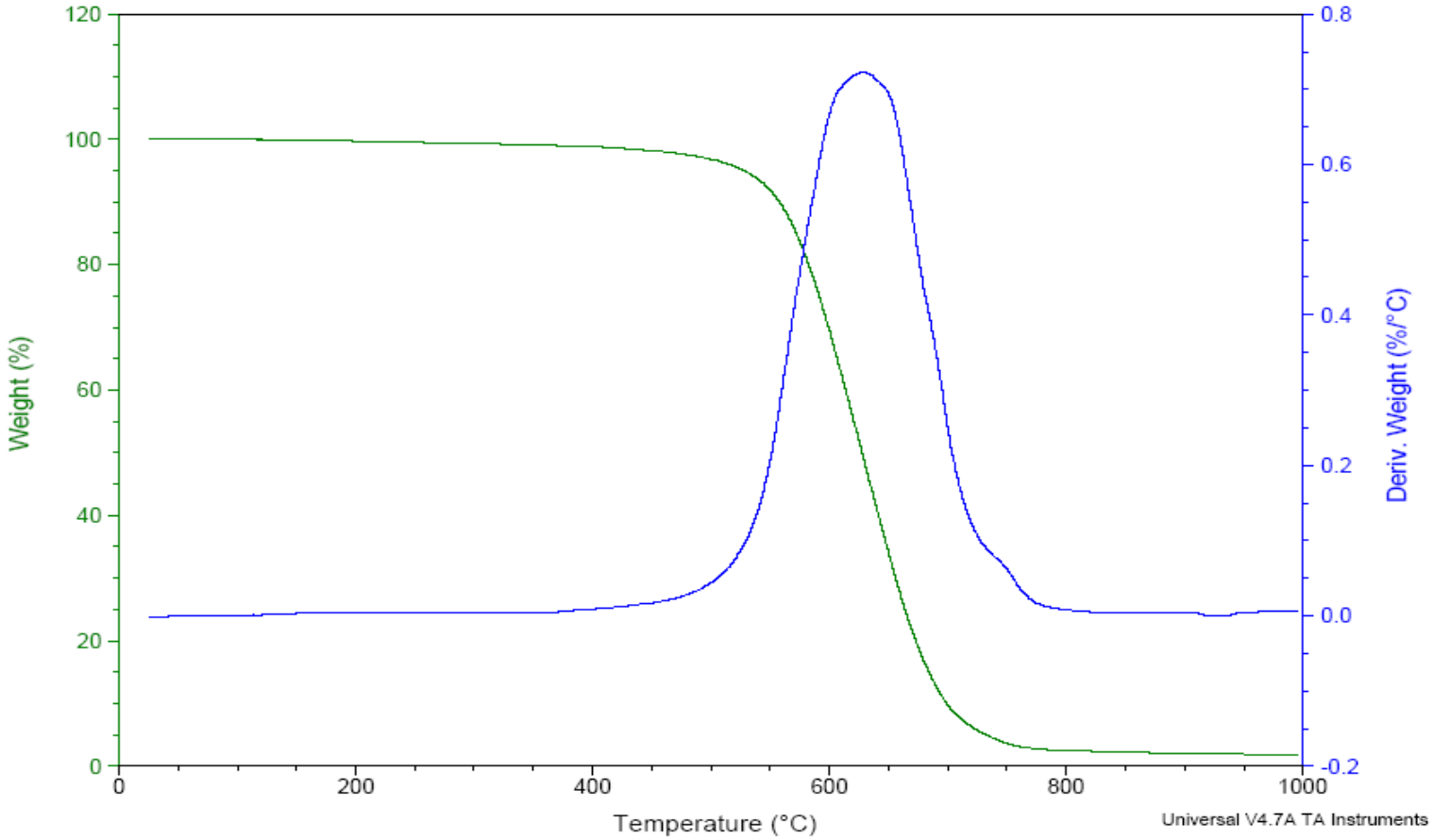

Figure 4.1.15: Thermogravimetric (TG) curve as green color Derivative thermogravimetric (DTG) curve as blue color for Modified CNFs

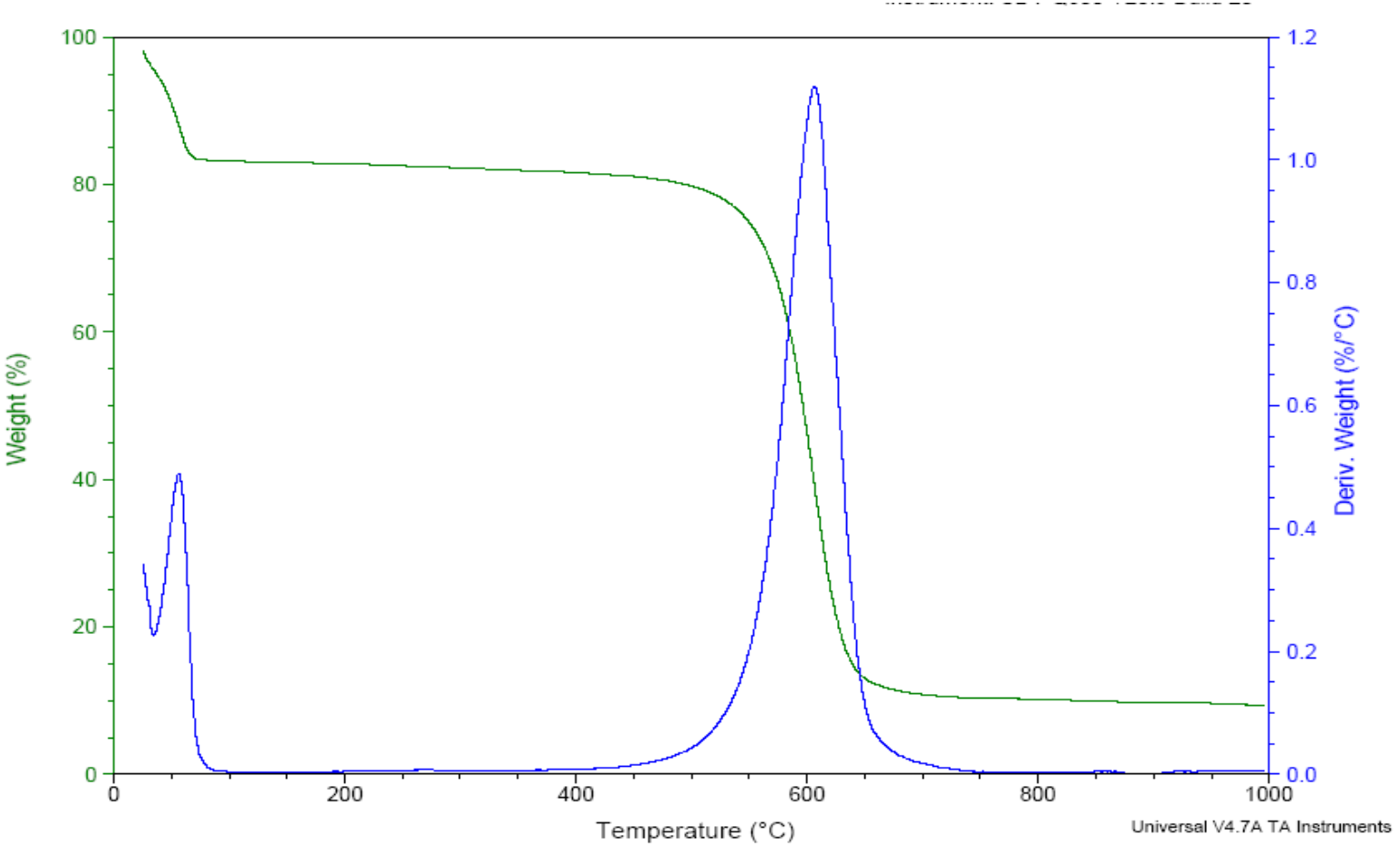

Figure 4.1.16: Thermogravimetric (TG) curve as green color Derivative thermogravimetric (DTG) curve as blue color for Modified Activated Carbon

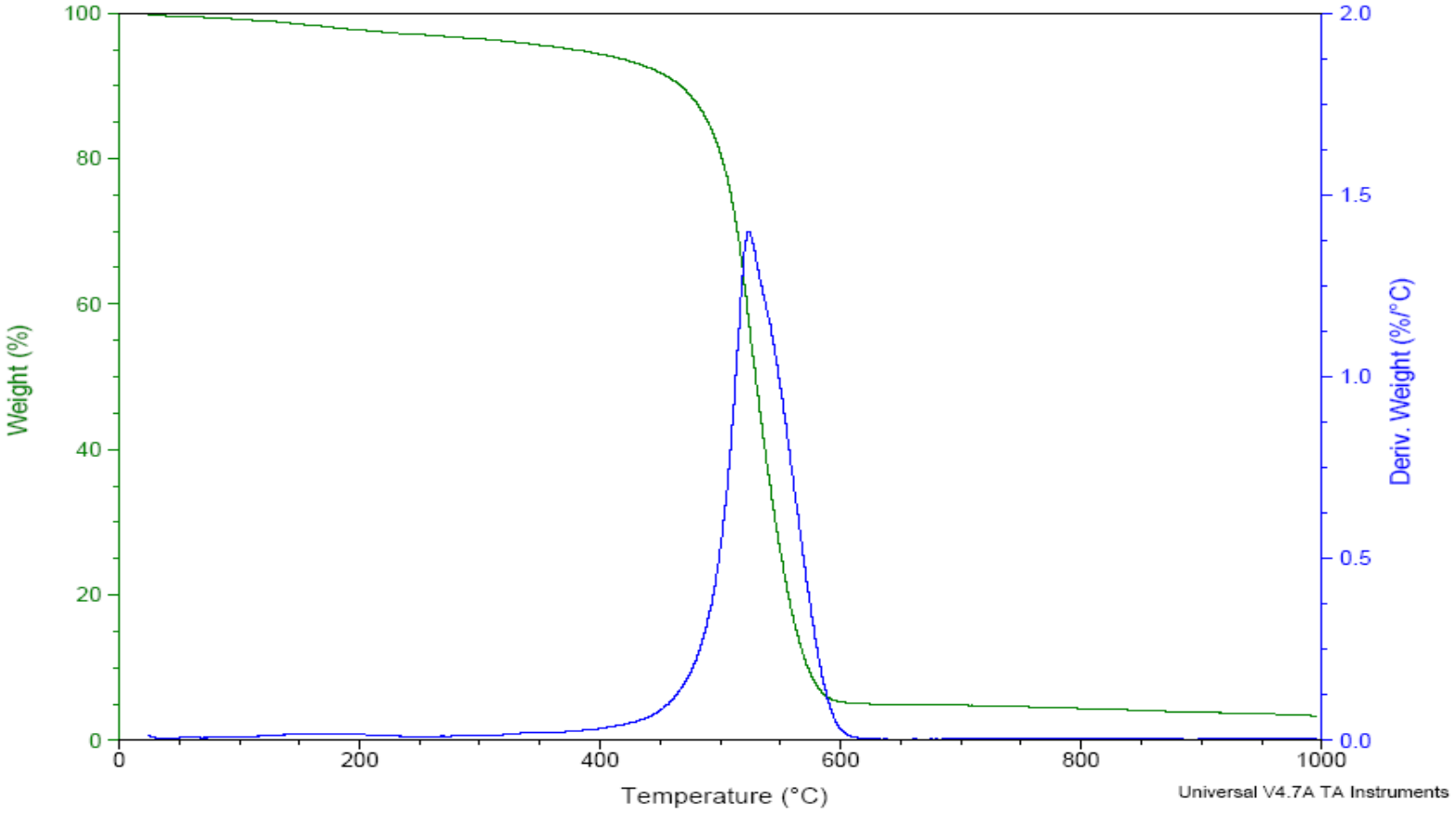

Figure 4.1.17: Thermogravimetric (TG) curve as green color Derivative thermogravimetric (DTG) curve as blue color for Modified Fly Ash.

FA modification (Figure-4.1.17) changes the TG carve significantly. While regular FA show a mix of different form of carbon based materials with three degradation zones, the modified FA becomes a pure material with single initial degradation temperature and single DTG peak. With regular FA 40%, by weight, of material remains available for temperature as high as 900°C. However, the modified FA is over 90% degradable for less than 600°C.

4.2 Removal of Cadmium and Chromium (VI) from Water

In this work of research, the effect of pH, agitation speed, contact time, and adsorbent dosage rate on the uptake of cadmium (II) and chromium (VI) were investigated to find the optimum conditions for the maximum removal of these heavy metals from water. The percent removals of cadmium (II) and chromium (VI) were determined to measure the adsorption capacity of each adsorbent.

4.2.1 Removal of Cadmium using Carbon Based Adsorbents

The parameters affect on the removal of Cadmium (II) are:

4.2.1.1 Effect of pH

The pH of aqueous solution is one of the important variables impacting the adsorption rate of heavy metal ions. The pH value controls the adsorption of ion at the solid-water interfaces and affects the solubility of the metal ions, concentration of the counter ions on the functional groups of the adsorbent and the degree of ionization of the adsorbate during the reaction.

The pH was found to be a predominant factor affecting the removal of cadmium ions under the conditions studied. Cadmium species can be present in dionized water in the forms of Cd^{2+}, $Cd(OH)^{+}$, $Cd(OH)_{2(s)}$ [58]. At low pH, the dominant cadmium species is Cd^{2+} in the form of complex $[Cd(H_2O)_6]^{2+}$ [58]. The removal of cadmium by the four adsorbents with various pHs has been studied and the results are shown in Figure-4.2.1.

The variations of pH used in the experiments are within the range of 2 to 8. The same phenomenon of the effect of pH was observed for all adsorbents. With the increasing of the pH from 4 to 7 the removal of cadmium in the solution, by CNTs, CNFs, and AC, increases. There was no removal for cadmium (Cd^{2+}), for these three adsorbents, at lower than pH 4. This happened due to the strong competition of H^{+} with $Cd2^{+}$ on the adsorption sites. At pH 7 the maximum percentage removals of cadmium, by CNTs, CNFs, and AC, were found to be approximately 27%, 34% and 38%, respectively. In contrast, FA shows much superior adsorption of metal ions from solution for the entire studied pH range. The reported adsorption capacity of FA, as shown in Figure-4.2.1, is 95% that is almost three times that for the other three carbon based adsorbents.

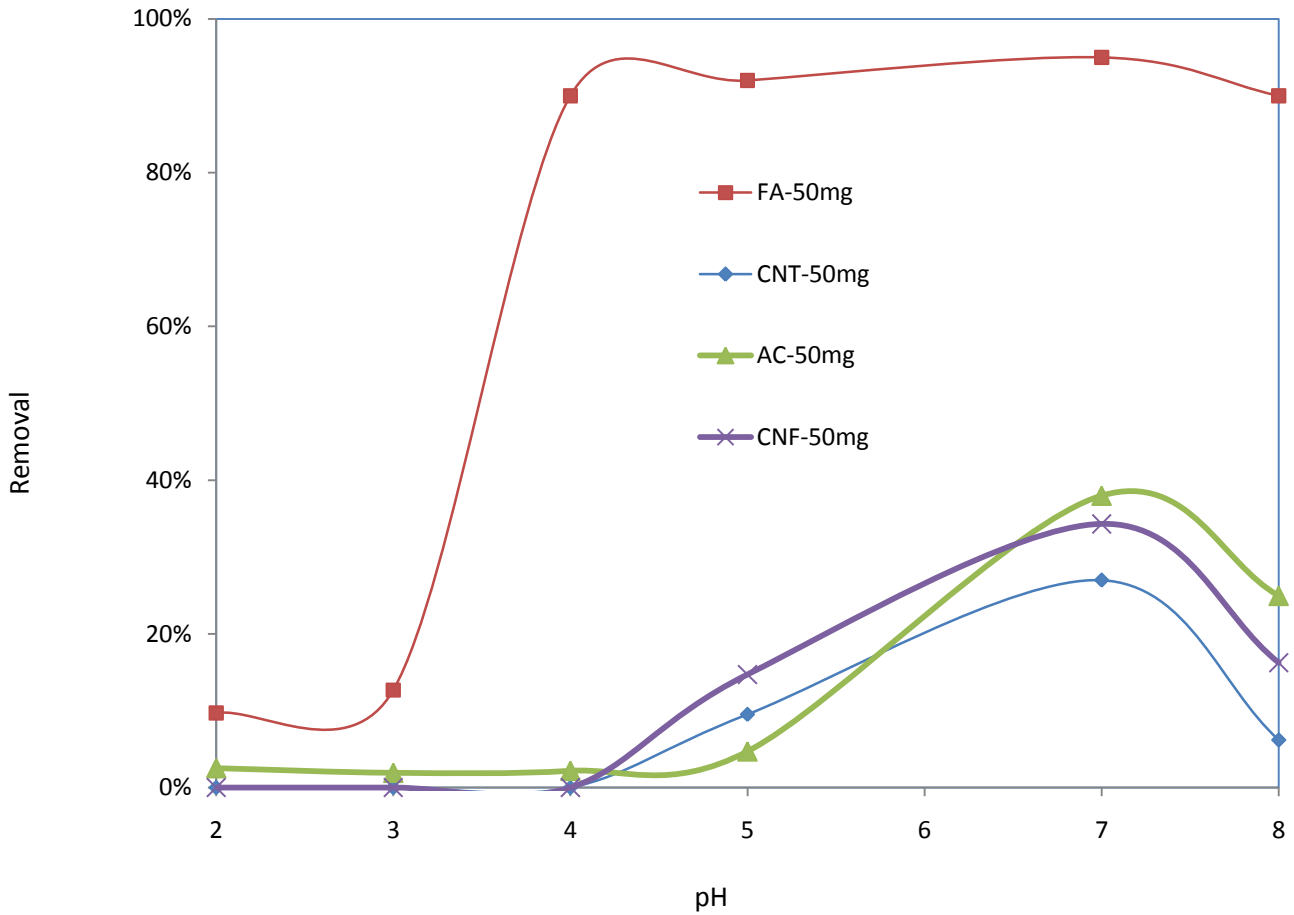

Figure 4.2.1: The effect of pH on percentage removal of Cadmium at 150 rpm.

The dominant metallic species at pH> 6.0 is $Cd(OH)_2$ and those at pH< 6.0 is Cd^{2+} and $Cd(OH)^+$ [70]. The increase in metal adsorption at pH above 6.0 can be related to the withholding of $Cd(OH)_2$ into microspores of carbon particles. The superior Cd^{2+} removal by FA can be related to the surface charge development between the fly ash and the concentration distribution of metal ions since both of them are pH dependent [71]. The maximum adsorption of Cd(II) ions, as Cd^{2+}, at equilibrium conditions for pH 7.0 is believed to occur by electrostatic attraction [58]. Ricou-Hoeffer and others suggested that the Cd(II) ions are perhaps adsorbed on the surface of alumina metal present in the fly ashes [72]. Therefore, the adsorption with alumina metal and possibly other metals present in fly ashes under study could be explained by the strong tendency towards chemical bonding between the Cd(II) ions and these metals.

The weakness of removal of Cd(II) at pH values lower than 4 can be explained by the competition between H^+ and Cd^{2+} ions present in low pH solution for the same sorption site [62].

The removal of cadmium by the four modified adsorbents with various pHs has been studied and the results are shown in Figure-4.2.2. The variation of pH used in the experimental work is within the range of 2 to 8. Similar phenomenon of the effect of pH was observed for all modified adsorbents. With the increasing of the pH from 3 to 7 the removal of cadmium in the solution, by the modified CNTs, CNFs, and FA, increases. At pH 7 the maximum percentage removals of cadmium, by M-FA, and M-CNFs, were found to be approximately 74% and 55%, respectively. In contrast, M-

CNTs and AC show much superior adsorption of cadmium ions from solution for the entire studied pH range. The observed adsorption removals of M-CNTs and M-AC, as shown in Figure-4.2.2, are around 93% and 98%, respectively.

Figure-4.2.1 demonstrates the removal percentage of cadmium ions from water as a function of pH by the four carbon based absorbents in their regular forms. From Figure-4.2.2 it can be shown that modification of CNTs, CNFs, and AC has significantly improved the removal capacity. In contrast, the modification of FA has adversely impacted the removal capacity. This lower removal by the modified FA is due to the washout of adsorbent-active surfaces from the fly ashes during the acid treatment of the oxidation process. In addition, the acid treatment was found to reduce porosity of fly ashes as explained by the SEM images.

The dominant metallic species at pH> 6.0 is $Cd(OH)_2$ and those at pH< 6.0 are Cd^{2+} and $Cd(OH)^{+}$ [58]. The increase in metal adsorption at pH above 6.0 can be related to the withholding of $Cd(OH)_2$ into microspores of carbon particles. The superior $Cd2^{+}$ removal by CNTs and AC can be related to the surface charge development by the carboxyl functional groups attached to the activated carbons and the concentration distribution of metal ions since both of them are pH dependent [70]. The maximum adsorption of Cd(II) ions, as $Cd2^{+}$, at equilibrium conditions for pH 7.0 is believed to occur by electrostatic attraction [71]. The low removal efficiency of cadmium at low pH values is due to the low dissociation of the carboxylic groups and competition between H^{+} and Cd^{2+} ions at this low pH value [58].

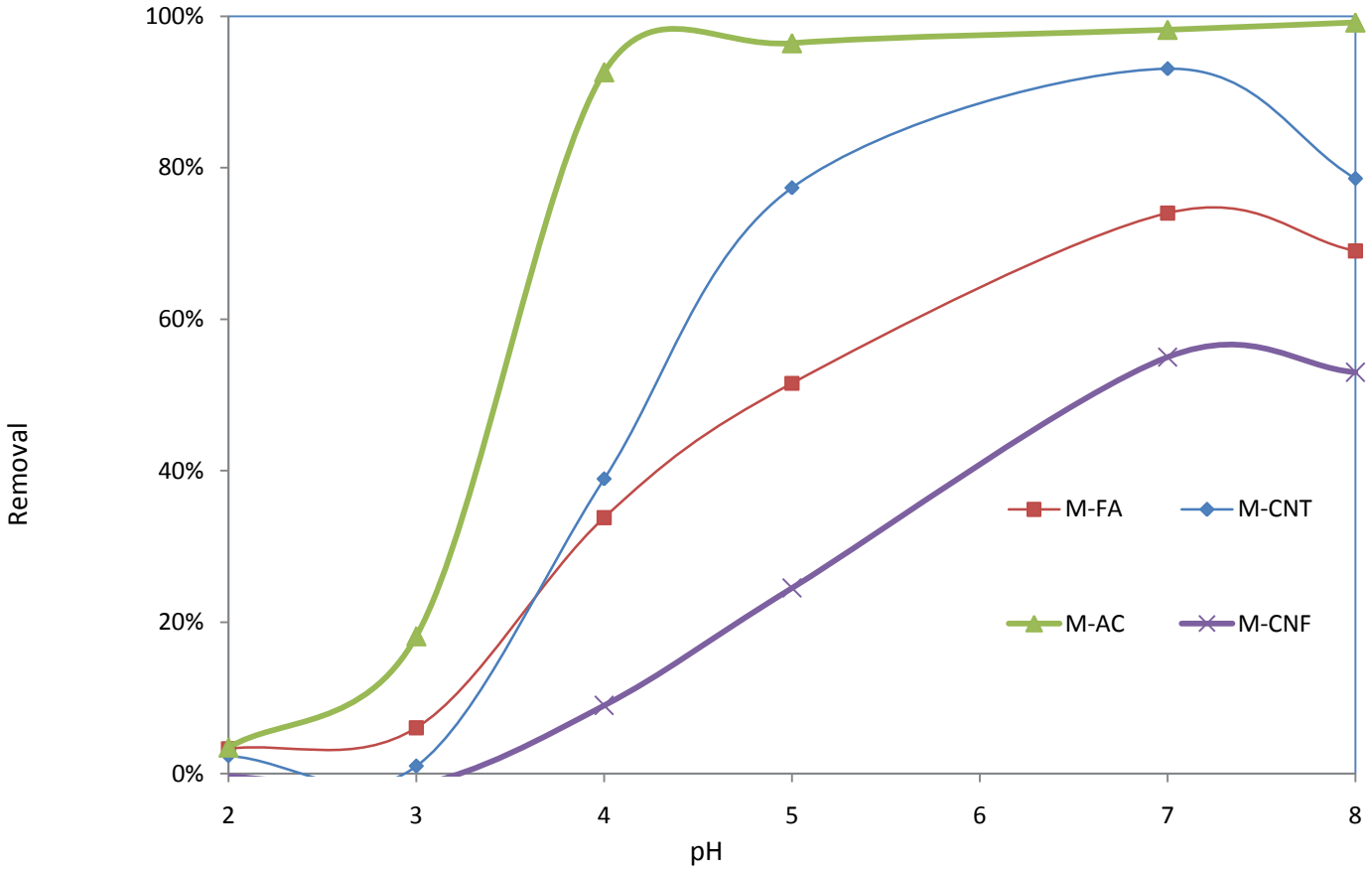

Figure 4.2.2: The effect of pH on percentage removal of Cadmium at 150 rpm.

4.2.1.2 Effect of Agitation Speed

The peak removal at pH 7 was used to study the effect of the agitation speed on adsorption capacity of cadmium by the four adsorbents. By varying the speed of agitation from 50 to 250 rpm as shown in Figure-4.2.3, it has been observed that the percentage of cadmium removal increases with increasing speed up to the agitation speed of 150 rpm for all adsorbents, then the speed start declining slightly with increasing agitation speed for CNTs, CNFs and FA; while the cadmium removal by AC continue increasing slightly with increasing speed beyond the 150 rpm.

Agitation facilitates proper contact between the metal ions in solution and the adsorbents binding sites and thereby promotes effective transfer of cadmium ions to the carbon active sites. This is due to the fact that, the increase of agitation speed, improves the diffusion of cadmium ions towards the surface of the adsorbents. From Figure-4.2.3, it can be concluded that the contact between solids and liquid is more effective at 150 rpm for cadmium removal under the removal condition stated under this study.

Similarly, the peak removal at pH=7 was used to study the effect of the agitation speed on adsorption capacity of cadmium by the four modified adsorbents. By varying the speed of agitation from 50 to 250 rpm as shown in Figure-4.2.4, it has been observed that the percentage of cadmium removal increases with increasing speed up to the agitation speed of 150 rpm for the M-CNTs, M-CNFs, and M-AC, then the speed start declining slightly or remain constant with increasing agitation speed.

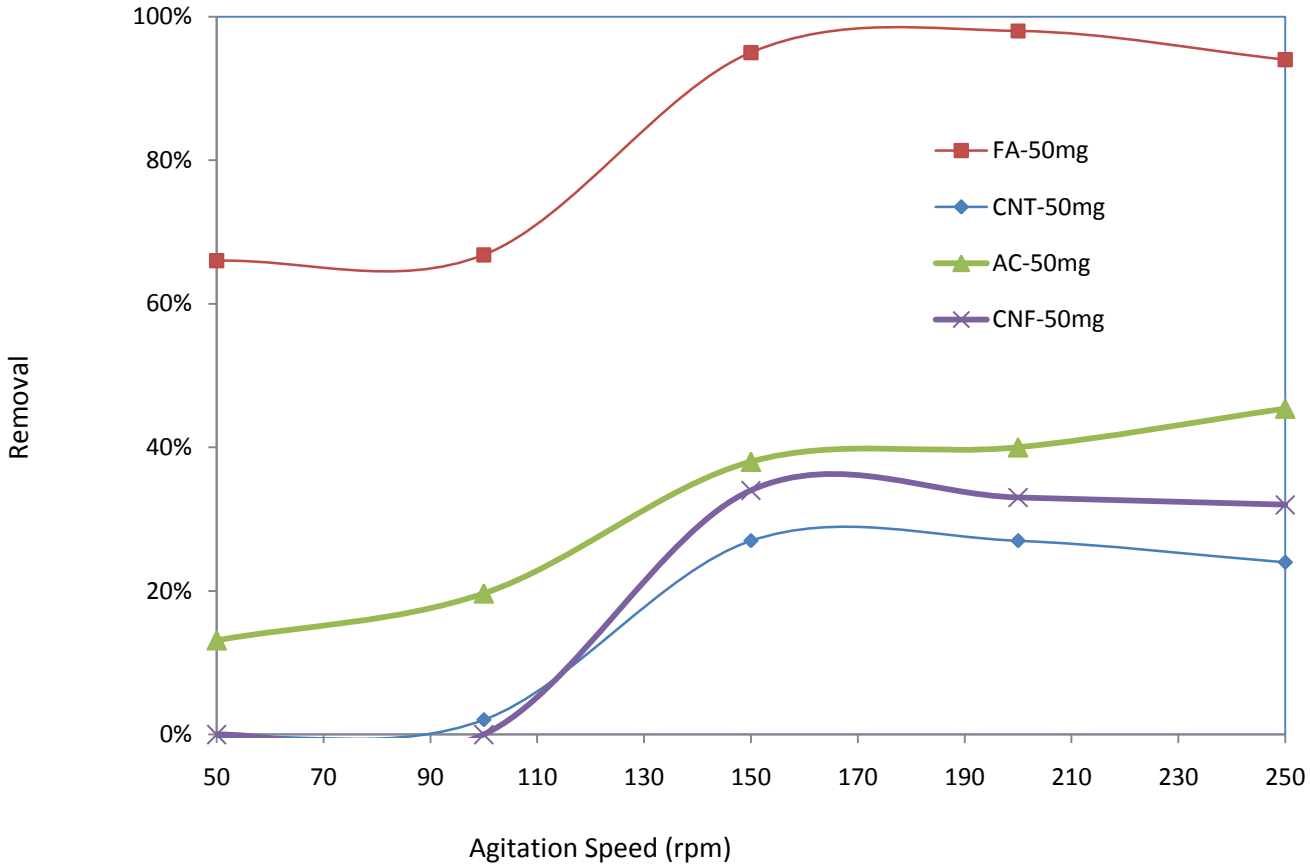

Figure 4.2.3: The effect of agitation speed on percentage removal of cadmium at pH 7.

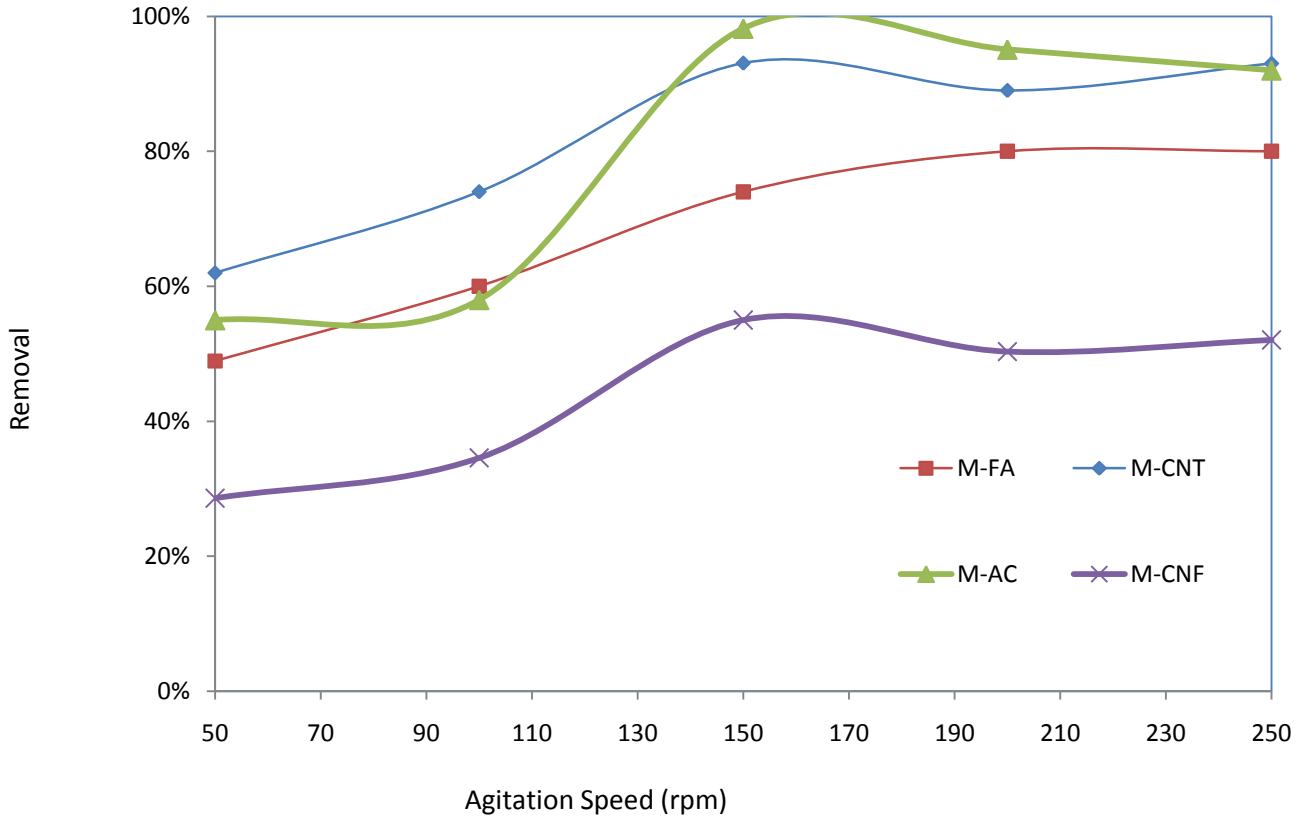

Figure 4.2.4: The effect of agitation speed on percentage removal of cadmium at pH 7.

For the modified FA, cadmium removal continue increasing with increasing speed up to 200 rpm; however, the maximum removal of M-FA is still below the removal achieved by regular FA at the same experimental conditions.

Agitation facilitates proper contact between the metal ions in solution and the adsorbents binding sites and thereby promotes effective transfer of cadmium ions to the carbon active sites. From Figure-4.2.4, it can be concluded that the contact between solids and liquid is more effective at 150 rpm for cadmium removal under the removal condition stated under this study for all adsorbents except for FA where higher removal was found to be still achievable at higher speed.

4.2.1.3 Effect of Contact Time

The adsorption behavior of Cadmium by these four adsorbents as a function of contact time was carried out by varying the equilibrium time from 10 minutes to 24 hours at a Cd concentration of 1 mg/L, a dose of adsorbent of 50mg/L, and optimum pH of 7. The agitation speed was kept constant at 150 rpm though out the experiments time.

The results presented in Figure 4.2.6 show that the adsorption rate reach to the equilibrium for all adsorbents after two hours and the removal rates of Cd were about 27%, 34%, 38% and 95 percent for the CNTs, CNFs, AC and FA, respectively. It is indicating that by using FA, the reaction is much faster and the adsorption sites are well exposed as compared to other adsorbents, which have much lower capacity for adsorption. No further increase in removal efficiency was observed with time for all the four adsorbents after two hours contact time.

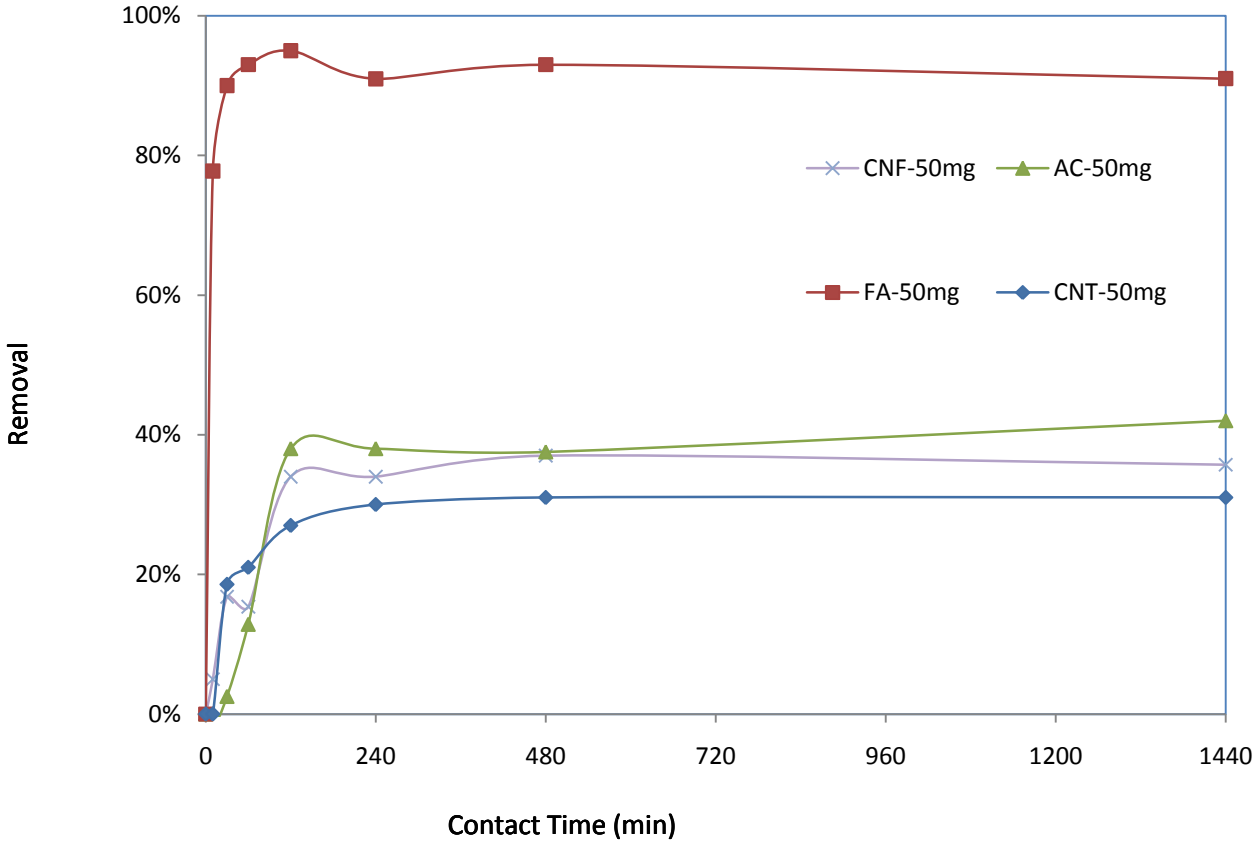

Figure 4.2.5: The effect of contact time on percentage removal of cadmium at 150 rpm at pH 7.

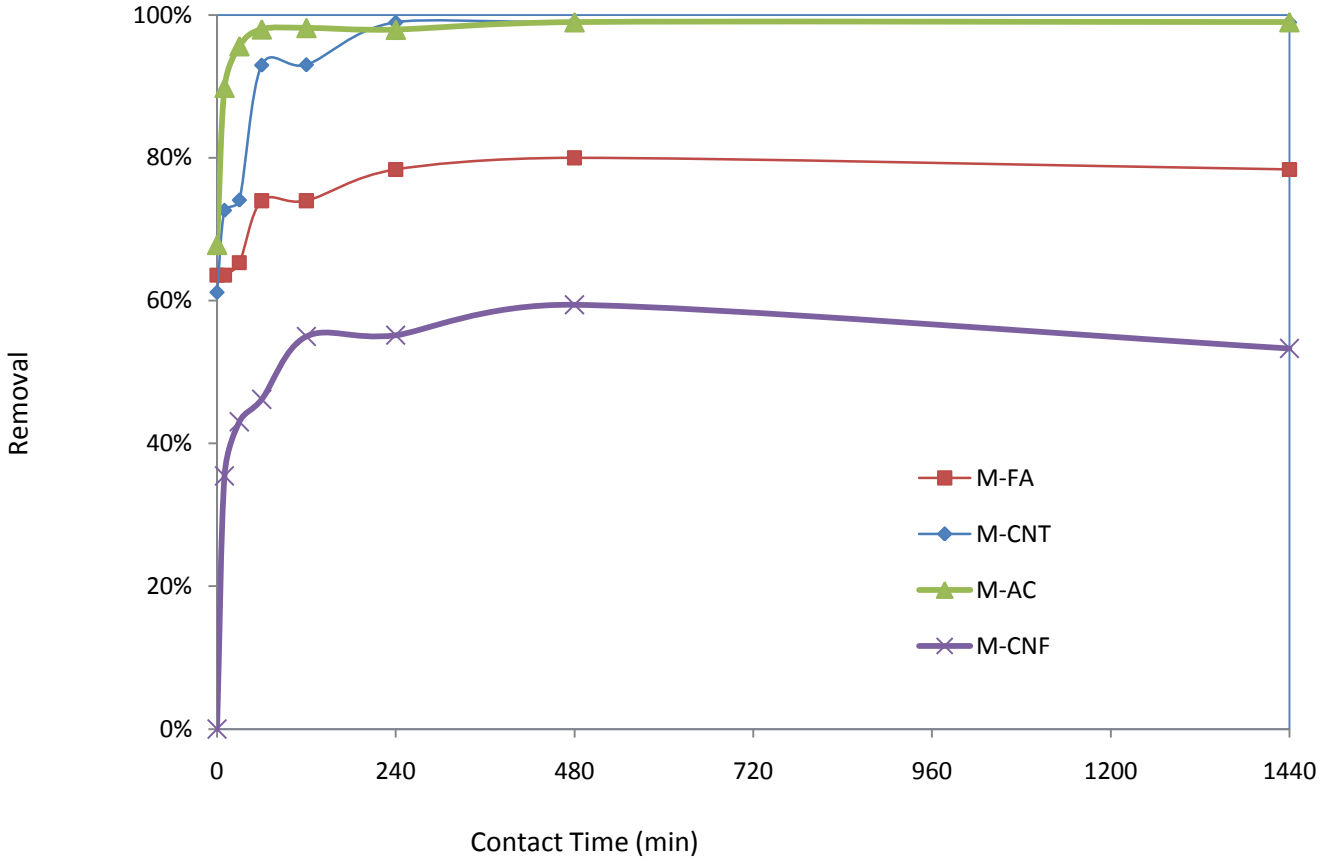

Figure 4.2.6: The effect of contact time on percentage removal of cadmium at 150 rpm at pH 7.

The adsorption behavior of Cadmium by the four modified adsorbents as a function of contact time was carried out by varying the equilibrium time from 10 minutes to 24 hours at a Cd^{2+} concentration of 1 mg/L, a dose of adsorbent of 50mg/L, and optimum pH of 7. The agitation speed was kept constant at 150 rpm though out the experiments time.

The results presented in Figure-4.2.6 show that the adsorption rate reach to the equilibrium for all adsorbents after two hours and the removal rates of Cd were about 93%, 55%, 98% and 75 percent for the M-CNTs, M-CNFs, M-AC and M-FA, respectively. It is indicating that by using M-CNTs and M-AC, the reaction is much faster and the adsorption sites are well exposed as compared to the other two adsorbents, which have relatively lower capacities for adsorption. No further increase in removal efficiency was observed with time for all the four modified adsorbents after two hours contact time.

4.2.1.4 Effect of Adsorbent Dosage Rate

The amount of adsorbent in the water is one of the major factors, which affect the adsorption capacity. The batch adsorption experiments were carried out by using various amounts of regular and modified adsorbents from 25 to 250 mg while the pH, agitation speed and contact time were fixed at 7, 150 rpm and 120 minutes, respectively. The results shown in Figure-4.2.7 indicated that the adsorption capacity increases with increases in adsorbent dosage up to 50 mg dosage, then remains almost constant for the rest of dosage range. For the range below 50 mg, the increase in

percentage removal with the increase in dosage rate is expected because the higher the dosage of adsorbents in the solution, the greater the availability of exchangeable sites for ions. However, after certain dosage rate, which is 50 mg in this study, the dosage rate was found to have no effect on the percentage removal. This would indicate that the Cd removal is a function of the concentration of the Cd2+ ions in the solution. From figure-4.2.7, it can be reported that the maximum Cd (II) removals, for the conditions specified under this study, remain the same: 27%, 34%, 38% and 95 percent for the CNTs, CNFs, AC and FA, respectively.

The batch adsorption experiments were carried out by using various amounts of the modified adsorbents ranging from 25 to 250 mg while the pH, agitation speed and contact time were fixed at 7, 150 rpm and 120 minutes, respectively. The results shown in Figure-4.2.8 indicated that the adsorption capacity increases with increases in adsorbent dosage up to 50 mg dosage for M-AC and M-FA, then remains almost constant for the rest of dosage range.

M-CNTs show similar behavior; however, M-CNFs continue increasing with increasing dosage but at very slow rate. The removal rate was found to be possible to increase from 93% to 98% but by doubling or tripling the dosage rate. M-CNFs show steady increase in removal with increases in dosage up to 150 mg. By using 150 mg dosage rate of M-CNFs, the cadmium removal was found to increase from 55% to around 80%. With higher dosage rate, M-CNFs was found to compete with M-FA. For the range below 50 mg, the increase in percentage removal with the increase in dosage rate is expected because the higher the dose of adsorbents in the solution, the greater the availability of exchangeable sites for ions.

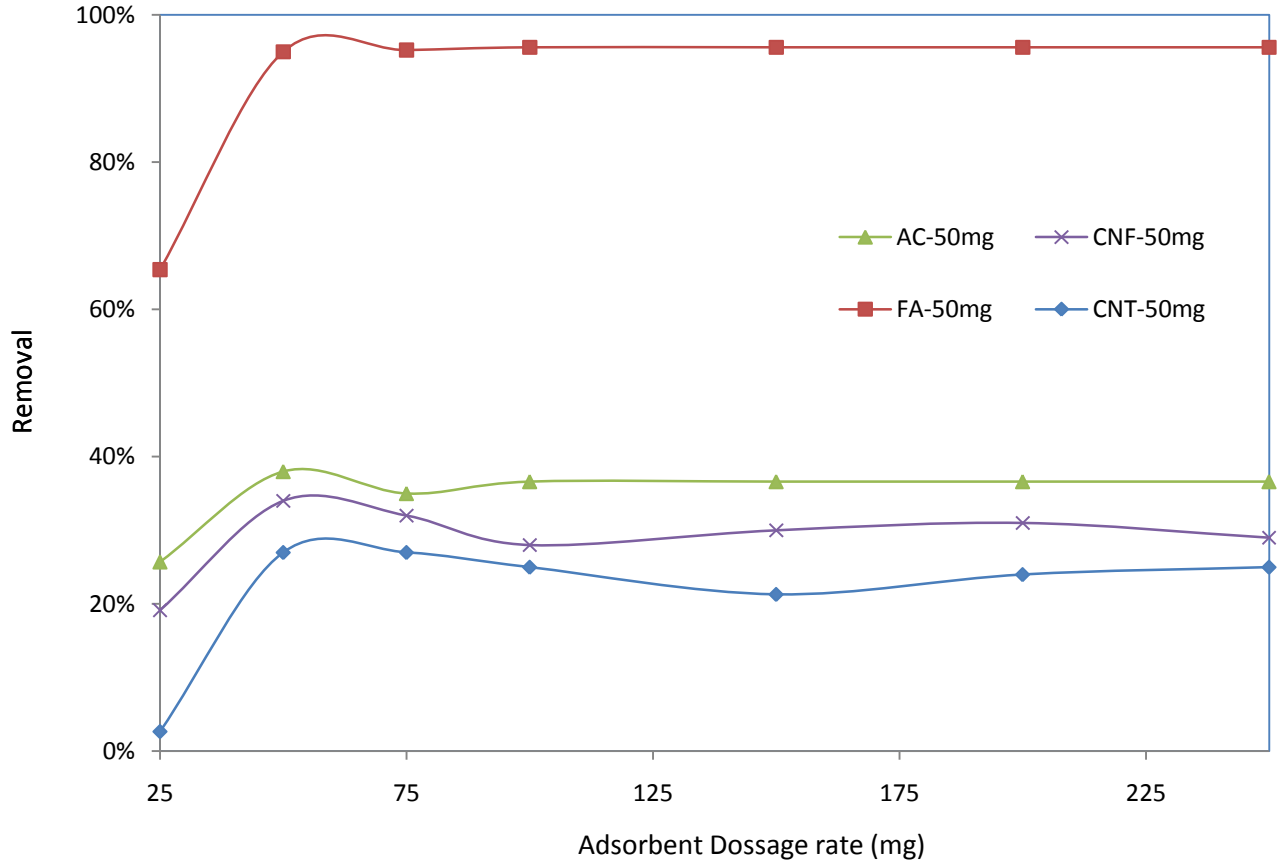

Figure 4.2.7: The effect of adsorbents dosage on percentage removal of cadmium at pH 7.

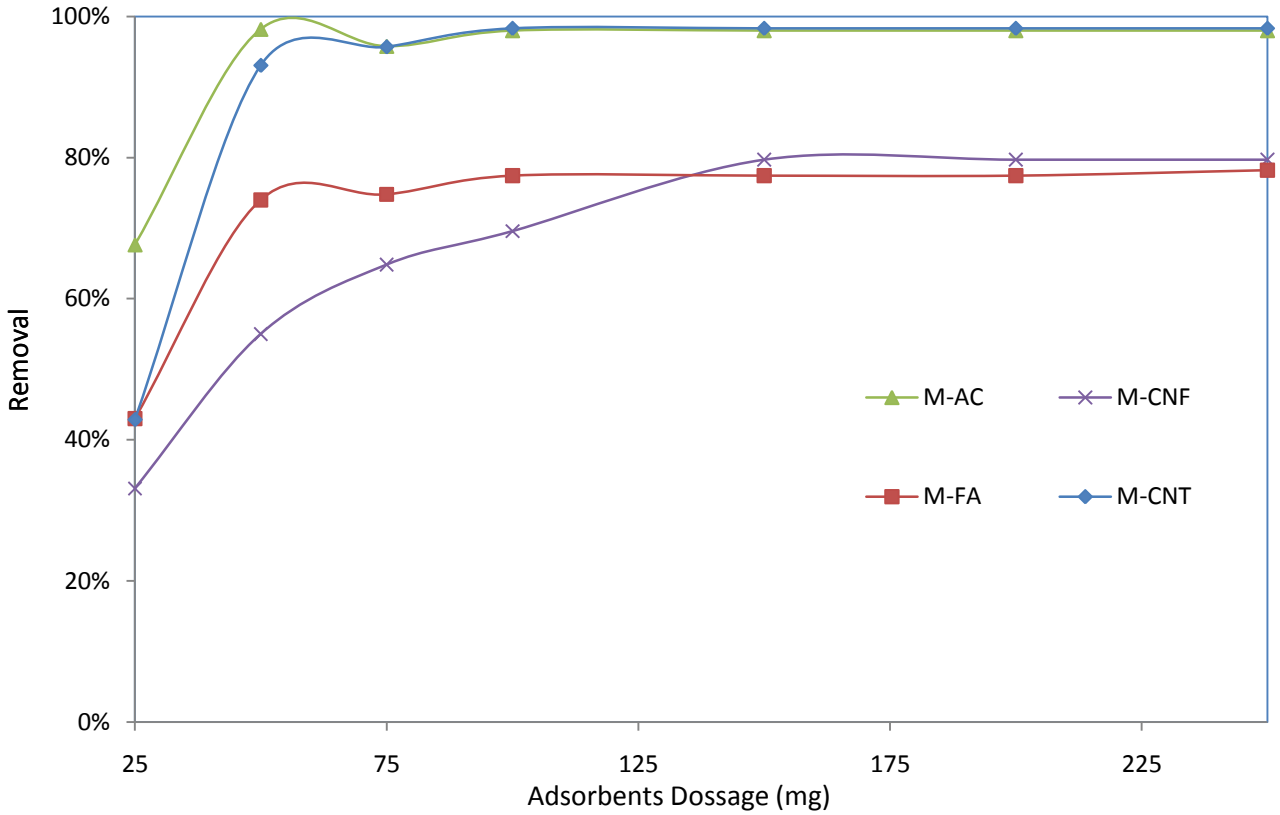

Figure 4.2.8: The effect of Modified Adsorbents Dosage on percentage removal of cadmium at pH 7.

However, after certain dosage rate, the dosage rate was found to have no effect on the percentage removal. This would indicate that the Cd removal is a function of the concentration of the Cd^{2+} ions in the solution. From figure-4.2.8, it can be reported that the maximum Cd (II) removals, for the conditions specified under this study, remain the same: 98%, 98%, 80%, and 74 percent for the M-CNTs, M-AC, M-CNFs, and M-FA, respectively.

4.2.2 Removal of Chromium (VI) Using Carbon Based Adsorbents

4.2.2.1 Effect of pH

The pH was found to be a major factor affecting the removal of Cr(VI) ions under the condition studied. The removal of chromium (VI) by the four regular and modified absorbents with various pHs has been studied and the results are shown in Figure-4.2.9.

The variations of pH used in the experiments are within the range of 2 to 8. From Figure-4.2.9 & 10, it can be concluded that the regular and modified CNFs and FA do not remove Cr(VI) from water at all pH range from 2 to 8. However, for CNTs and AC the highest removal were achieved at pH 3 to 4. The maximum percentage removals of chromium (IV), by CNTs, AC, M-CNTs and M-AC, were found to be approximately 47%, 44%, 42%, and 55%, respectively. It can be seen that modification improves the removal efficiency of Cr(VI) by AC, but have negligible effect on CNTs.

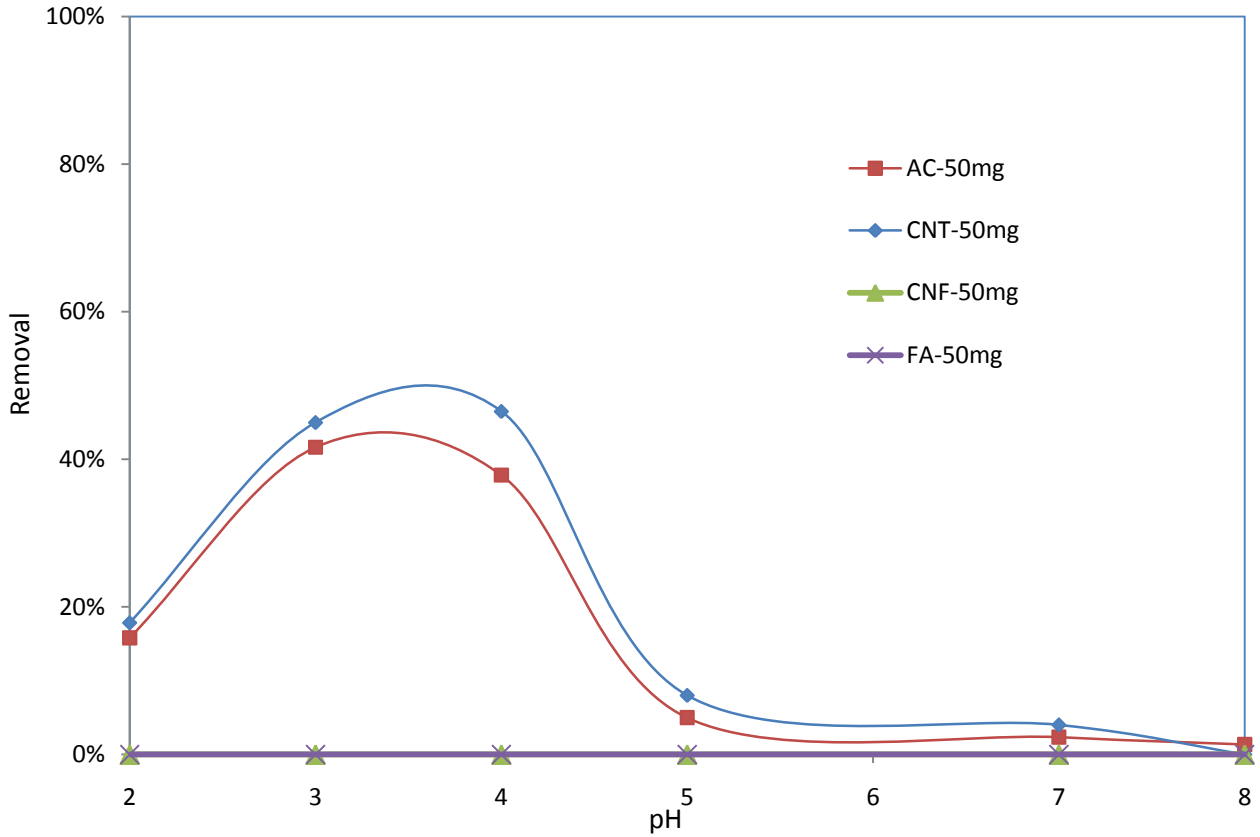

Figure 4.2.9: The effect of pH on percentage removal of chromium (VI) by the Carbon Based Adsorments

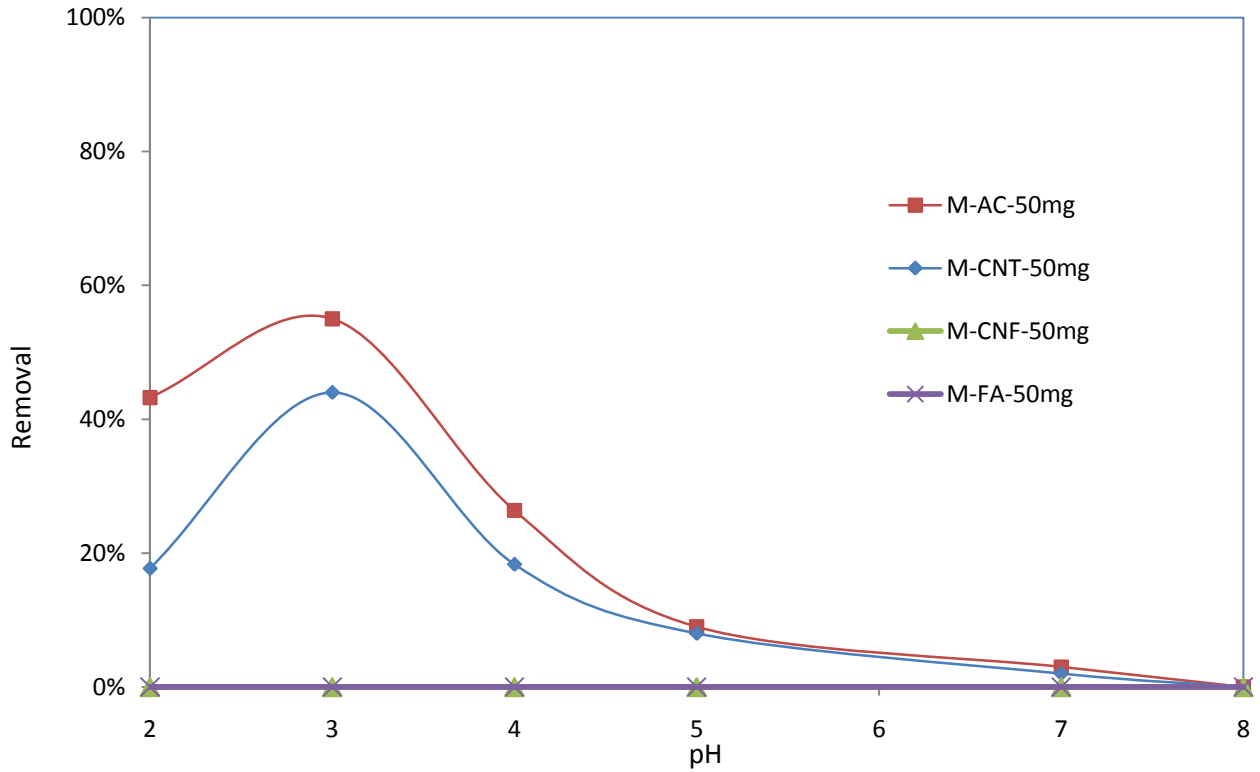

Figure 4.2.10: The effect of pH on percentage removal of chromium (VI) by the Modified Carbon Based Adsorments

4.2.2.2 Effect of Agitation Speed

The peak removal at pH 3 was used to study the effect of the agitation speed on adsorption capacity of chromium (VI) by the four absorbents. The agitation speed was also found to have no effect on Cr(VI) removal by CNFs and FA for the regular and modified forms. By varying the speed of agitation from 50 to 250 rpm, as shown in Figure-4.2.11, it has been observed that the percentage of chromium removal increased with increasing speed up to the agitation speed of 200 rpm for the AC and M-AC, whereas it has almost no influence on CNTs and M-CNTs for the whole speed range.

From Figure-4.2.11, it can be shown that the modification of CNTs has no effect on Cr(VI) removal efficiency; in contrast, with increased agitation speed to above 200 rpm, the removal efficiency by M-AC was improved by almost 10% over the removal by the regular AC.

This is due to the fact that, the increase of agitation speed, improves the diffusion of chromium ions towards the surface of the AC.

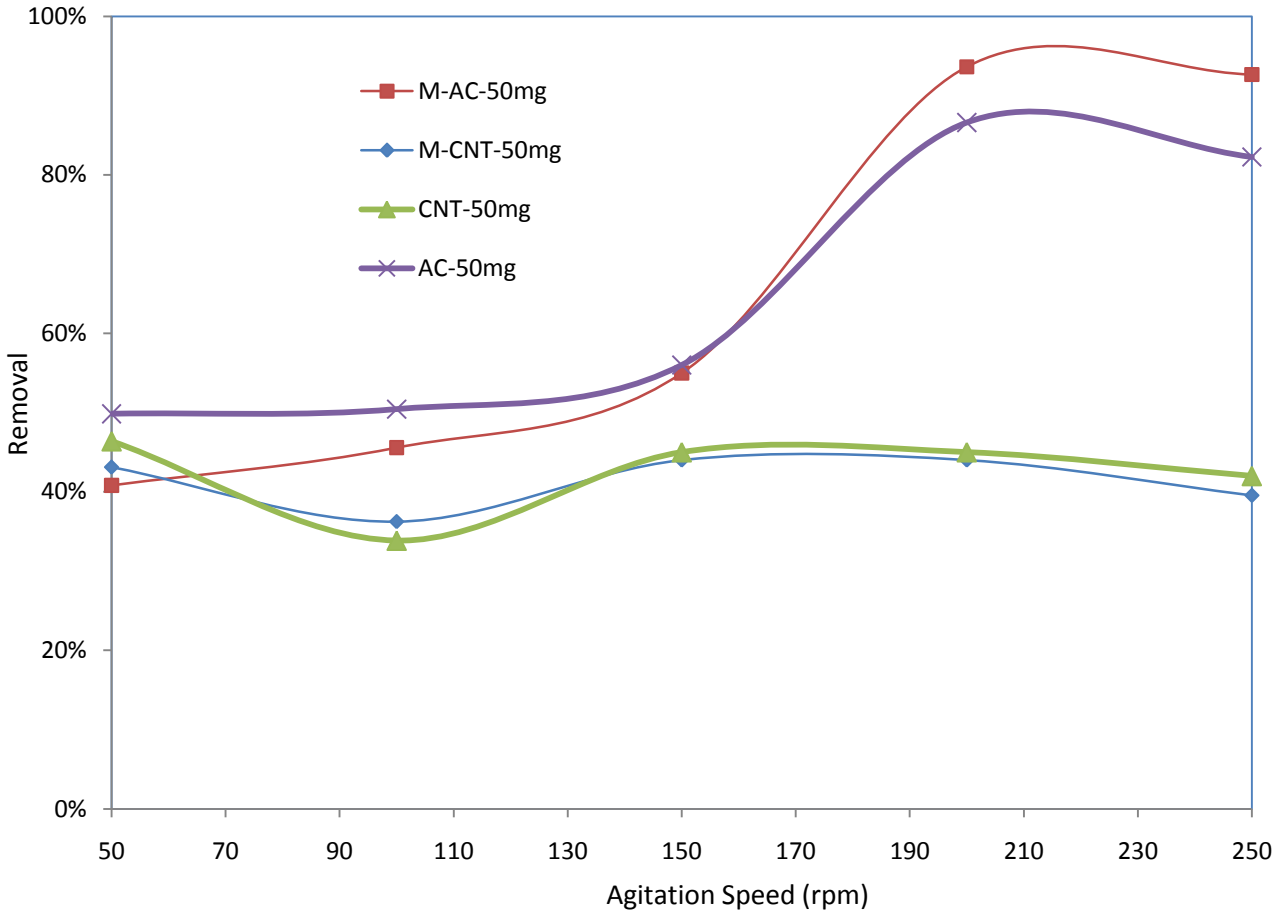

Figure 4.2.11: The effect of agitation speed on percentage removal of chromium (VI) at pH 3.

4.2.2.3 Effect of Contact Time

The adsorption behavior of Chromium by CNFs and FA were also studied for pH 3 and 150 rpm, but no removals were recorded. Therefore, it was concluded that Cr(VI) by CNFs and FA is not a function of contact time, too. The adsorption behavior of Chromium by CNTs and AC as a function of contact time was carried out by varying the equilibrium time from 10 minutes to 24 hours for initial Cr(VI) concentration of 1 mg/L, adsorbent dosage rate of 50mg/L, and optimum pH of 3. The agitation speed was kept constant at 150 rpm for CNTs and modified CNTs and 200 rpm for AC and modified AC though out the experiments time.

The results presented in Figure-4.2.12 show that the adsorption rate reach to the equilibrium for AC and M-AC after slightly above two hours and the removal rates of Cr(VI) were about 88% and 95% for the AC and M-AC, respectively. It was found that CNTs and M-CNTs reach most of the removal after two hours and both show similar behavior with the equal maximum Cr(VI) removal rate of about 45%. This indicates that by using AC and M-AC, the reaction is much faster and the adsorption sites are well exposed as compared to the other two absorbents.

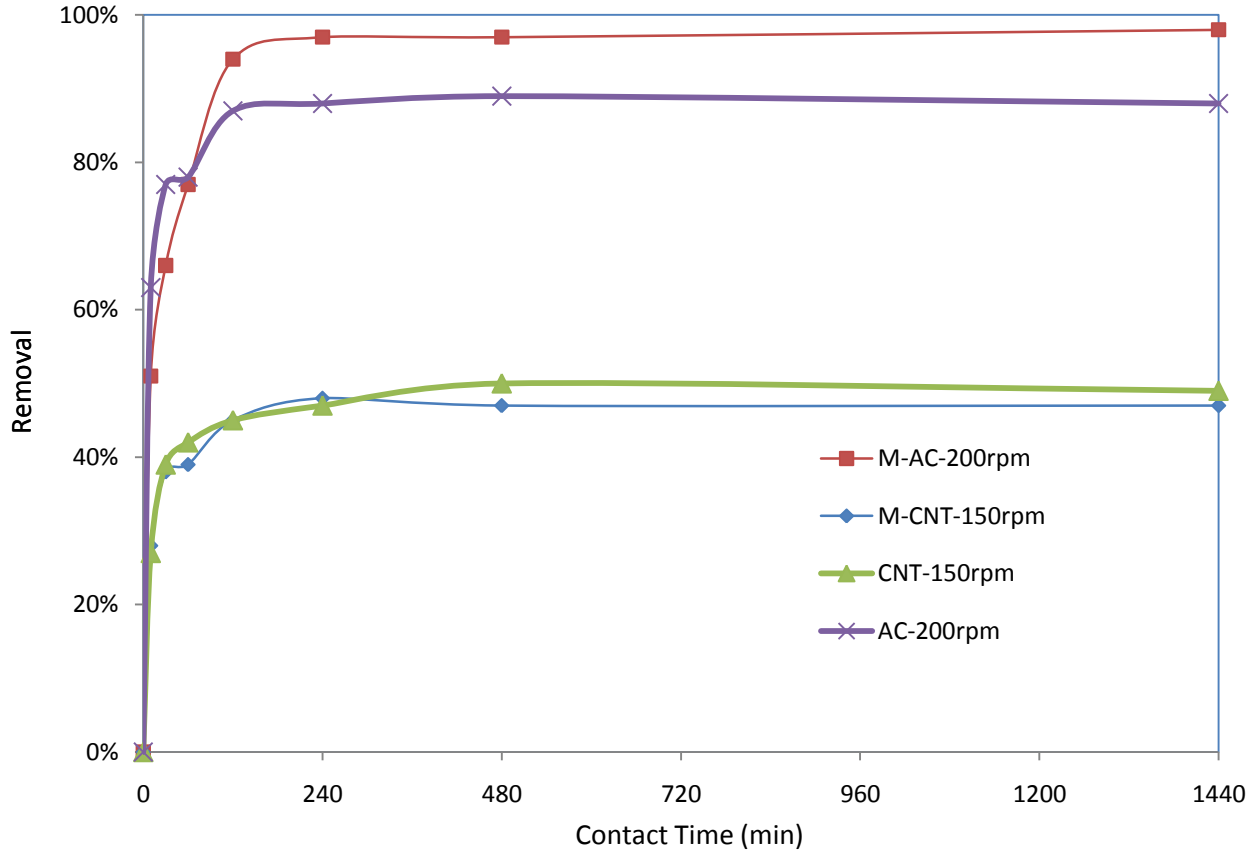

Figure 4.2.12: The effect of contact time on percentage removal of chromium at pH 3.

4.2.2.4 Effect of CNTs Dosage

The amount of adsorbent in water is one of the major factors, which affect the adsorption capacity. The batch adsorption experiments were carried out by using various amounts of absorbents ranging from 25 to 250 mg while the pH, agitation speed and contact time were fixed at 3, 150 rpm and 120 minutes, respectively, for CNTs, M-CNTs. For AC and M-AC, the experiments were carried out with similar condition but at 200 rpm agitation speed.

The results shown in Figure-4.2.13 indicated that the adsorption capacity increases with increases in adsorbent dosage up to 50 mg dosage for AC and M-AC, then remains almost constant for the rest of dosage range. In contrast, CNTs and M-CNTs continue increasing with increasing dosage beyond the 50 mg. M-CNTs show steady increases in removal with increases in dosage up to 200 mg, while the regular CNTs stop increasing at 150 mg.

By using 150 mg dosage rate for CNTs and 200 mg of M-CNTs, the chromium removals were found to increase to 80% and 87%, respectively. However, after certain dosage rate, which is 50 mg for AC and M-AC, 150 mg for CNT, and 200 mg for M-CNT, the dosage rate was found to have no effect on the percentage removal. This would indicate that the Cr(VI) removal is a function of the concentration of the Cr^{6+} ions in the solution.

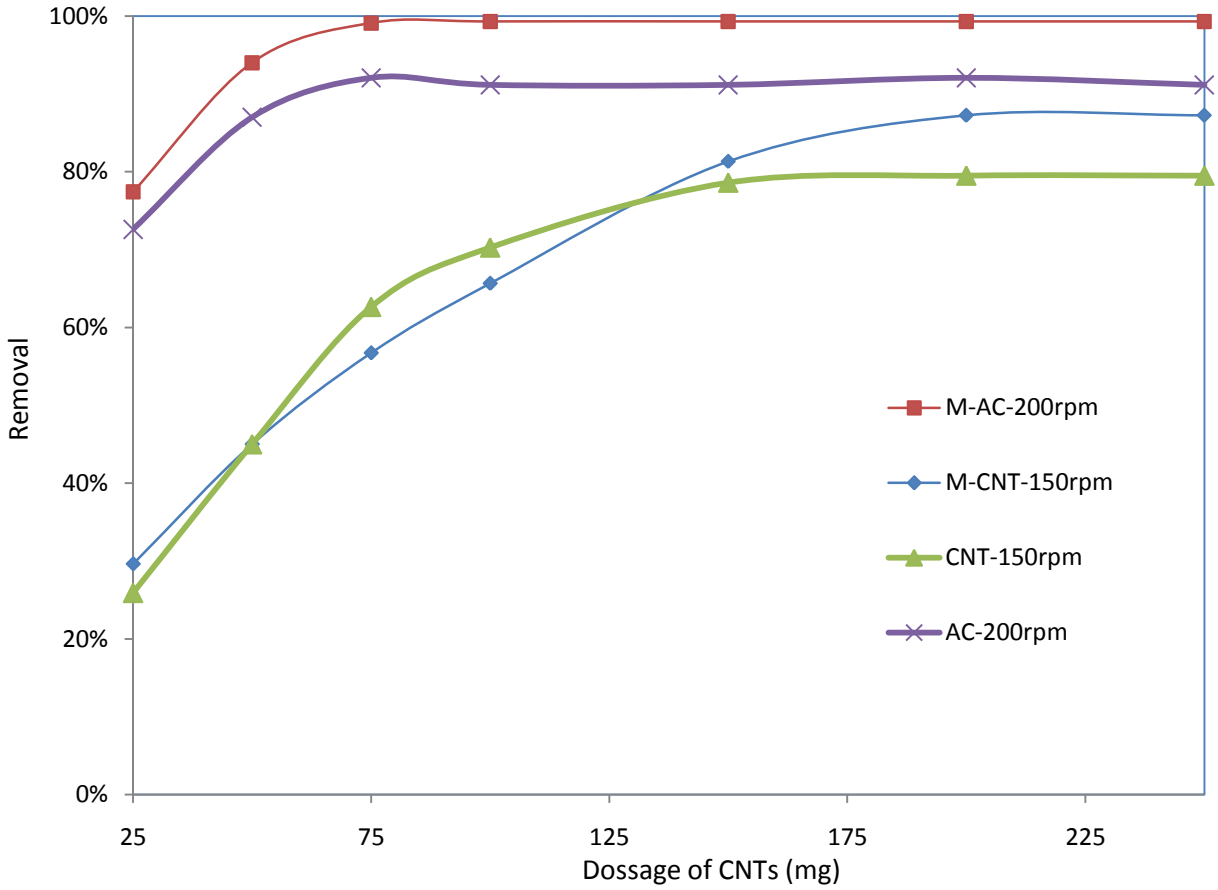

Figure 4.2.13: The effect of Adsorpate Dosage on percentage removal of chromium (VI) at pH 3.

The adsorption behavior of Chromium by CNFs and FA were also studied for pH 3, 150 rpm and 2 hours contact time, but no removal were recorded.

4.3 Freundlich and Langmuir Isotherms Models

Freundlich and Langmuir isotherms relate the coverage or adsorption of molecules on a solid surface to gas pressure or concentration of a medium above the solid surface at a fixed temperature.

The experimental data for Cd^{2+} and Cr^{6+} adsorption on the four adsorbents at different pH values could be approximated by the isotherm models of Langmuir (1) and Freundlich (2)

$$q = \frac{q_m K_L C}{1 + K_L C} \qquad \text{.....(1)}$$

Where C is the equilibrium of cadmium or chromium (VI) concentration (mg/l), q is the amount adsorbed (mg/g) and q_m and K_L are Langmuir constants related to adsorption capacity and energy of adsorption, respectively.

$$q = K_F C^{1/n} \qquad \text{.....(2)}$$

Where K_F and n are Freundlich constants related to adsorption capacity and adsorption intensity, respectively.

The equations (1) and (2) can be written as:

$$\frac{C}{q} = \frac{1}{(K_L q_m)} + \frac{C}{q_m} \qquad \text{.....(3)}$$

$$\log q = \frac{1}{n} \log C + \log K_F \qquad \text{.....(4)}$$

4.3.1 Adsorption Isotherm Models for Cadmium

The equilibrium adsorption is important in the design of any adsorption system. Equilibrium studies in adsorption indicate the maximum capacity of the adsorbent during the treatment process. Taking into account that the percentage removal is the highest at pH 7, thus, the condition was used to further optimize the adsorption process parameters. The equilibrium curve was modeled in Figure-4.3.1.

The Langmuir and Freundlich equations were used to describe the data derived from the adsorption of Cd (II) by the different adsorbents over the entire parameters range studied. Based on Figure 4.3.1, the adsorption capacities (q_e) and adsorption intensities were determined from the slope and intercept of each adsorbent graph, respectively.

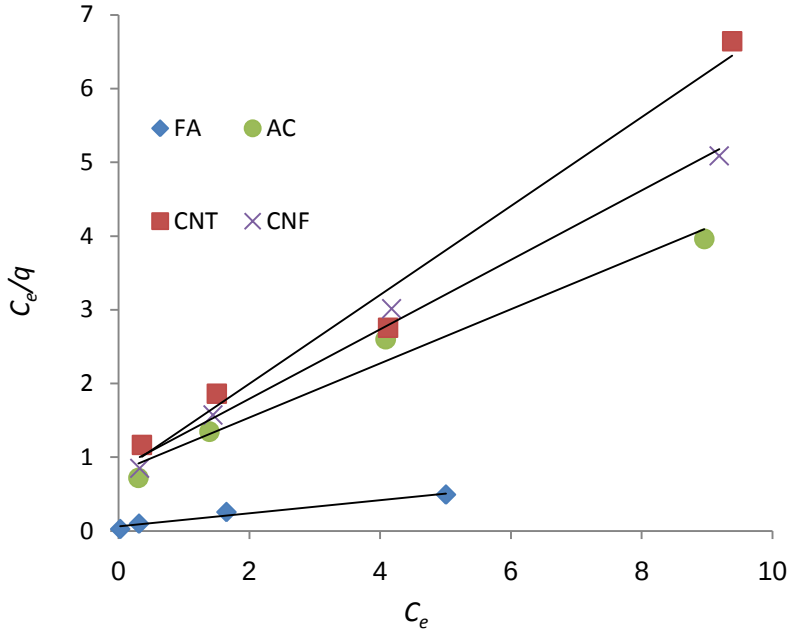

(a)

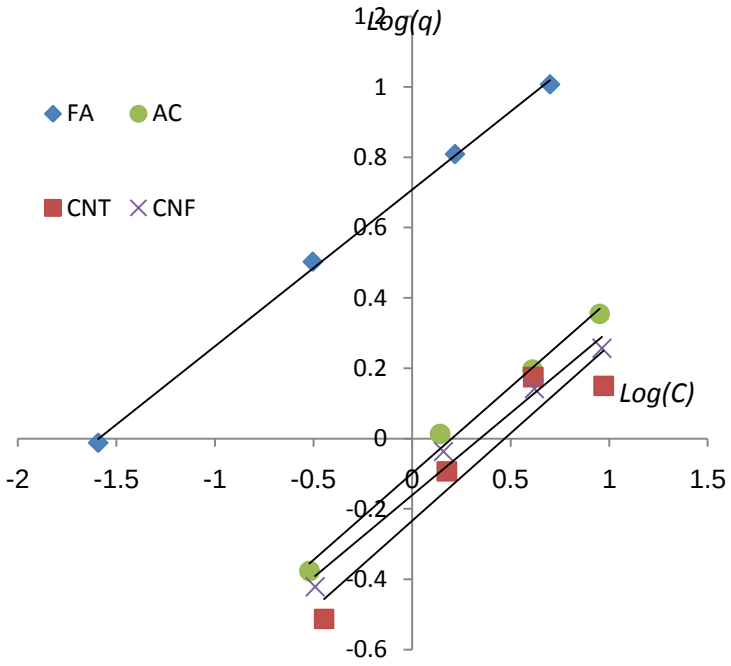

(b)

Figure 4.3.1: Adsorption isotherm models for cadmium at pH 7: (a) Langmuir and (b) Freundlich.

By comparison of Langmuir and Freundlich isotherms, Freundlich Isotherm shows better fitting model with higher correlation coefficients for the activated carbon and fly ash; whereas the data for both nanocarbon types (CNT and CNF) are better represent by Langmuir Isotherm. However, the Langmuir isotherm application for AC and FA is still within the acceptable range (above 95%); therefore, the applicability of monolayer coverage of Cd (II) ions on the surface of the four adsorbent is a valid assumption. This is due to the fact that all the four adsorbents have high surface area for metal adsorption. The above analysis also indicates that Cd (II) ions strongly adsorbed to the surface of these adsorbents suggesting that these forms of carbon based adsorbents have great potential to be good adsorbents for the removal of Cd (II) ions in water treatment.

	Langmuir			Freundlich		
Adsorbent	qm	K_L	R^2	n	K_F	R^2
CNT	1.661	0.761	0.979	2.008	0.791	0.912
CNF	2.123	0.555	0.993	2.141	0.851	0.982
AC	2.725	0.456	0.976	2.033	0.906	0.991
FA	11.236	1.435	0.968	2.247	2.028	0.998

Table 4.3.1: Langmuir and Freundlich Isotherm Parameters for cadmium.

From Table-4.3.1 it can be seen that FA has a greater adsorption capacity when compared to other three adsorbents. Each gram of FA can uptake three to four times the adsorption capacity by other three adsorbents. This high adsorption capacity could

be related to the high surface area but could be also explained by the metal content of the FA as suggested by Belgin [9].

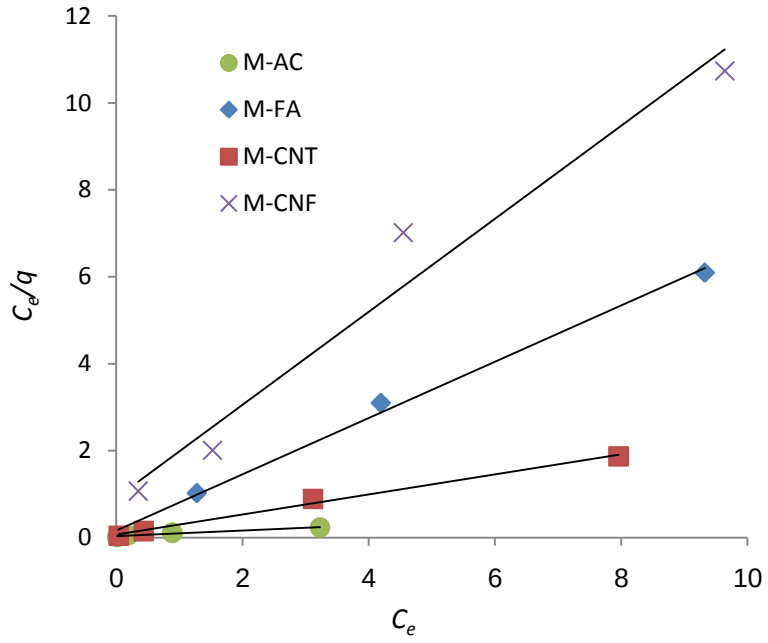

(a) Langmuir

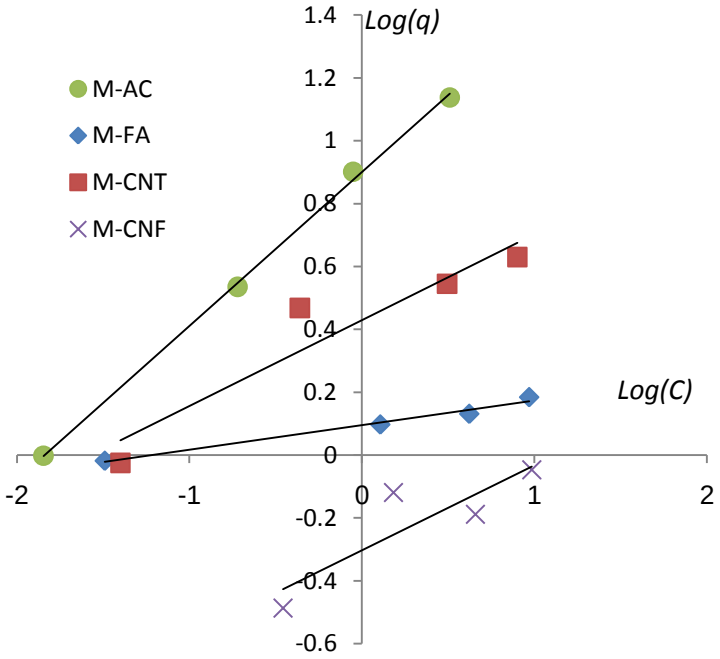

(b) Freundlich.

Figure 4.3.2: Adsorption isotherm models for cadmium by Modified Adsorbents at pH 7

The Langmuir and Freundlich equations were also used to describe the data derived from the adsorption of Cd (II) by the different modified absorbents over the entire parameters range studied. Based on Figure 4.3.2, the adsorption capacities (q_e) and adsorption intensities were determined from the slope and intercept of each absorbent graph, respectively.

By comparison of Langmuir and Freundlich isotherms, Langmuir Isotherm shows better fitting model with higher correlation coefficients for all except for the modified activated carbon, in which Freundlich Isotherm provide better fit for the data available. However, the Langmuir isotherm applications for M-AC is still within the acceptable range (above 95%); therefore, the applicability of monolayer coverage of Cd (II) ions on the surface of the four modified adsorbents is a valid assumption. This is due to the fact that all the four adsorbents have great surface area for metal adsorption. The above analysis also indicates that Cd (II) ions strongly adsorbed to the surface of these modified adsorbents suggesting that these forms of modified carbon based absorbents have great potential to be good adsorbents for the removal of Cd (II) ions in water treatment.

	Langmuir			Freundlich		
Adsorbent	qm	K_L	R^2	n	K_F	R^2
M-CNT	4.348	3.239	0.993	3.663	1.536	0.898
M-CNF	0.935	1.177	0.965	3.704	0.739	0.770
M-AC	15.873	1.800	0.965	2.045	2.462	0.998
M-FA	1.546	3.994	0.996	12.821	1.099	0.982

Table 4.3.2: Langmuir and Freundlich Isotherm Parameters for Cd (Modified).

From Table-4.3.2 it can be seen that M-AC and M-CNTs have greater adsorption capacities when compared to the other two absorbents. These high adsorption capacities for M-CNTs and M-AC could be related to the chemisorptions caused by the available carboxylic group on the surfaces of these adsorbents. The adsorption of Cd^{2+} by carboxylic functionalized carbon nanotubes is believed to be a chemisorptions process rather than a physisorption process [73]. However, the higher adsorption capacity of M-CNTs when compared to R-CNT indicates that the introduced carboxylic functional groups, is most probably, are involved in chemisorptions process. Moreover, acidic oxygen-containing groups might behave as ion-exchange by extracting cations Cd^{2+} by the anions charge of the oxygen groups [65].

In contrast, modification of FA with carboxylic functions reduced the adsorption capacity of the carbon based fly ashes. The reduction in adsorption can be explained by the following:

- The acid treatment extracted some of the metal content of the as-received fly ashes. As can be seen in Table 4.3.3 for EDX of modified FA, the metal content has decreased from the amount shown in the as-received FA (Table 2.3.1). This is an indication of metal losses during the acid treatment process.

- The acid treatment reduced the fly ash porosity limiting the diffusion rate toward internal surface area.

Spectrum	Sum
C	73.70
O	17.37
Na/Mg	0.23
S	2.90
Others	5.8
Total	100.0

Table 4.3.3: The Energy Dispersive X-ray analysis for Modified FA

The adsorption models using BET and TEMKIN adsorption isotherms were also tested for cadmium removal. The table below summarizes the correlation coefficients for the for used adsorption isotherms:

Adsorbent	Langmuir	Freundlich	BET	TEMKIN
CNT	0.979	0.912	0.979	0.907
CNF	0.993	0.982	0.993	0.992
AC	0.976	0.991	0.976	0.969
FA	0.968	0.998	0.968	0.919

Adsorbent	Langmuir	Freundlich	BET	TEMKIN
M-CNT	0.993	0.898	0.993	0.962
M-CNF	0.965	0.770	0.965	0.763
M-AC	0.965	0.998	0.965	0.888
M-FA	0.996	0.982	0.996	0.96

As can be seen from above tables, the BET correlation coefficients approach Langmuir isotherms correlations which confirm monolayer assumption. The TEKIN shows much lower correlation indicating that the interaction between adsorbed molecules can be neglected.

4.3.2 Adsorption isotherm models for Cr (VI)

Equilibrium studies in adsorption for Cr (VI) indicate the maximum capacity of the adsorbent during the treatment process. Taking into account that the percentage removal is the highest at pH 3, thus, the condition was used to further optimize the adsorption process parameters. The equilibrium curve was modeled in Figure-4.3.3.

The Langmuir and Freundlich equations were used to describe the data derived from the adsorption of Cr (VI) by the different absorbents over the entire parameters range studied. Based on Figure-4.3.3, the adsorption capacities (qe) and adsorption intensities were determined from the slope and intercept of each absorbent graph, respectively.

By comparison of Langmuir and Freundlich isotherms, Langmuir Isotherm shows better fitting model with higher correlation coefficients for all except for the regular activated carbon, in which Freundlich Isotherm provide much better fit for the data available. However, the Langmuir isotherm applications for R-AC is still within the acceptable range (above 90%); therefore, the applicability of monolayer coverage of Cr (VI) ions on the surface of the four adsorbents is a valid assumption.

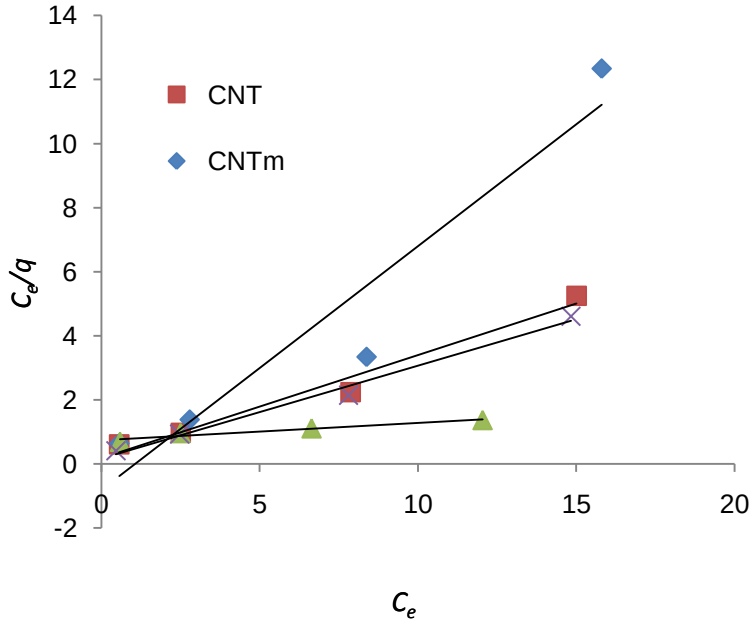

(a) Langmuir

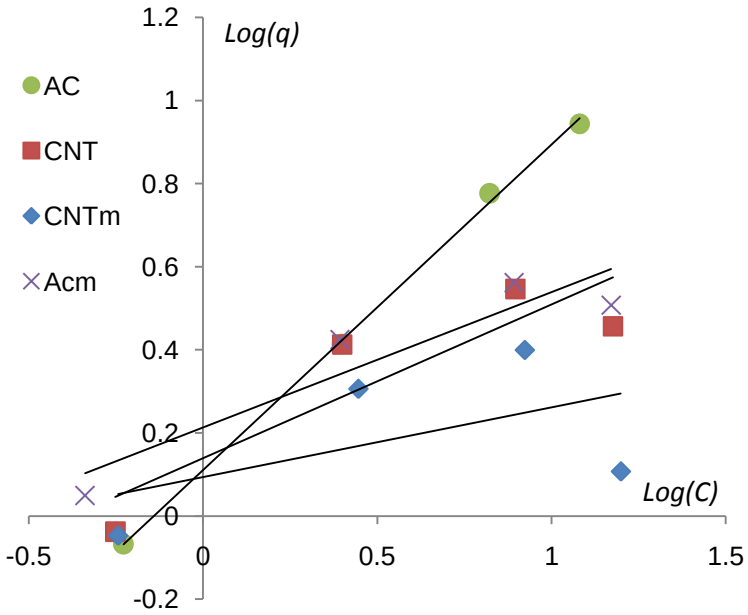

(b) Freundlich

Figure 4.3.3: Adsorption isotherm models for chromium (VI) at pH 3:

	Langmuir			Freundlich		
Adsorbent	qm	K_L	R^2	n	K_F	R^2
R-CNTs	3.115	1.773	0.994	2.008	0.791	0.826
M-CNTs	1.314	-0.929	0.979	5.988	1.099	0.351
R-AC	18.519	0.073	0.937	1.279	1.117	0.999
M-AC	3.460	1.690	0.992	4.695	2.462	0.874

Table 4.3.4: Langmuir and Freundlich Isotherm Parameters for Chromium.

This is due to the fact that all the four adsorbents have great surface area for metal adsorption. The above analysis also indicates that Cr (VI) ions are strongly adsorbed to the surface of these adsorbents suggesting that these forms of carbon based absorbents have great potential to be good adsorbents for the removal of Cr (VI) ions in water treatment.

From Table-4.3.3 it can be seen that R-AC has much higher adsorption capacity than M-AC; however, it was shown earlier that M-AC has the highest Cr(VI) removal for water with Cr(VI) initial concentration of 1 ppm. This indicates that as the solution concentration increases, R-AC will be able to absorb high quantity of Cr(VI). For instances, the removal percentage of Cr(VI) by regular AC doe a solution with initial concentration of 10 ppm will be around 30% compared to 20% by M-AC and even much lower by CNTs and M-CNTs. From the analysis above it can be concluded that M-AC should be selected for Cr(VI) removal from low initial concentration solutions, while regular AC provides better application for high initial concentrations of Cr(VI).

The lower adsorption capacities by modified AC and modified CNTs when compared to their regular forms at high concentrations may also be explained by the existence of carboxylic functional groups on these carbon based absorbents. The lower adsorption capacity of M-AC and M-CNTs when compared to R-AC and R-CNT at high initial concentrations indicates that the introduced carboxylic functional groups, is most probably, are involved in a repulsion effect caused by the negative charges in carboxylic group with the negative charges carried by hydrogen chromate ions ($HCrO_4^-$).

Similarly, the adsorption models using BET and TEMKIN adsorption isotherms were also tested for chromium (VI) removal. The table below summarizes the correlation coefficients for the for used adsorption isotherms:

Adsorbent	Langmuir	Freundlich	BET	TEMKIN
R-CNTs	0.994	0.826	0.994	0.869
M-CNTs	0.979	0.351	0.979	0.251
R-AC	0.937	0.999	0.937	0.916
M-AC	0.992	0.874	0.992	0.889

4.4 Modeling of Kinetics Adsorption

Kinetic modeling of adsorption data is fundamental information for the application of adsorption in real industries. Modeling of adsorption kinetics gives information for selecting from different adsorbents under different operational conditions to the optimal design that suite a given operational conditions for pollutants, such as heavy metals, removal from potable water and wastewater systems [74].

The kinetics for Cadmium (II) and Chromium (VI) were studied using the experimental data obtained from the effect of adsorbents dosage rate (dry-weight basis) at 25◦C at several different time intervals up to 480 minutes. The kinetic was calculated and plotted for the three kinetics Models: the first-order equation, the pseudo-second-order rate equation and the second-order rate equation shown below on their liner forms:

$$\log\frac{\mathrm{q_e} - q_\mathrm{t}}{\mathrm{q_e}} = -\frac{\mathrm{K_L t}}{2.303} \quad (8)$$

$$\frac{t}{q_t} = \frac{1}{2K_s q_e^2} + \frac{t}{q_e} \quad (9)$$

$$\frac{1}{q_e - q_t} = \frac{1}{q_e} + kt \quad (10)$$

The selection of kinetic model for each adsorbent is based on the degree of correlation for the fitted data defined by the correlation Coefficient (R^2).

4.4.1 Kinetics Adsorption Model of Cadmium (II)

Table-4.4.1 shows the correlation coefficients for each model used to describe each of the four regular adsorbents. Per Table-4.4.1, the pseudo first-order kinetic equation can be used to describe Cd^{2+} adsorption by AC; however, the pseudo first-order kinetic equation was not applicable for CNTs, CNFs, and FA because R^2s for these adsorbents are small comparing to R^2 of pseudo-second-order equation. Therefore, the pseudo-second-order equation was used in this study in order to investigate the mechanism of adsorption of Cd(II) by the three adsorbents, CNTs, CNFs, and FA, and the potential rate-controlling steps, such as mass transport and chemical reactions.

Adsorbent (50 mg)	1st Order	Pseudo 2nd Order	2nd Order
CNTs	0.974	0.999	0.809
CNFs	0.937	0.976	0.826
AC	0.956	0.725	0.913
FA	0.904	0.999	0.971

Table 4.4.1: Correlation Coefficients for Kinetic Models of Cadmium

The pseudo second-order equation for the mechanism of adsorption of Cadmium (II) by the CNTs, CNFs, and FA is derived by:

$$\frac{dq_t}{dt} = k_2(q_e - q_t)^2 \qquad .....(4.5)$$

Where q_e and q_t are the sorption capacity at equilibrium and at time (mg/g) respectively and k_2 is the rate constant of the pseudo second-order sorption

($g.mg^{-1}.min^{-1}$). For the boundary conditions t=0 to t=t and q_t=0 and q_t=q_t, the integrated form of equation 4.5 becomes:

$$\frac{1}{q_e - q_t} = \frac{1}{q_e} + k_2 t \qquad .....(4.6)$$

Putting this equation on a linear form:

$$\frac{1}{q_t} = \frac{1}{k_2 q_e^{\,2}} + \frac{t}{q_e} \qquad ..... (4.7)$$

The integrated form of the above equation is:

$$\frac{t}{q_t} = \frac{1}{h} + (\frac{1}{q_e})t \qquad .....(4.8)$$

Where h ($g.mg^{-1}.min^{-1}$) can be regarded as the initial sorption rate $q_t/t \longrightarrow 0$, hence $h= k_2 q_e^{\,2}$

Based on the good correlation coefficients for CNTs, CNFs, and FA, the pseudo second-order kinetics should be applicable to the experimental data and the plot of t/q_e versus time of equation 4.8 should give linear relationship from which q_e, k and h can be determined from the slope and intercept for each adsorbent.

The parameters for the kinetics adsorption model for cadmium (II) at pH 7 are shown in Table-4.4.2 for CNTs, CNFs and FA. Plotting t/qt versus time (Figure-4.4.1) yields

very good straight lines. From the second order rate constant, shown in Figure-4.4.1 and Table-4.4.2, it can be concluded that the time to achieve equilibrium concentration of Cd (II) using FA is less than the time required by using CNTs and CNFs. For the AC, it is best represented by first-order equation with a correlation of R^2=0.956.

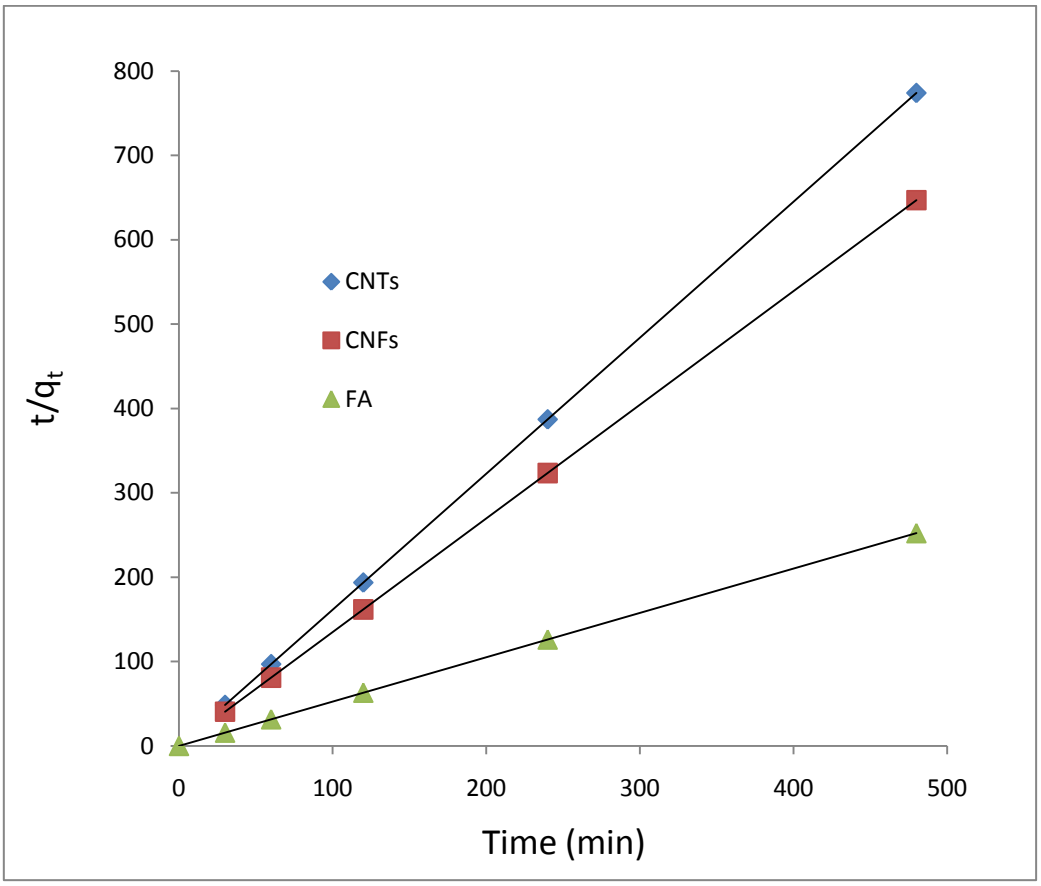

Figure 4.4.1: Pseudo-second-order kinetics of Cd (II) using R-CNTs, R-CNFs and R-FA.

The equilibrium adsorption capacity, q_e obtained from the graph and Table-4.4.2 also implies that FA has much higher adsorption capacity (q_e = 1.838 mg/g) when compared to all other adsorbents. Activated carbon still show approximately equal adsorption capacity (q_e = 0.8 mg/g) when compared to nano-carbons.

Adsorbent (50 mg)	qe (mg/g)	K2 (g.mg-1.h-1)	R2
CNT	0.657	0.028	0.999
CNF	0.840	0.010	0.976
FA	1.838	1.156	0.999

Table 4.4.2: Kinetic parameters for pseudo-second-order model of cadmium.

Similar analysis carried out for the kinetics of cadmium (II) removal by the modified carbon based adsorbents. The parameters for the kinetics adsorption model for cadmium (II) at pH 7 are shown in Table-4.4.3 for M-CNTs, M-CNFs, M-AC, and M-FA. Plotting t/qt versus time (Figure-4.4.2) yields very good straight lines.

Adsorbent (50 mg)	qe (mg/g)	K2 (g.mg-1.h-1)	R2
M-CNT	2.020	0.031	0.999
M-CNF	1.222	0.024	0.999
M-AC	1.984	0.197	1.000
M-FA	1.580	0.041	0.999

Table 4.4.3: Kinetic parameters for pseudo-2nd-order model of Cd (modified)

From the second order rate constant, shown in Figure-4.4.2 and Table-4.4.3, it can be concluded that the time to achieve equilibrium concentration of Cd (II) using M-CNTs and M-AC is less than the time required by using M-CNFs and M-FA.

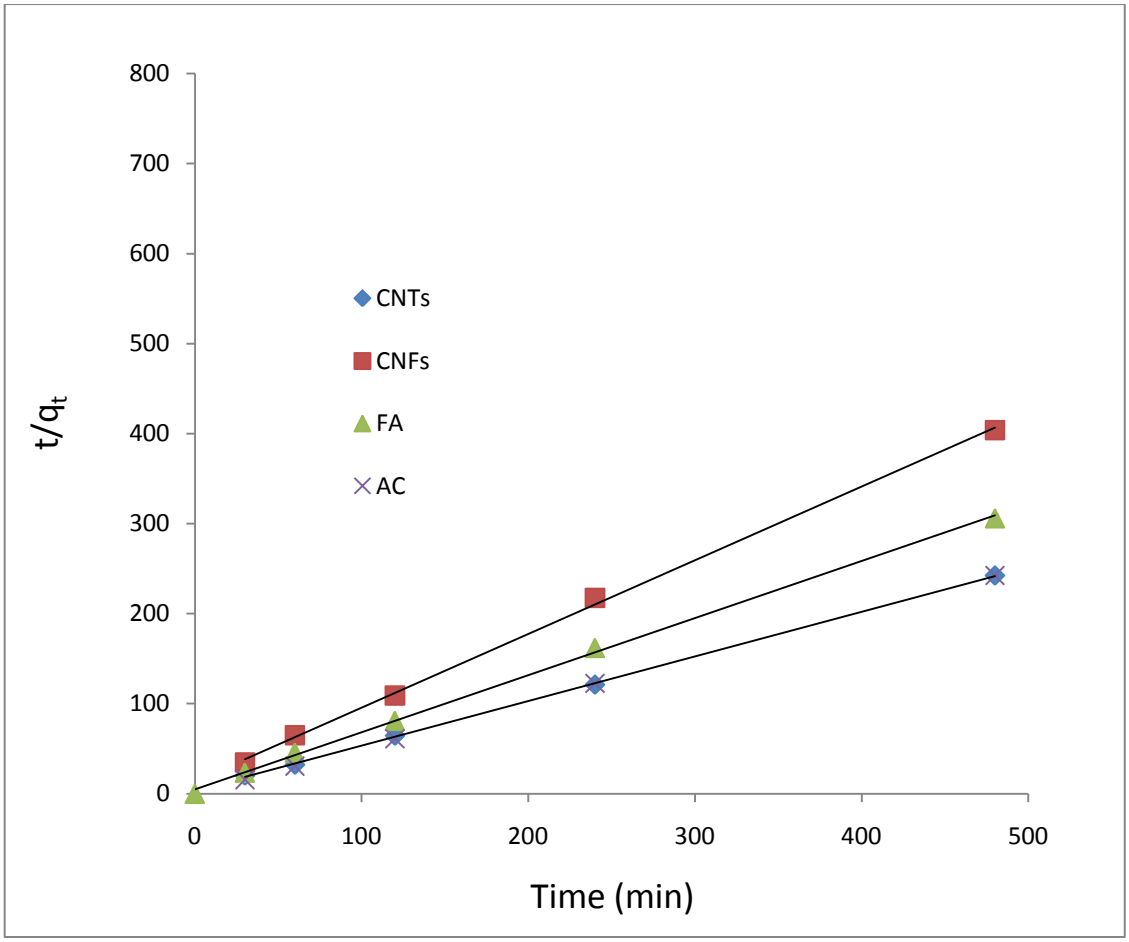

Figure 4.4.2: Pseudo-second-order kinetics of Cd (II) using M-CNTs, M-CNFs, M-AC and M-FA.

The equilibrium adsorption capacity, qe obtained from the graph and Table-4.4.3 also implies that modified CNTs and modified AC have high adsorption capacities comparable to the non-modified FA adsorption capacity of 1.838 mg/g. M-CNFs has the lowest adsorption capacity (qe = 1.222 mg/g) but still higher than non-modified CNTs, CNFs, and AC of 0.657, 0.840, and 0.8 mg/g, respectively.

4.4.2 Kinetics Adsorption Model of Chromium (VI)

The constants for the kinetics adsorption model for chromium (VI) at pH 3 are shown in Table-4.4.4 for the four absorbents. Plotting t/qt versus time (Figure-4.4.3) yields very good straight lines. From the second order rate constant, shown in Figure-4.4.3

and Table-4.4.4, it can be concluded that the time to achieve equilibrium concentration of Cr (VI) using M-CNTs is least and by M-AC is the slowest.

Adsorbent (50 mg)	qe (mg/g)	K2 (g.mg-1.h-1)	R2
R-CNTs	1.021	0.035	0.999
M-CNTs	0.964	0.059	0.999
R-AC	1.805	0.044	0.999
M-AC	2.024	0.011	0.994

Table 4.4.4: Kinetic parameters for pseudo-2nd-order model of chromium (VI).

The equilibrium adsorption capacity, q_e obtained from the graph and Table-4.4.4 also implies that AC and modified AC have high adsorption capacities compared to the two carbon nanotubes based absorbents. The CNTs and M-CNTs have relatively comparable adsorption capacities ($qe \approx 1$ mg/g) and similarly AC and M-AC have, also, relatively comparable adsorption capacities ($qe \approx 2$ mg/g). This implies that the modification of the carbon based absorbents used in this study has no major effect on Cr(VI) removal efficiency.

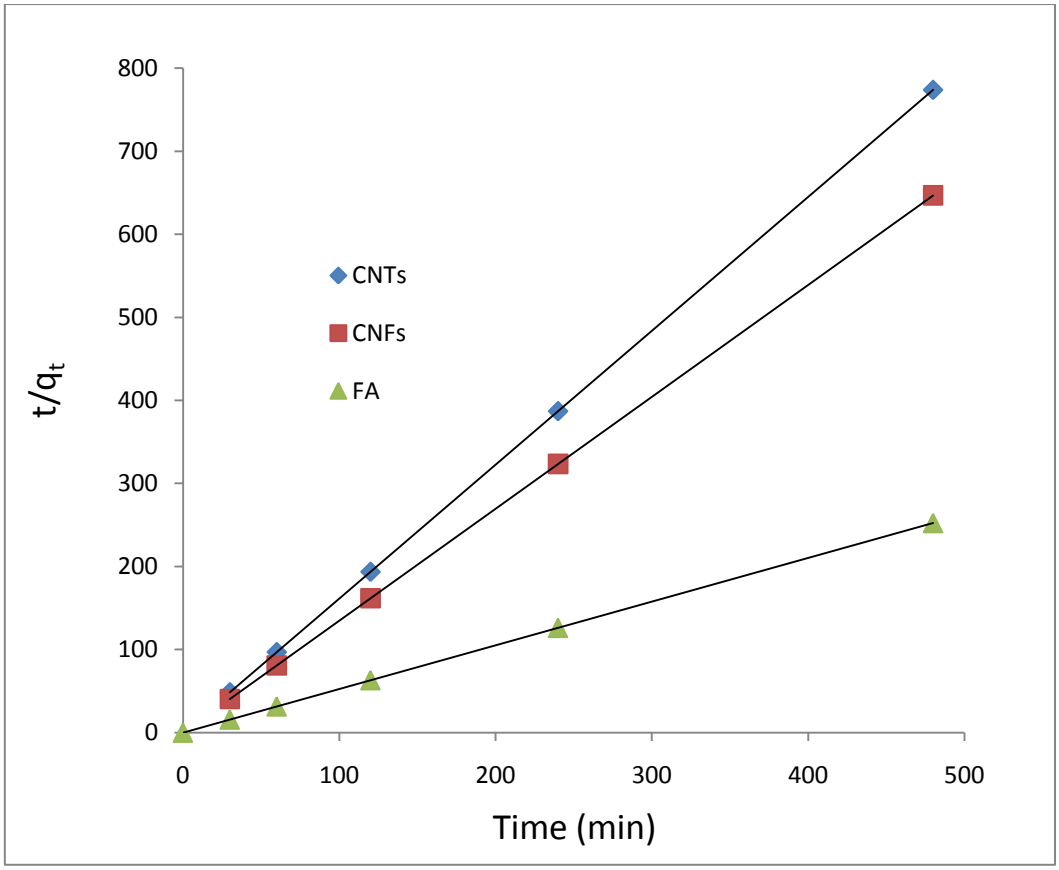

Figure 4.4.3: Pseudo-second-order kinetics of Cr (VI).

4.5 Comparative Analysis of Various Adsorbents for Cadmium and chromium removal

In this section, a comparison for removing Cd (II) and Cr (VI) ions using CNTs, CNFs, AC, and FA are listed in Table 4.5.1.

Table 4.5.1: Comparison of various adsorbents for Cd (II) and Cr (VI)

Sorbents	Metal Ions	pH	q_m (mg/g)	Reference
FA (Afsin-Elbistan)	Cd (II)	7.0	0.2949	[9]
FA (Seyitomer)	Cd (II)	7.0	0.2160	[9]
R-CNTs	Cd (II)	8.0	1.29	[62]
M-CNTS (Oxidized)	Cd (II)	8.0	22.32	[62]
M-CNTS (Oxidized)	Cd (II)	7.0	22.74	[61]
M-CNTS (Oxidized)	Cr (VI)	2.05	4.2615	[10]
Nitric acid oxidized CSC	Cr (VI)	3-4	10.88	[10]
Nitric acid oxidized CAC	Cr (VI)	3-4	15.47	[10]
Sulfuric acid oxidized CSC	Cr (VI)	3-4	4.05	[10]
Sulfuric acid oxidized CAC	Cr (VI)	3-4	8.94	[10]
CSC-nonmodified	Cr (VI)	3-4	3.65	[10]
Acid Treated AC	Cr (VI)	1.5	71.4	[63]
AC	Cr (VI)	1.5	25.6	[63]

coconut shell charcoal (CSC) and commercial coconut shell activated carbon (CAC)

Other values for Cr(VI) removal reported by D. Mohan [45] shown under Section 2.6 of the Thesis, list the adsorption capacities for many carbon based adsorbents. The value under this table varies significantly. The adsorption capacity, based on the adsorbent selected and operating condition, may vary from as low as lower than 1mg/g to as high as more than 500 mg/g of adsorbent.

Literature results of the adsorption of Cd^{2+} ions by various adsorbent.

Adsorbent	q_{max} (mg g^{-1})	b (L mol^{-1})	References
Carbon nanotubes			
CNT (HNO_3)	2.92	1,180,000	[14]
Nitrogen-doped MWCNT (HNO_3)	31		[43]
Cup-stacked MWCNT (HNO_3)	20	–	
CNT grown on microsized Al_2O_3 particles	8.89	14,613	[44]
CNT ($KMnO_4$)	11.0	–	[45]
MWCNT (HNO_3)	10.86	32,598.9	[46]
MWCNT (HNO_3)	7.42	–	[47]
Carbon			
Unmodified carbon	207.3	–	[31]
Triton X-100-modified carbon	232.9	–	
Oxidized granular activated carbon	5.74	31,860	[48]
Commercial activated carbon	4.29	11,061	[49]
Ash			
Rice husk ash	3.03	21,014	[50]
Biomass			
Cystine-modified biomass	11.63	170,863	[21]
Biomass grafted with polyamic acid	95.2	1,829,727	[22]
Agricultural waste			
Peanut hulls	6	–	[51]
Phosphoric acid modified corncob	52.8	–	[52]
Natural corncob	5.38	105,665.4	[53]
Citric acid oxidized corncob	55.7	219,199.5	
Nitric acid oxidized corncob	19.3	64,073.7	
Native starch	8.9	1.24	[54]
Oxidized starch	14.6	4.72	
Sugar beet pulp	24.39	6920	[55]
Algae			
Pelvetia caniculata	75	8430.7	[56]
Caulerpa lentillifera	4.70	8346.1	[57]
Aquatic moss			
Fontinalis antipyretica	28	14,613.3	[58]
Bacterium			
Sphaerotilus natans	45	1124.1	[59]
Inorganic			
Nano-B_2O_3/TiO_2 composite	49.9	786.8	[60]
Silica			
Amino-functionalized silica	18.25	28,395	[61]
Zeolite			
HEU-type zeolite	12.2	–	[62]
Resin			
Thio chelating resins	78.7	2800	[63]
Chelating resins containing N,N donor sets	16.64	–	[64]
Commercial resins			
Duolite GT-73	105.7	–	[51]
Amberlite IRC-718	258.5	–	
Lewatit TP 207	50	–	[53]
e-MWCNT	25.7	465,265	This study

CHAPTER VI

CONCLUSION AND RECOMMENDATION

Carbon based adsorbents were found to be efficient for the adsorption of Cd (II) in aqueous solution. The characterization of Cd (II) uptake showed that, the Cadmium ions binding is dependent on initial pH, agitation speed, amount of dosage, and contact time. Percentage uptake increased with an increased in pH from pH 2 to pH 7. The optimum pH found in this study is pH 7 in which it gave approximately 30% to 40% removal of Cd (II) ions by using regular CNTs, CNFs and activated carbon, whereas the FA shows a removal close to 95%. The percentage uptake increase slightly with an increase in agitation speed from 50 to 150 rpm, in which 150 rpm gave slightly higher removal for cadmium. While the percent removal of Cd (II) was observed to increase with increases in dosage, it was found that beyond 50 mg the dosage rate has no effect on percentage removal of Cd ions for the conditions specified under this study.

Carboxyl modified carbon based absorbents were found to be efficient, too, for the adsorption of Cd (II) in aqueous solution. The adsorption process of the regular forms of these carbon based materials is basically physisorption process. However, when these carbon based absorbents were modified for addition of carboxylic functional groups, the cadmium removal in general significantly enhanced and this can be

explained by the chemisorptions process caused by the existing of active carboxyl groups.

The characterization of Cd (II) uptake showed that, the Cadmium ions binding is dependent on initial pH, agitation speed, amount of dosage, and contact time. Percentage uptake increased with an increased in pH from pH 2 to pH 7. The optimum pH found in this study is pH 7 in which it gave approximately high removal of Cd (II) ions (≈95%) by using modified CNTs and AC, whereas the modified FA and CNFs show removal of 55% and 74%, respectively. The percentage uptake increase slightly with an increase in agitation speed from 50 to 150 rpm, in which 150 rpm gave slightly higher removal for cadmium. While the percent removal of Cd (II) was observed to increase with increases in dosage, it was found that beyond 50 mg the dosage rate has no effect on percentage removal of Cd ions for all substances except for the modified CNFs, in which the dosage was found to continue influencing the removal rate up to 150 mg. The maximum achieved removal with modified CNFs is 80%, which is slightly higher than the modified FA removal.

Among the four carbon based adsorbents and their four modified forms, R-FA, M-CNTs, and M-AC have the highest removal capacities and can be considered good adsorbents for application of cadmium removal from water. M-CNFs is also a good candidate for cadmium removal from water, but at relatively high dosage rate.

In this study it was shown that regular FA, a waste material, could be used in water treatment. This should help both: improve waste management and establish a new low cost water treatment material. It was also concluded that the regular FA, without the

need to modify it for extra cost, still shows the highest removal when compared to all other absorbents with and without modification. The high removal of Cd (II) by FA is due to the strong tendency towards chemical bonding between the Cd(II) ions and these metals. Although, FA was found to be a good Cd (II) absorbent, FA is a waste material that contains many other heavy metals, such as vanadium, which may cause pollution to the water being treated. One more concern with FA is the fact that FA composition changes with the change in source, therefore, the result of this study cannot be applied to all FA types.

Modified and nonmodified carbon nanotubes and activated carbon were found to be effective absorbents for Cr (VI) removal from aqueous solution. The adsorption process is basically physisorption process. For Cr(VI) removal the oxidation treatment of absorbents, for addition of carboxylic functional groups, was found to have no major effect on removal efficiency.

The characterization of Cr (VI) uptake showed that, the Chromium ions binding is dependent on initial pH, agitation speed, amount of dosage, and contact time. Percentage uptake increased with an increased in pH from pH 2 to pH 3 and then start to decline. The optimum pH found in this study is pH 3 in which it gave approximately high removal of Cr (VI) ions, around 95% and 90% by using modified AC and regular AC, respectively. CNTs and M-CNTs achieved 80% and 85% removal but at much higher dosage rate. While CNTs and M-CNTs show no major change in the percentage uptake with increase in agitation speed from 50 to 250 rpm, AC and M-AC show significant improvement, almost double removal, beyond 200 rpm.

In contrast, while the dosage rate was found to have no major effect on Cr(VI) removal my AC and M-AC after 75 mg dosage rate of absorbent, absorbent dosage rate was found to be a major influential factor for Cr(VI) removal percentage by CNTs and M-CNTs. The percentage removal by 50 mg CNTs and M-CNTs of 45% was almost doubled for dosage rate higher than 150 mg. The maximum removal by CNT and M-CNTs were found to be 80% and 87% using 150 mg CNTs and 200 mg M-CNTs, respectively.

In this study it was shown that the adsorption isotherm for these for absorbents can be represented by Langmuir model; although Freundlich model gives better representation for regular AC. Moreover, the adsorption kinetics for chromium (VI) by all the four absorbents, CNT, M-CNTs, AC, and M-AC, can be best represented by the pseudo-second-order equation.

REFERENCES

[1] World Health Organization (WHO) Guidelines, www.who.int

[2] Carbon Nanotubes and Related Structures: New Materials for the Twenty-First Century, by Harris, Peter, Cambridge University Press, 2001

[3] Kratschmer, K.; Lamb, L. D.; Fostiropoulos, K.; Huffman, R. D. Nature 1990, pp 347, 354.

[4] Dresselhaus, M. S., Dresselhaus, G. & Avouris, P. (EdsCarbon Nanotubes: Synthesis, Structure, Properties, and Applications. Germany: Springer, (2000).

[5] Iijima, S. , Helical microtubes of graphitic carbon, Nature 354 (1991), pp. 56–58. J.K. Ong, N.R. Franklin, C. Zhou, M.G. Chapline, S. Peng and K. Cho et al., Science 287 (2000), p. 622.

[6] Bethune, D. S.; Kiang, C. H.; de Vries, M. S.; Gorman, G.; Savoy, R.; Vazquez, J.; Bevers, R. Nature 1993, 363, 605.

[7] M. A. DAOUS, "Utilization of Cement Kiln Dust and Fly Ash in Cement Blends in Saudi Arabia" JKAU: Eng. Sci., vol. 15 no. 1, pp. 33-45 (1425 A.H./ 2004 A.D.)

[8] Atsuko Sato, Satoshi Nishimoto, “Effective Reuse of Coal Fly Ash as Civil Engineering Materials", 2005 World of Coal Ash (WOCA) April 11-15, 2005, Lexington, Kentuck, USA.

[9] Belgin Bayat, “Comparative study of adsorption properties of Turkish fly ashes: The case of chromium (VI) and cadmium (II),” Journal of Hazardous Materials B95 (2002) 275–290

[10] Jun Hu, Changlun Chen, et al., “Removal of chromium from aqueous solution by using oxidized multiwalled carbon nanotubes” Journal of Hazardous Materials 162 (2009) 1542–1550

[11] Allotrope in IUPAC Compendium of Chemical Terminology, Electronic/ version, http://goldbook.iupac.org/A00243.html. Accessed March 2007.

[12] Wang, X.; Li, Q.; Xie, J.; Jin, Z.; Wang, J.; Li, Y.; Jiang, K.; Fan, S. (2009). "Fabrication of Ultralong and Electrically Uniform Single-Walled Carbon Nanotubes on Clean Substrates". Nano Letters 9 (9): 3137–3141. doi:10.1021/nl901260b. PMID 19650638.

[13] http://en.wikipedia.org/wiki/Carbon_nanotube

[14] Dimitrios Tasis, Nikos Tagmatarchis, Alberto Bianco, and Maurizio Prato," Chemistry of Carbon Nanotubes" Chem. Rev. 2006, 106, 1105-1136

[15] Saito, R., Dresselhaus, M. S. & Dresselhaus, G. Physical Properties of Carbon Nanotubes. Singapore: Imperial College Press. (2001).

[16] D. S. Bethune, C-H. Kiang, M. S. de Vries, G. Gorman, R. Savoy, J. Vazquez, and R. Beyers, "Cobalt-catalysed growth of carbon nanotubes with single-atomic-layer walls", Nature 363, 605-607 (1993)

[17] Ebbesen T. W., Ajayan PM., "Large-scale synthesis of carbon nanotubes". Nature 1992; pp.220-358

[18] Thoteson, E. , Z. Ren and T. Chou, "Advances in the science and technology of carbon nanotubes and their composites: a review", Compos Sci Technol 61 (2001) (13), pp. 1899–1912.

[19] Yi, W. , L. Lu, D.L. Zhang, Z.W. Pan, S.S. Xie, "Linear specific heat of carbon nanotubes", Phys. Rev. B 59 (1999) R9015.

[20] Hone, J. , M. Whitney, C. Piskoti, A. Zettl, "Thermal conductivity of single-walled carbon nanotubes", Phys. Rev. B 59 (1999) R2514.

[21] Collins, P.G. and P. Avouris, "Nanotubes for electronics", Sci Am 283 (2000), pp. 62–69.

[22] S. Niyogi, M. A. Hamon, H. Hu, B. Zhao, P. Bhowmik, R. Sen, M. E. Itkis, and R. C. Haddon, "Chemistry of Single-Walled Carbon Nanotubes", Acc. Chem. Res. 2002, 35, 1105-1113

[23] Mickelson, E. T.; Chiang, I. W.; Zimmerman, J. L.; Boul, P.; Lozano, J.; Liu, J.; Smalley, R. E.; Hauge, R. H.; Margrave, J. L. J. Phys. Chem. B 1999, 103, 4318.

[24] Khabashesku, V. N.; Billups, W. E.; Margrave, J. L. Acc. Chem. Res. 2002, 35, 1087.

[25] Boul, P. J.; Liu, J.; Mickelson, E. T.; Huffman, C. B.; Ericson, L. M.; Chiang, I. W.; Smith, K. A.; Colbert, D. T.; Hauge, R. H.; Margrave, J. L.; Smalley, R. E. Chem. Phys. Lett. 1999, 310, 367.

[26] Saini, R. K.; Chiang, I. W.; Peng, H.; Smalley, R. E.; Billups, W. E.; Hauge, R. H.; Margrave, J. L. J. Am. Chem. Soc. 2003, 125, 3617.

[27] Tietze, L. F.; Bratz, M., "Dialkyl Mesoxalates by Ozonolysis of Dialkyl Benzalmalonates", Org. Synth., ; Coll. Vol. 9: 314 (1998), www.orgsyn.org.

[28] Banerjee, S.; Wong, S. S. J. Phys. Chem. B 2002, 106, 12144.

[29] Ivanov, V.; Fonseca, A.; Nagy, J. B.; Lucas, A.; Lambin, P.; Bernaerts, D.; Zhang, X. B. Carbon 1995, 33, 1727.

[30] The Smalley Group at Rice University, http://www.ruf.rice.edu

[31] C. Journet and P. Bernier, “Production of carbon nanotubes”, Appl. Phys. A (1998), pp. 1–9.

[32] H. Dai, Carbon nanotubes: opportunities and challenges, Surface Sci 500 (2002) (1–3), pp. 218-241.

[33] L. V. Radushkevich and V. M. Lukyanovich, Zh. Fiz. Khim. 26, 88 s1952d.

[34] Koyama, T. and Endo, M.T. “Structure and Growth Processes of Vapor-Grown Carbon Fibers”, O. Buturi, 42 (1973):690.

[35] Morgan, P. “Carbon Fibers and Their Composites”, Taylor & Francis Group, CRC Press, Boca Raton, FL (2005).

[36] Schlogl; Robert ; et al., "Carbon Nanotubes and Carbon Nanofibers For Oil Spill Remediation", U.S. Patent Application 20090220767 published in September 2009.

[37] Goodman, D.W., R.D. Kelley, T.E. Madey, and J.T. Yates. 1980. J. Catal. 63: 226.

[38] Kim , Pand C.M. Lieber. Nanotube Nanotweezers, Science 286 (1999), p. 2148.

[39] Y. Hamerlinck, D.H. Mertens, in: E.F. Vansant (Ed.), Activated Carbon Principles in Separation Technology, Elsevier, New York, 1994.

[40] C.L. Mantell, Carbon and Graphite Handbook, Interscience, New York, 1968.

[41] D. Mohan, K.P. Singh, Granular activated carbon, in: J. Lehr, J. Keeley, J. Lehr (Eds.), "Water Encyclopedia: Domestic, Municipal, and Industrial Water Supply and Waste Disposal", Wiley/ Interscience, New York, 2005.

[42] T. Otowa, Y. Nojima, T. Miyazaki, "Development of KOH activated high surface area carbon and its application to drinking water purification", Carbon 35 (9) (1997) 1315–1339.

[43] J.S. Mattson, H.B. Mark Jr., "Activated Carbon", Marcel Dekker, NewYork, 1971.

[44] http://en.wikipedia.org/wiki/Activated_carbon

[45] Dinesh Mohan, Charles U. Pittman Jr., " Activated carbons and low cost adsorbents for remediation of tri- and hexavalent chromium from water" Journal of Hazardous Materials B137 (2006) 762–811

[46] Managing Coal Combustion Residues in Mines, Committee on Mine Placement of Coal Combustion Wastes, National Research Council of the National Academies, 2006

[47] Human and Ecological Risk Assessment of Coal Combustion Wastes, RTI, Research Triangle Park, August 6, 2007, prepared for the U.S. Environmental Protection Agency

[48] http://www.sierranevadaconcrete.com/pubs/Fly_Ash_Bulletin.pdf

[49] Whellock, John G., "Treatment of Fly Ash", US Patent Application# US2010/031293, Publication Date October 28, 2010.

[50] Kenneth Wark, CECIL F. Warner, and Wayne T. Davis, Air Pollution: Its Origin and Control, Addison Wesley, 3rd Edition England, 1998.

[51] Dinesh Mohana and Charles U. Pittman, "Activated carbons and low cost adsorbents for remediation of tri- and hexavalent chromium from water", Journal of Hazardous Materials B137 (2006) 762–811.

[52] C. Raji, T.S. Anirudhan, "Batch Cr(VI) removal by polyacrylamide-grafted sawdust: kinetics and thermodynamics", Water Res. 32 (1998) 3772–3780.

[53] J. Fang, Z.M. Gu, "Cr(VI) removal from aqueous solution by activated carbon coated with quaternized poly(4-vinylpyridine)", Environ. Sci. Technol. 41 (2007) 4748–4753.

[54] D. Mohan, K.P. Singh, V.K. Singh, “Trivalent chromium removal from wastewater using low cost activated carbon derived from agricultural waste material and activated carbon fabric cloth”, J. Hazard. Mater. 135 (2006) 280–295.

[55] Jun Hu, Changlun Chen, Xiaoxiang Zhu, Xiangke Wang, "Removal of chromium from aqueous solution by using oxidized multiwalled carbon nanotubes", Journal of Hazardous Materials 162 (2009) 1542–1550

[56] Dionex, Determination of Cr(VI) in water, wastewater and solid waste extracts, Technical Note 26, http://www.dionex.com/

[57] http://cadmium.org/

[58] R. Leyva-Ramos, J.R. Rangel-Mendez, et al., "Adsorption of cadmium(II) from aqueous solution onto activated carbon", Wat. Sci. Technol. 35 (1997) 205–211.

[59] Ahalya, N.; Kanamadi, R. D.; Ramachandra, T. V., "Biosorption of Chromium (VI) from aqueous solution by the husk Bengal gram" (Cicer Arientinum). Eelect. J. Biotech. 8 (3), (2005) 258-264

[60] Li, Y.H. ,J. Ding, Z. Luan, Z. Di, Y. Zhu, C. Xu, D. Wu and B. Wei, “Competitive adsorption of Pb2+, Cu2+ and Cd2+ ions from aqueous solutions by multiwalled carbon nanotubes”, Carbon 41 (2003) (c) , pp. 2787–2792.

[61] Maryam Ahmadzadeh Tofighy, Toraj Mohammadi, " Adsorption of divalent heavy metal ions from water using carbon nanotube sheets", Journal of HazardousMaterials (2010), Article in Press

[62] Goran D. Vukovi´c, Aleksandar D. Marinkovi´c, et al., "Removal of cadmium from aqueous solutions by oxidized and ethylenediamine-functionalized multi-walled carbon nanotubes", hemical Engineering Journal 157 (2010) 238–248

[63] A. A. Attia, S. A. Khedr and S. A. Elkholy, "ADSORPTION OF CHROMIUM ION (VI) BY ACID ACTIVATED CARBON", Brazilian Journal of Chemical Engineering, Vol. 27, No. 01, pp. 183 - 193, January - March, 2010

[64] Badu, B. V. and Gupta, S., "Adsorption of Cr(VI) using activated neem leaves, kinetic studies". Adsorption 14, 85 (2008).

[65] Raoa, G., Lu, C. and Su, F., "Sorption of divalent metal ions from aqueous solution by carbon nanotubes: A review". Separation and Purification Technology, 58 (2007) pp. 224-231.

[66] http://www.nanoamor.com

[67] Chilton Nga, Jack N. Lossoa, et al., "Physical and chemical properties of selected agricultural byproduct-based activated carbons and their ability to adsorb geosmin," Journal of Bioresource Technology, September 2002, Pages 177-185.

[68] Wenzhong Shen, Zhijie Li and Yihong Liu, "Surface Chemical Functional Groups Modification of Porous Carbon", Recent Patents on Chemical Engineering 2008, 1, 27-40.

[69] A. A. Muataz, Omer Yahya Bakather, et al., “Removal of Chromium (III) from Water by Using Modified and Nonmodified Carbon Nanotubes,” Journal of Nanomaterials Volume 2010, Article ID 232378, 9 pages.

[70] Amir Fouladi Tajar, Tahereh Kaghazchi, et al., "Adsorption of cadmium from aqueous solutions on sulfurized activated carbon prepared from nut shells" Journal of Hazardous Materials, 165 (2009) 1159–1164.

[71] C.H. Weng, C.H. Huang, in: C.R. O’Melia (Ed.), Proceedings of the 1990 Environmental Engineering Speciality Conference ASCE, New York, 1990, pp. 923–924.

[72] P. Ricou-Hoeffer, I. Lecuyer, P. Le Cloirec, Water Res. 35 (4) (2001) 965.

[73] D. Xu, X. Tan, C. Chen, X. Wang, “Removal of Pb(II) from aqueous solution by oxidized multiwalled carbon nanotubes”, J. Hazard. Mater. 154 (2008) 407–416.

[74] A. Nassereldeen, A. A. Muataz, A. Abdullah, E. S. Mohamed, M. D. Alam, and N. Yahya, “Kinetic adsorption of application of carbon nanotubes for Pb(II) removal from aqueous solution,” Journal of Environmental Sciences, vol. 21, pp. 539–544, 2009.

[75] Omar Yahya Bakather, "Removal of Lead & Chromium from Water Using Modified and Nonmodified Carbon Nanotubes", MSc Thesis, Chem Engineering Dept. King Fahd University of Petroleum & Minerals, June 2009.

APPENDIXES

APPENDIX A

EXPERIMENTAL RESULTS FOR

Table A.1: Hexavalent- Chromium removal % by all Adsorbents

Table A.2: Cadmium removal % by Non-modified Adsorbents

Table A.3: Cadmium removal % by Modified Adsorbents

Table A.1: Hexavalent- Chromium removal % by all Adsorbents

pH	CNT-50mg	AC-50mg	M-CNT-50mg	M-AC-50mg
2	18%	16%	18%	43%
3	45%	42%	44%	55%
4	47%	38%	18%	26%
5	8%	5%	8%	9%
7	4%	2%	2%	3%
8	0%	1%	0%	0%

rpm	CNT-50mg	AC-50mg	M-CNT-50mg	M-AC-50mg
50	46%	50%	43%	41%
100	34%	50%	36%	46%
150	45%	56%	44%	55%
200	45%	87%	44%	94%
250	42%	82%	40%	93%

Time	CNT-150rpm	AC-200rpm	M-CNT-150rpm	M-AC-200rpm
0	0%	0%	0%	0%
10	27%	63%	28%	51%
30	39%	77%	38%	66%
60	42%	78%	39%	77%
120	45%	87%	45%	94%
240	47%	88%	48%	97%
480	50%	89%	47%	97%
1440	49%	88%	47%	98%

mg	CNT-150rpm	AC-200rpm	M-CNT-150rpm	M-AC-200rpm
25	26%	73%	30%	77%
50	45%	87%	45%	94%
75	63%	92%	57%	99%
100	70%	91%	66%	99%
150	79%	91%	81%	99%
200	80%	92%	87%	99%
250	80%	91%	87%	99%

Table A.2: Cadmium removal % by Non-modified Adsorbents

pH	CNT-50mg	FA-50mg	AC-50mg	CNF-50mg
2	0%	10%	3%	0%
3	0%	13%	2%	0%
4	0%	90%	2%	0%
5	10%	92%	5%	15%
7	27%	95%	38%	34%
8	6%	90%	25%	16%

rpm	CNT-50mg	FA-50mg	AC-50mg	CNF-50mg
50	0%	66%	13%	0%
100	2%	67%	20%	0%
150	27%	95%	38%	34%
200	27%	98%	40%	33%
250	24%	94%	45%	32%

Time	CNT-50mg	FA-50mg	AC-50mg	CNF-50mg
0	0%	0%	0%	0%
10	0%	78%	0%	5%
30	19%	90%	3%	17%
60	21%	93%	13%	15%
120	27%	95%	38%	34%
240	30%	91%	38%	34%
480	31%	93%	38%	37%
1440	31%	91%	42%	37%

mg	CNT-50mg	FA-50mg	AC-50mg	CNF-50mg
25	3%	65%	26%	19%
50	27%	95%	38%	34%
75	27%	95%	35%	32%
100	25%	96%	37%	28%
150	21%	96%	37%	30%
200	24%	96%	37%	31%
250	25%	96%	37%	29%

Table A.3: Cadmium removal % by Modified Adsorbents

pH	M-CNT	M-FA	M-AC	M-CNF
2	2%	3%	3%	0%
3	1%	6%	18%	-2%
4	39%	34%	93%	9%
5	77%	52%	96%	25%
7	93%	74%	98%	55%
8	79%	69%	99%	53%

rpm	M-CNT	M-FA	M-AC	M-CNF
50	62%	49%	55%	29%
100	74%	60%	58%	35%
150	93%	74%	98%	55%
200	89%	80%	95%	50%
250	93%	80%	92%	52%

Time	M-CNT	M-FA	M-AC	M-CNF
0	61%	64%	68%	0%
10	73%	64%	90%	35%
30	74%	65%	96%	43%
60	93%	74%	98%	46%
120	93%	74%	98%	55%
240	99%	78%	98%	55%
480	99%	80%	99%	59%
1440	99%	78%	99%	53%

mg	M-CNT	M-FA	M-AC	M-CNF
25	43%	43%	68%	33%
50	93%	74%	98%	55%
75	96%	75%	96%	65%
100	98%	77%	98%	70%
150	98%	77%	98%	80%
200	98%	77%	98%	80%
250	98%	78%	98%	80%

APPENDIX B

Table B.1: Materials for the experiment.

MATERIALS
1. Sample Adsorbents • Raw carbon nanotubes (R-CNTs) • Modified carbon nanotubes (R-CNTs) 2. Stock Pb (II) solution 3. Stock Chromium (III) Solution 4. 0.1 N Sodium Hydroxide 5. 6 M nitric acid 6. Deionized water

APPENDIX C

Table C.1: Equipment for the Experiment

EQUIPMENTS		
No.	**Equipments**	**Model**
1.	Transmission Electron Microscopy, TEM	JEOL JEM-2010F
3.	Scanning Electron Microscopy, SEM	SHAKER SK-600
4.	Inductive coupled plasma (ICP)	
5.	Mechanical Shaker	SHAKER SK-600
6.	pH Indicator	METTLER TOLEDO MP 220
9.	Magnetic Stirring Heater	-
10	Sonicator	
10.	100 ml Conical flasks	-
11.	1000 mL Volumetric flasks	-
12.	1-5 mL, petites	-
13.	Balancer	-
14.	Test Tube rack	-
15.	Scott Bottles (100 mL)	-

APPENDIX D

Experimental Figures

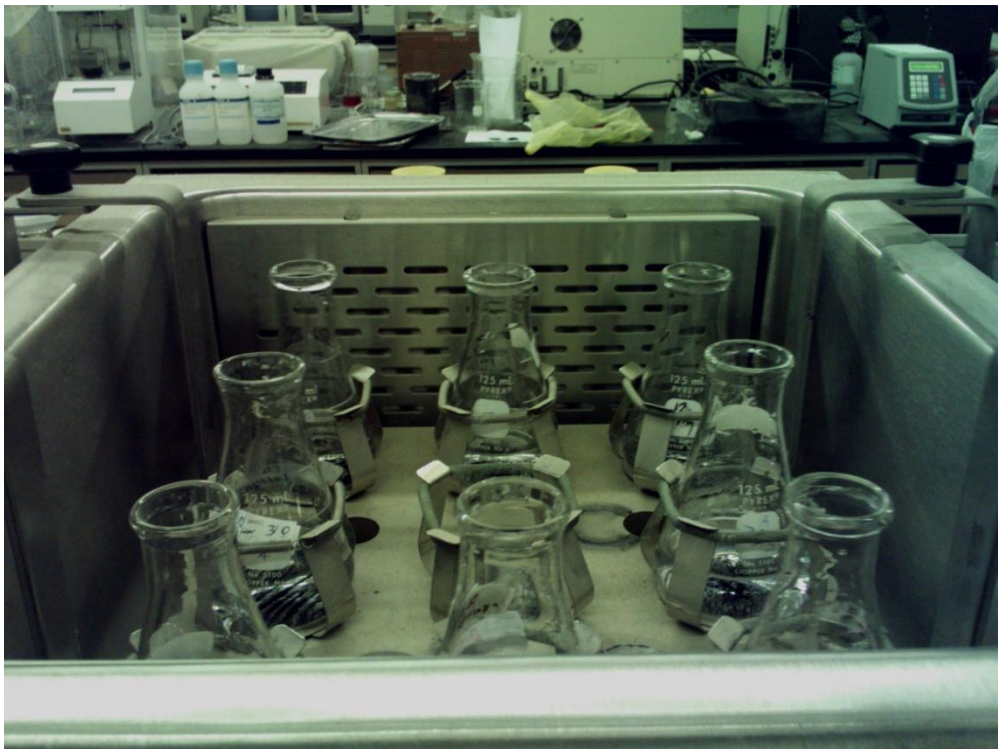

Figure D.1: Photograph of Batch Mode Adsorption Experiment

Figure D.2 :A photograph of SEM JEOL 6400

Figure D.3: A photograph of TEM Hitachi H-7100

Figure D.4: A Sonicator

APPENDIX E

Experimental Flowchart for Final Year Project

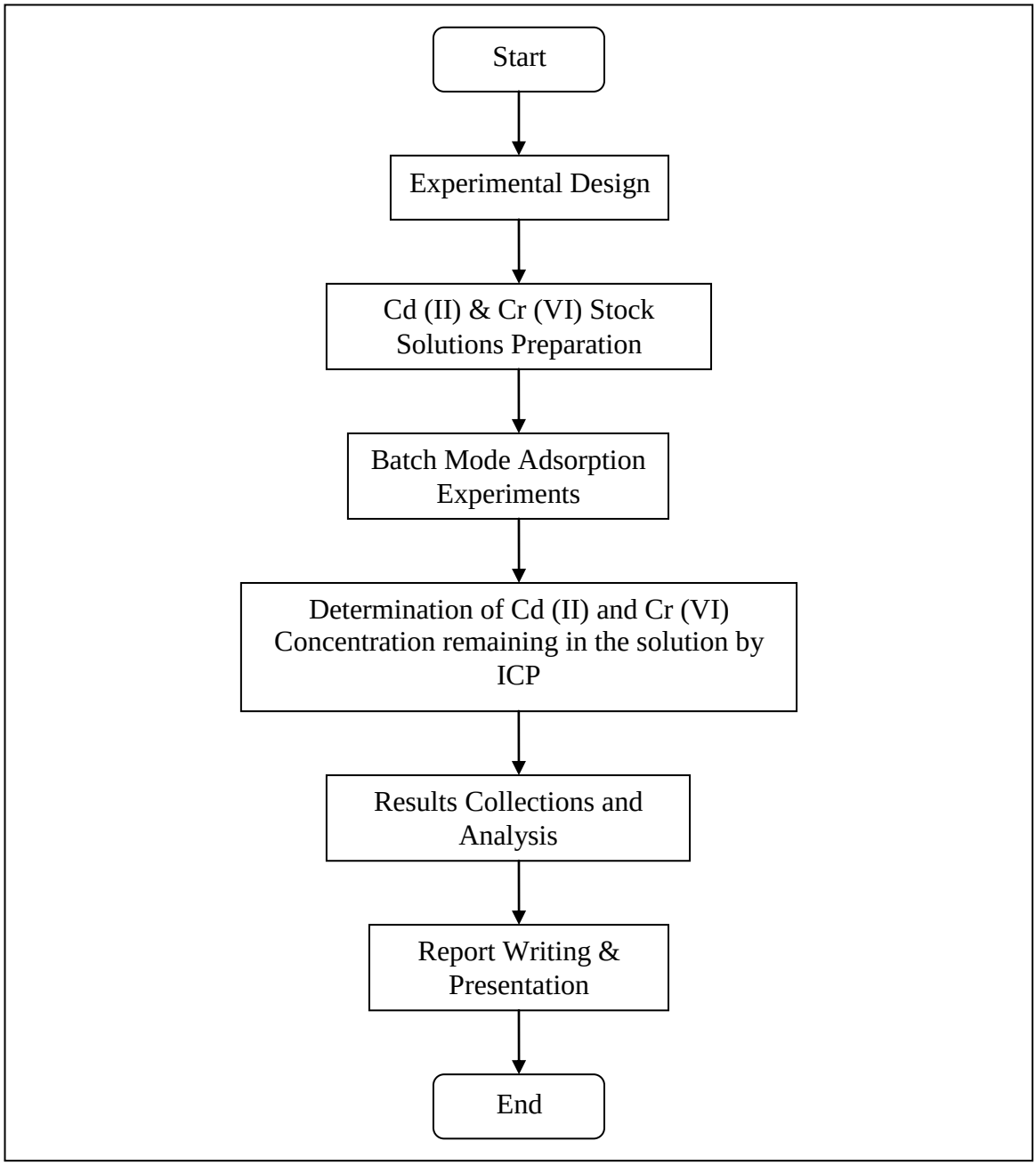

VITA

- Fahad Abdulaziz A. Al-Khaldi
- Saudi - Born in Anak-Qatif, 28/11/1962.
- Married.
- Received B.Sc. degree in Chemical Engineering from King Fahd University of Petroleum & Minerals in June 1988.
- Received Master of Business Administration from King Fahd University of Petroleum & Minerals in July 1992.
- Received Master of Science degree in Civil Engineering from King Fahd University of Petroleum & Minerals in July 1996.
- Received Doctor of Philosophy degree in Chemical Engineering from King Fahd University of Petroleum & Minerals in June 2011.
- Worked as Operation Engineer, then as Senior Efficiency Engineer in Saline Water Conversion Corporation, Al-Khobar Power and Desalination Plant (Dec. 1988 – Nov. 1996).
- Facilities Planning Engineer in Saudi Aramco (Dec. 1996 – Now).
- Current/Permanent Address: P.O Box 12538, Dhahran 31311, Saudi Arabia
  Tel.: +966505856525
- Email: khaldifahad@yahoo.com